C 51.17/12:987/7
C 51.17/12:987/7
AUG 0 8 1987

Tech Notes

JULY 1987

PB87-925907

CONTIN

PENNSYLVANIA STATE UNIVERSITY
JAN 14 1988
DOCUMENTS COLLECTION

Feature Article:
Cooperative Research Programs at

C P M VL

NTIS
U.S. DEPARTMENT OF COMMERCE
National Technical Information Service
Center for the Utilization of Federal Technology

Tech Notes

Highlighting Selected U.S. Government Technology & Resources

JULY 1987

Contents

Agriculture & Food 619

Computers 623

Electrotechnology 629

Energy 638

Engineering 644

Environmental Science & Technology 657

Manufacturing, Machinery, & Tools 661

Materials 674

Medicine & Biology 690

Natural Resources Technology & Engineering 695

Physical Sciences 699

Transportation 715

Published monthly by the National Technical Information Service (NTIS), Tech Notes bring togeather individual one to two page fact sheets prepared by Federal agencies, their laboratories, or contractors. These fact sheets highlight current Federal technology determined to have commercial or practical application. Topics cover new processes, materials, techniques, software, instrumentation, and resources.

Some of the current sources are the Department of the Navy, Department of the Army, NASA, Department of Energy , Environmental Protection Agency, Department of the Interior, and the Department of Agriculture.

Special assistance is provided by the Federal Laboratory Consortium.

Change of address or questions concerning subscriptions should be sent to:
Subscriptions Department
National Technical Information Service
Springfield, VA 22161
(703) 487-4630

Suggestions, comments, or questions concerning Tech Notes should be directed to:
Tech Notes Editor
Room 11R
National Technical Information Service
Springfield, VA 22161
(703) 487-4838

U. S. Depository Copy

How to Use Tech Notes

Every Tech Notes fact sheet lists a source for additional information. The source of this information may be a special support package from the originating agency, a personal contact, a licensing opportunity, or a backup report available from NTIS.

Each fact sheet also is perforated to allow for easy removal for those subscribers who may wish to keep a special fact sheet file or route to others in their organization

Sources of Further Backup Information

Below are two representative examples of how each Tech Note fact sheet provides you with a source of further information. In most cases, this information is provided directly by the agency or its laboratory. However, there are cases where NTIS is the source for backup documentation. In these cases, use the order form at the end.

Examples:

significant distance from the endwalls. Therefore, a radial variation in efficiency should be used when designing small stators.
Project Officer Jeffrey E. Haas
(216) 433-4000.

FOR ADDITIONAL INFORMATION

You can learn more about this technology by ordering the NTIS report(s):
Cold-Air Performance of Compressor Drive Turbine
Order number: AD-A101066/NAA
Price code: A02
Order from:
National Technical Information Service
5285 Port Royal Road
Springfield, VA 22161
(703) 487-4650

158

Agency contact who can supplement the information contained in the backup report.

NTIS Order Number*

NTIS Price Code*

* See the order form and price code table at the end of the issue.

Suggested applications include other kinds of refrigerators, heat engines, thermal instrumentation, and heat switches.
This work was done by Emanuel Tward of Caltech for NASA's Jet Propulsion Laboratory.
NPO-15479/TN

FOR ADDITIONAL INFORMATION
Contact: Director, Technology Transfer Division, P.O. Box 8587, BWI Airport, MD 21240: (301) 621-0100 Ext.241.
REFER TO THE NUMBER LISTED AT THE END OF THE ARTICLE

178

Agency reference number

Source of more information about the technology described in the fact sheet

Page number

Tech Notes Title List for July 1987

Agriculture & Food

619 Computer Keeps Potatoes Breathing Easy
620 Potential Agricultural Impacts of Large-Scale Biomass Production
621 Uniform Cost-Estimation Method for Biomass Production and Conversion Technologies

Testing & Instrumentation

622 Animal Electronics Make Cows Bionic Bovines

Computers

623 Natural Language Processing: A Tutorial
624 An Integrated Fault Tree Environment
625 Optical Interferometric Parallel Data Processor—Image data would be processed much faster than in present electronic systems.
626 Parallel Analog-to-Digital Image Processor—Compact circuitry performs conversions.

Software

627 Program Assesses Software Reliability During its Testing

Electrotechnology

629 Optical-Data Processing With Liquid-Crystal TV—Even in its present state of development, this miniature flat-screen television can be used for pattern recognition.
630 Small-Screen Displays—A literature search examines size, protocols, abbreviations, and vocabulary.
631 Better Radiation-Hardened Memory Chips Possible—Computer model predicts how much radiation can be withstood.
632 Tape Interconnect Materials and Processes for Military Electronic Packages
633 Millimeter-Wave Traveling-Wave-Tubes Circuits Produced at Reduced Costs
634 Designing High-Frequency Inductors—Procedures for both ferrite-core and Molypermalloy-core inductors are detailed.
635 CMOS Clock Synchronizer—A circuit synchronizes clock and gate signals within one-quarter of a clock cycle. (Licensing Opportunity)
636 Two-Layer, Full-Color Electroluminescent Display—A matrix-addressed, flat-panel display features increased resolution, brightness, and contrast. (Licensing Opportunity)

Testing & Instrumentation

637 Double-Referenced, Pulsed, Phase-Locked Loop—DRP2L2—The phase shift between two tone-burst signals is measured precisely. (Licensing Opportunity)

Other items of interest

622 Animal Electronics Make Cows Bionic Bovines
679 New Anisotropic Ceramic-Air Composites Improve the Strength and Operational Capability of Ceramic Electronic Devices

Energy

638 Benefits of Replacing Residential Central Air Conditioning Systems
639 New Polymer Electrolyte for Batteries
640 Liquid-Crystal Thermal-Control Panels—Radiative temperature regulators would have no moving parts. (Licensing Opportunity)
641 Solar Cells With Reduced Contact Areas—Silicon cells are more efficient because less metal touches the semiconductor. (Licensing Opportunity)
642 More Efficient Solar Thermal-Energy Receiver—Thermal stresses and reradiation are reduced. (Licensing Opportunity)

Testing & Instrumentation

643 Monitoring the Heat Output of a Wood-Burning Stove

Other items of interest

670 Screening Mechanically-Defective Solar Cells—A flexure test eliminates failure-prone wafers before further processing.
712 One-Dimensional Simulation of Isotropic Radiation—Solar cells are tested for effects of radiation in a unidirectional beam.
718 Acceptance, Verification, and Performance Test Results for the Bedford CF Electric Van

Engineering

644 Predicting the Impulse of Blast Waves—A computer code predicts potentially hazardous effects with acceptable accuracy.
645 The POP Pipe-Joining System—Tests evaluate the suitability of the system for gap or river crossings.
646 Zirconia-Bonded Zirconia Fiber Insulation Structures
647 Energy-Absorbing Passenger Seat for Aircraft—Tests show probability of passenger survival to be high.
648 Improved Heat-Transfer Calculations for Hypersonic Flow—The Lewis number is corrected for extremely high airspeeds.
649 Multiple-Scale Turbulence Model—The turbulence in complex, recirculating flows is not in spectral equilibrium.

Testing & Instrumentation

650 Propeller Flows Studied Using Doppler Velocimetry
651 Depth Gauge for Liquids Under High Pressure—An ultrasonic transducer is protected from high pressure and is easy to connect. (Licensing Opportunity)
652 Measuring Room Area or Volume Electronically—Results would be obtained rapidly with minimal effort.
653 Measuring Fluid Velocities With Glowing Particles—Particle trajectories are recorded photographically. (Licensing Opportunity)
654 Taking Impressions of Hidden Cavity Walls—A device for field checks makes casts of internal contours.
655 Environmental Testing of Glass-Fiber/Epoxy Pressure Vessels—Strength diminishes during long exposure to the environment.

Engineering (Cont.)

656 Identifying Vibration Parameters in Large Structures—An analytical method separately examines low-frequency and high-frequency behavior.

Environmental Science & Technology

657 Process Eliminates 99% of NOx from Exhaust in Lab Tests

658 Geotextiles for Drainage, Gas Venting, and Erosion Control at Hazardous Waste Sites

659 Waste Characterization and Analysis Activities in Support of the INEL Solidification Development Program

Testing & Instrumentation

660 Air Monitoring Device Developed—New meter measures light scattered by particulates.

Other items of interest

695 Underground Channels Mapped by Radar

Manufacturing, Machinery, & Tools

661 Low-Loss Coherent Fiber-Optic Arrays—Multifibers can be made from fused silica glass.

662 Robot Carts Given Flexibility with New Software

663 Part Geometry Data Used to Direct Robot Deburring

664 Cleaner Vacuum-Bag Curing—An improvement upon recommended procedures saves time and expense. (Licensing Opportunity)

665 Hot-Air-Pulse Generator—Mixer blades interrupt airflow for rapid testing of insulating materials.

666 Remotely Adjustable Hydraulic Pump—Outlet pressure can be adjusted to match varying loads. (Licensing Opportunity)

667 Local Data Processing for a Robot Hand—Integrated-circuit microcomputers process signals among sensors, external controls, and the end-effector motor.

668 Simplified Explosive Joining of Tubes to Fittings—A ribbon explosive and mild detonating fuse allow the use of a smaller charge. (Licensing Opportunity)

Software

669 NASA Test File—Comparisons among different computer-aided design systems are facilitated.

Testing & Instrumentation

670 Screening Mechanically-Defective Solar Cells—A flexure test eliminates failure-prone wafers before further processing.

671 Eddy-Current Detection of Weak Bolt Heads—An electronic test identifies flawed units that pass hardness tests.

672 Eddy-Current Detection of Cracks in Tubes—A nondestructive device tests narrow, sharply-bent metal tubes.

673 Measuring Hole Elongation in Bolted Joints—The measurement does not affect joint parameters. (Licensing Opportunity)

Other items of interest

633 Millimeter-Wave Traveling-Wave-Tubes Circuits Produced at Reduced Costs

677 Rubber-Processing Studies—Processing of natural rubber and styrene/butadiene was studied.

682 Fast-Response Heating of Silicon Melts—Heating would be confined to a small mass near the growing crystal.

Materials

674 Hot Isostatic Pressing of Sintered Ceramics—A model of the process has been developed and analyzed.

675 Self-Propagating High-Temperature Synthesis—A new method of preparing ceramics offers many advantages.

676 Properties of Sintered Beta Silicon Carbide at High Temperature—Commerically produced material is compared with earlier samples made in the laboratory.

677 Rubber-Processing Studies—Processing of natural rubber and styrene/butadiene was studied.

678 Hypersonic Plane Material—Basic tests on aluminum-lithium alloys will be conducted.

679 New Anisotropic Ceramic-Air Composites Improve the Strength and Operational Capability of Ceramic Electronic Devices

680 Fracture Analysis of Welded Type 304 Stainless Steel Pipe

681 Microstructure and Aging of Powder-Metallurgy Al Alloys—Peak hardness is achieved at lower aging temperatures than with standard ingot-metallurgy alloys.

682 Fast-Response Heating of Silicon Melts—Heating would be confined to a small mass near the growing crystal.

683 Evaluation of GaAs Fracture Mechanics—These data can aid the design of solar cells.

684 Radiation Effects on Polymer Properties—Tables present lowest doses for which effects are noticeable.

685 Fire-Retardant, Decorative Inks—The effectiveness of fire-retardant additives is evaluated. (Licensing Opportunity)

686 Polyimide Pregregs With Improved Tack—Drape and tack are improved without loss of strength.

Testing & Instrumentation

687 Mechanical Tests of Coated Carbon/Carbon Composite—The duplex coating performs its function despite nonuniformity, cracks, and debonding.

688 Damping Capacity Measurements for Characterization of Degradation in Advanced Materials

689 Furnace for Tensile Testing of Flexible Ceramics—Ceramic cloth and thread are tested quickly at temperatures up to 1,250°C. (Licensing Opportunity)

Other items of interest

646 Zirconia-Bonded Zirconia Fiber Insulation Structures

Medicine & Biology

690 Neural Tissues Available

691 Advance Computer System Probes Molecular Structure of Proteins

Testing & Instrumentation

692 Portable Beta Spectrometer for Tissue Dose Measurement

Medicine & Biology (Cont.)

693 Magnetic Study of Bioelectric Phenomena (Licensing Opportunity)

694 Surgical Borescopes Remove Contaminants—Borescope instruments are put to use in extracting hard-to-reach particles.

Natural Resources Technology & Engineering

695 Underground Channels Mapped by Radar

Software

696 Tidal Data Available through Microcomputer Software

697 HARPA (Hamiltonian Acoustic Ray-tracing Program for the Atmosphere)—Traces the three-dimensional paths of acoustic rays through continuous model atmospheres

698 Program for Thermospheric Calculations—Atmospheric properties at high altitudes are predicted.

Physical Sciences

699 Cleaning With Ultraviolet Radiation and Ozone—The combustion of radiation and active oxidation removes contaminants quickly and clearly.

700 Chemist's Workbench for Molecular Mechanics—A suite of programs allows modeling, analysis, and display

701 Temperature and Concentration Profiles in Hydrogen/Nitrous Oxide Flames—Raman spectroscopy and laser-induced fluorescence yield data on constituents and temperatures over a range of flame mixtures.

702 New Fischer-Tropsch Catalysts Derived from Zeolitic Aluminoferrisilicates

703 High Pressure Studies Show Rare Behavior of Bonding in Actinide Metals

704 Determining Optical Axes of Uniaxial Crystals

705 Monolithic Isolated Single-Mode Ring Laser—The MISER uses a four-sided ring to lase nonreciprocally. (Licensing Opportunity)

706 Rapid Synthesis of Nonstoichiometric Lanthanum Sulfide—A new process is relatively fast and simple.

707 Thermoelectric Properties of Lanthanum Sulfide—At 300 to 1,400 K, Gamma-phase La(3-x)S4 is an extrinsic semiconductor.

708 A Model-Parameter Extraction Procedure—The procedure accommodates multiple input excitations.

709 Preventing Cracks in Silicon-Reactor Liners—Correct placement may help to prevent contamination while eliminating crack-causing deposits.

Testing & Instrumentation

710 Monitoring Ion-Implantation Progress—A conventional implanter can be modified to perform ion acoustic microscopy.

711 Automatic Measurement of Rain Rate—Standard rain gauges are assembled into an electronic collection, storage, and processing sytem.

712 One-Dimensional Simulation of Isotropic Radiation—Solar cells are tested for effects of radiation in a unidirectional beam.

713 Versatile X-Ray Telescope—Spatial and spectral resolutions are increased. (Licensing Opportunity)

714 Wide-Angle, Flat-Field Telescope—An all-reflective system is unvignetted. (Licensing Opportunity)

Other items of interest

639 New Polymer Electrolyte for Batteries

660 Air Monitoring Device Developed—New meter measures light scattered by particulates.

675 Self-Propagating High-Temperature Synthesis—A new method of preparing ceramics offers many advantages.

684 Radiation Effects on Polymer Properties—Tables present lowest doses for which effects are noticeable.

697 HARPA (Hamiltonian Acoustic Ray-tracing Program for the Atmosphere)—Traces the three-dimensional paths of acoustic rays through continuous model atmospheres

Transportation

715 Small-Scale and Full-Scale Models of Helicopter Rotors—Data on noise and on hovering and forward flight are compared.

716 Testing Helicopter Crashworthiness—A simulated crash shows that an energy-absorbing design is effective in protecting the crew.

717 Circulation-Control Variable-Pitch Propeller—Blown aerodynamics concept would improve reliability and reduce costs.

718 Acceptance, Verification, and Performance Test Results for the Bedford CF Electric Van

Other items of interest

647 Energy-Absorbing Passenger Seat for Aircraft—Tests show probability of passenger survival to be high.

678 Hypersonic Plane Material—Basic tests on aluminum-lithium alloys will be conducted.

Agriculture & Food

619 Computer Keeps Potatoes Breathing Easy

620 Potential Agricultural Impacts of Large-Scale Biomass Production

621 Uniform Cost-Estimation Method for Biomass Production and Conversion Technologies

Testing & Instrumentation

622 Animal Electronics Make Cows Bionic Bovines

Digitized by the Internet Archive
in 2013

http://archive.org/details/technxxxxxxxxx00cent

United States Department of Agriculture

Research Technology
Agricultural Research Service

Computer Keeps Potatoes Breathing Easy

Agricultural engineer Lewis Schaper inspects vertical and horizontal air sampling tubes during bin-filling operation.

When a 500-ton bin of potatoes is about to rot, storage managers need to take action in a hurry.

Now a new computerized system developed by USDA Agricultural Research Service scientists at East Grand Forks, MN, can give them a hand in deciding which action is best.

Researchers at the Red River Valley Potato Research Laboratory have linked a personal computer to gas monitoring devices, temperature and wind sensors, and ventilating fans to give early warning of spoilage or other storage problems.

The computer system helps most in controlling bin atmospheres during and soon after harvest. That's when potatoes recover from harvest damage and use large amounts of oxygen and produce high concentrations of carbon dioxide. Normal respiration in the dark conditions adds to a bin environment that promotes the outbreak of disease. "Disease micro-organisms love an anaerobic atmosphere where they have the advantage of living and growing without oxygen," says biochemist Jerry L. Varns.

Storage managers provide needed oxygen for the potatoes by forcing outside air into bins through ducts connected to an electric fan. Ventilation helps potatoes suberize, or cure. This process, which takes about 2 weeks, toughens potato skins and heals wounds inflicted by handling during harvest.

But the decision of how much ventilation to use is not as simple as it may seem. The bins used for potatoes intended for potato chips are typically 25 feet wide by 80 feet long. Potatoes are normally piled 16 to 18 feet deep in these bins. Excessive fan operation supplies "too much air too soon and causes them to shrink and flatten," says agricultural engineer Lewis A. Schaper. "Those on the bottom bruise from the weight of those above them."

Restricting air circulation too much can be harmful. Varns explains it this way, "Potatoes are alive. In storage they use up oxygen and respire carbon dioxide. The poor tubers on the bottom

of the bin are the first to show breathing problems because of the weight stress. The added stress becomes too much and that's when diseases take over. They start in small areas commonly called disease pockets and, if not contained, will quickly spread by the liquid generated in these pockets."

Varns says potato bins should have sufficient ventilation to keep carbon dioxide levels from rising above 2 percent during curing. After curing, levels should be kept even lower.

Experience in managing potato storages doesn't always provide the best insurance against disease problems. That's mainly because changes in temperature, humidity, and windspeed during harvest and bin-filling can create the need for individualized management for each bin. Such attention has not been possible for the majority of farmers who both grow and store potatoes.

After the researchers tested the computerized monitoring system in a commercial-sized research bin, they installed a second, modified system at an eight-bin commercial storage facility. Air samples from over 60 locations within the bins are automatically pumped via nylon tubing to a gas chromatograph for analysis.

The chromatograph acts as a mechanical nose by identifying key stress gases in the air much sooner than a human can detect them. Also, when carbon dioxide levels get too great, the computer turns on the fans to remove the heavy concentrations. Without ventilation, or if wind conditions are calm outside of storage buildings, accumulations can easily reach unfavorable levels of 4 to 6 percent. Conversely, windspeeds exceeding 10 mph can remove accumulations and the monitoring system turns off the fans. Computerized monitoring of each bin thus helps provide disease protection and minimize water loss from excessive ventilation.

Both laboratory research and fieldwork in commercial bins are being done in cooperation with the Minnesota and North Dakota Agricultural Experiment Stations and the Red River Valley Potato Growers' Association.—By **Linda Cooke-Stinson,** ARS.

Jerry L. Varns and Lewis A. Schaper are in the USDA-ARS Red River Valley Potato Research Laboratory, P.O. Box 113, East Grand Forks, MN 56721.

(214) 773-2473

Above: Biochemist Jerry Varns evaluates potato storage environment by computerized monitoring of windspeed, temperature, relative humidity, and gases released by potatoes.

energygram

Potential Agricultural Impacts of Large-Scale Biomass Production

DOE/TIC/EG-86/151
OFFICE OF SCIENTIFIC AND TECHNICAL INFORMATION

This technical note was based on research conducted by Argonne National Laboratory for the U.S. Department of Energy.

Argonne National Laboratory

The long-run potential costs of producing up to 11 quads of biomass energy and the effects of biomass production on conventional agriculture in the United States have been investigated. The report presents the results of the investigation.

A national, interregional, linear programming model of the U.S. agricultural sector, adapted to the year 2000, was used.

The report presents a detailed discussion and analysis of the impacts of large-scale biomass production on all aspects of agriculture. Among the conclusions reached are:

(1) Adequate land resources exist for producing 11 quads of energy from biomass while simultaneously meeting projected food demands.

(2) The increases in the cost of producing conventional crops and livestock which are the result of biomass production are significant and at certain levels of biomass production may be greater than the direct costs of producing biomass.

(3) Higher yielding biomass species, even if their direct production costs are lower than lower-yielding biomass species, may be more costly to grow.

(4) Increases in soil loss may be large and in an unacceptable range.

(5) There are advantages to developing region-specific species of biomass crops.

(6) Lower levels of biomass production can be achieved with reasonable costs.

FOR ADDITIONAL INFORMATION

Reference(s):
A. F. Turhollow, Jr., Sinyan Shen, G. E. Oamek, and E. O. Heady, The Potential Impacts of Large-Scale Biomass Production on U.S. Agriculture, May 1985.

For program-related information, contact:
Sinyan Shen
Argonne National Laboratory
9700 South Cass Avenue
Argonne, IL 60439
Telephone No.: (312) 972-6276

energygram

Uniform Cost-Estimation Method for Biomass Production and Conversion Technologies

DOE/TIC/EG-86/152
OFFICE OF SCIENTIFIC AND TECHNICAL INFORMATION

This technical note was based on research conducted by Argonne National Laboratory for the U.S. Department of Energy.

Argonne National Laboratory

A uniform cost-estimating and reporting method for all biomass production and conversion technologies has been developed. The report summarizes the procedure and provides worksheets with full instructions along with three sets of worked examples.

The cost-estimating method has been designed to meet the following general requirements:

(1) It does not impose an onerous burden on researchers supplying data.

(2) It uses only conventions and assumptions that are generally accepted by industrial users and by Biomass Energy Technology Division program participants.

(3) It is equally applicable to biomass production technologies and conversion technologies and allows them to be compared with energy production technologies based on other resources.

(4) It takes into account the effects of economies of scale.

(5) It is sufficiently flexible to incorporate different assumptions concerning industrial financial criteria, financing methods, tax structures, responses to risk and uncertainty, and other unanticipated factors.

(6) It enables results to be reported in the form of ranges reflecting uncertainties in the estimates.

Application of this uniform cost-estimating method will aid in:

(1) Identifying research and development needs and priorities by pinpointing high cost areas.

(2) Establishing research goals by translating improved performance into cost reductions.

(3) Assessing program performance by measuring product cost.

(4) Comparing investments in biomass technologies with investments in other energy technologies.

(5) Analyzing the effects on the cost of biomass technologies of changes in federal energy policies.

The method should not be used as a substitute for detailed engineering cost estimates since it uses average default values and simplified tax and accounting assumptions, but it can be used to compare commercial and developing technologies on a consistent basis.

FOR ADDITIONAL INFORMATION

DOE report(s):
Uniform Cost-Estimation Method for Biomass Production and Conversion Technologies.
Report number: ANL/CNSV-TM-128/NAB
Order number: DE85011714/NAB
Price: $11.95

Order from:
National Technical Information Service
5285 Port Royal Road
Springfield, VA 22161

For program-related information, contact:
Sinyan Shen
Argonne National Laboratory
9700 South Cass Avenue
Argonne, IL 60439
Telephone No.: (312) 972-6276

United States Department of Agriculture

Research Technology
Agricultural Research Service

Animal Electronics Make Cows Bionic Bovines

Farmers and ranchers may soon electronically monitor their livestock just as routinely as computers now monitor engine functions in some modern automobiles.

Already, some dairy farmers have installed computer-controlled devices that automatically meter feed to cows based on their individual milk production records. This ensures that high-producing cows get more feed than low-producing ones.

Roger J. Gerrits, National Program Director for Animal Production and Protection, USDA Agricultural Research Service, Beltsville, MD, says, "Scientists and commercial firms are currently developing and testing several devices for research or use on farms or in animal- and food-processing plants. The sensing and imaging technology has moved very rapidly in the last 10 years. Many devices have been developed for diagnosis and early detection of human diseases, and several of these are now available for animal research at considerably reduced cost."

"Electronic sensors are being used to measure animal weight, carcass composition, body temperature, and fertility. We will see tremendous progress in the next 5 years in the use of sensing technology for animal identification, diagnosis or detection of diseased tissue, and the refinement of current methods that will permit electronic analysis of meat. Commercial animal- and food-processing plants will use the technology to identify quality and composition of meat."

For consumers, the new technology will ensure the quality and safety of meat products.

For producers, the technology will mean an equitable price for the delivery of high-quality products and will reduce cost of production. For example, electronic monitoring of livestock may cut losses farmers now experience due to late detection of illnesses.

Also, electronic sensors can measure an animal's weight gain from miles away. For the beef producer, rapid weight gain is of paramount economic importance. Farmers and ranchers who know which animals are lagging behind others can take steps to treat them if they are sick or cull them from the herd if they are inferior producers. Not only would culling eliminate inefficient gainers, it would help ensure that only superior genetics pass to the next generation.

But weighing livestock, especially on open ranges, is time consuming and expensive. Cattle have to be herded into pens and driven onto scales. The extra handling upsets livestock and can disrupt a research project.

In May 1986, ARS scientists at Miles City, MT, started testing an electronic system that automatically weighs cattle every time they come for water.

When a thirsty cow enters a small enclosure containing a water basin at the opposite end, she breaks a light beam. Much like the door operation in some grocery stores, the beam controls a gate that shuts automatically behind her. Once she is locked in the stall leisurely drinking water, the electronics go to work.

Each cow has a donut-shaped ear tag about the size and thickness of three stacked quarters. As she lowers her head to drink, the ear tag comes close to a box that emits low-level microwaves. This energy bombards the ear tag, bringing to life a miniature radio transmitter inside that broadcasts her identification number. After this ID is verified by a microcomputer, the time and date are recorded and measuring begins.

The bottom of the stall is a scale. The cow's weight is read electronically 30,000 times a second. An average of these weights, computed each second, eliminates variations caused by the cow jostling around—something similar to weight differences people can get by shifting their bodies on bathroom scales.

Other devices measure volume and weight of water each cow drinks. When the cow has finished, she starts to back out of the stall, breaking another light beam that triggers the release mechanism on the privacy gate. She returns to her pasture, and the

microcomputer calibrates the scale, setting it to read zero just before the next cow enters. This eliminates errors that might occur if cows track in mud or defecate. The scale also has heating coils to keep snow or ice from accumulating in cold weather.

Researchers, 5 miles away in an office at the Fort Keogh Livestock and Range Research Station, receive the data via radio. A computer stores this data for analysis and gives information on how individual animals are faring on the range as well as overall herd performance.

Bradford W. Knapp, a statistician at the research station says, "We use repeaters that pick up the electronic signals from our seven scales, amplify their intensity, and boost them over hills that make line-of-sight transmission impossible. With more repeaters, we could collect information from the very edges of our 55,000-acre experimental ranch—some 8 miles distant."

"Our system is 'water driven,' meaning the cow's reward for entering the stall is a drink. It can be modified so the treat is a feed supplement when the research requires it," says Don C. Adams, a range nutrition scientist.

Weights are not the only bovine secrets being exposed by ARS electronic surveillance—implanted electronic sensors have proven more than 90 percent accurate in detecting when cows are ready for mating.

The sensors also predict when cows will give birth. This will help cut cow and calf deaths. If farmers know when the calf is due, they can be present to assist in difficult deliveries.

In Maryland at the Beltsville Agricultural Research Center, biomedical engineer Alan Marc Lefcourt says, "The key to these sensors' operation is resistance of reproductive tissue to small electrical pulses, about one-twelfth of the 5-milliamp current used in most human heart pacemakers. When a cow is in heat, these tissues swell with water, making them less resistant to the current. This information is relayed electronically to a recording device."

The sensors and monitoring electronics, if commercially mass-produced, coupled with a standard computer, shouldn't cost the farmer more than $30 per cow per year. The equipment cost is minimal compared with the expense of feeding an unproductive dairy cow 21 more days (the length of the estrous cycle) for each breeding time missed—and paying another breeding fee.

In Ames, IA, at the National Animal Disease Center, electronic engineer Joseph L. Riley has a sensor and radio transmitter to check stomach wall movements or contractions in cattle.

Riley says, "The unit is encased in a capsule small enough to be placed in the rumen through a stomach tube. It will broadcast readings on the rumen's response to feed toxins or to diseases for about 2 months, depending on the life of the batteries."

Animal electronic sensors coupled with computer technology have been largely research tools in the study of animal physiology and behavior to date, but the information gained will lead to practical uses for farmers and ranchers in the future.

Roger J. Gerrits is on the USDA-ARS National Program Staff, Bldg. 005, Beltsville Agricultural Research Center-West, Beltsville, MD 20705.

(301) 344-3066

Computers

623 Natural Language Processing: A Tutorial

624 An Integrated Fault Tree Environment

625 Optical Interferometric Parallel Data Processor—Image data would be processed much faster than in present electronic systems.

626 Parallel Analog-to-Digital Image Processor—Compact circuitry performs conversions.

Software

627 Program Assesses Software Reliability During its Testing

Natural Language Processing: A Tutorial

A special report was prepared by the Rome Air Development Center to serve as an entry level, practical guide to research in the field of Natural Language processing by computer. Its design and composition are meant to provide a good basis for further study and practice in the field. The first section defines the varied goals of researchers involved in producing computer programs that process Natural Language and attemps to provide a feeling for the full challenge of the task by outlining the problems that require solution.

As a subfield of Artificial Intelligence (AI), describing Natural Language processing often requires a subset of the terminology of AI, a section of this report defines members of that subset in the context of the Natural Language processing task.

Various schemes for categorizing approaches to processing Natural Language exist. The most referenced scheme, from Terry Winograd's influential book Understanding Natural Language [Winograd; 1972], partitions approaches into four groups based on their representation and use of knowledge: "special format" systems were the early, keyword and pattern matching systems, "text-based" systems had a prestored text and indexing schemes to retrieve pertinent data, "limited-logic" systems were those whose databases were stored in some formal notation and which retrieved information using simple logical inferences, and lastly, "general deductive" systems were those using a uniform notation for representing problems and knowledge. This report divides Natural Language technologies, basically, into 'linguistics-based' and alternative approaches. Methods are described which are primarily derived from Linguistic theories. The last section describes research into alternative approaches: simple pattern matching systems, and more complex systems which attempt to work from, and develop, representations of meaning.

Appendices include a glossary of field-related terms. For each term, an index directs the reader to an explanation of the term in the report. The names of computer systems used in the report as examples of concepts are also listed in the glossary, each with page numbers of where the system is mentioned. None of the systems are described in detail. The first mention of any system includes a reference to a source for more in-depth information.

Examples of concepts in the text are meant to demonstrate concept "basics": they may, or may not, be wholly descriptive of those concepts. Many examples have been taken directly (or with modifications for simplification) from previously published work. References are provided.

FOR ADDITIONAL INFORMATION: A copy of the report is available from NTIS, Springfield, VA 22161; (703) 487-4600.
NTIS order number: AD-A173386/NAC
Price code: A05

energygram

An Integrated Fault Tree Environment

DOE/TIC/EG-86/160
OFFICE OF SCIENTIFIC AND TECHNICAL INFORMATION

This technical note was based on research conducted by Idaho National Engineering Laboratory for the U.S. Department of Energy.

INEL
Idaho National Engineering Laboratory

The Integrated Fault Tree Environment (IFTREE) is an interactive, graphics-based tool for fault tree design. This report presents the design philosophy of IFTREE.

Probabilistic Risk Assessment (PRA) techniques are used to perform safety analyses of complex defense-in-depth systems. A major effort in PRA development is fault tree construction. IFTREE uses a unique rule-based solution algorithm founded in artificial intelligence (AI) techniques. IFTREE has been developed to handle the design and maintenance of full-size living PRAs and is currently in use at Idaho National Engineering Laboratory.

IFTREE provides integrated building, editing, and analysis features on a personal workstation. The impact of the AI approach on the program design is stressed.

This code is applicable to all risk-based safety assessments.

FOR ADDITIONAL INFORMATION

DOE report(s):
An Integrated Fault Tree Development Environment.
Report number: EGG-M-05086/NAB
Order number: DE87000474/NAB
Price: $9.95

Order from:
National Technical Information Service
5285 Port Royal Road
Springfield, VA 22161

For additional information, contact:
Brent W. Dixon
EG&G Idaho, Inc.
P.O. Box 1625
Idaho Falls, ID 83415
Telephone No.: (208) 526-0717

or

J. M. Welch
EG&G Idaho, Inc.
P.O. Box 1625
Idaho Falls, ID 83415
Telephone No.: (208) 526-8318

NASA Tech Brief
National Aeronautics and Space Administration
NASA's Jet Propulsion Laboratory, Pasadena, California

Optical Interferometric Parallel Data Processor

Image data would be processed much faster than in present electronic systems.

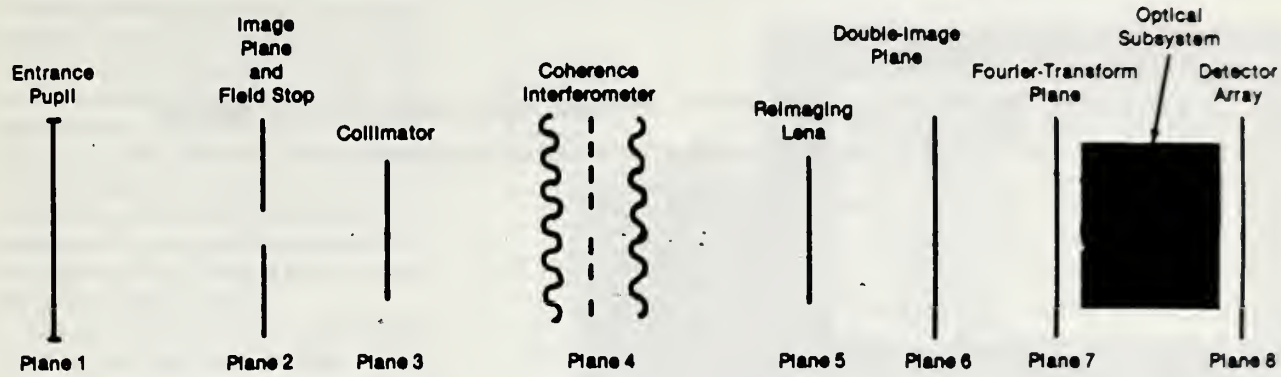

Figure 1. The Optical Parallel-Processing System would effectively calculate two-dimensional Fourier transforms in the time required by light to travel from plane 1 to plane 8.

A conceptual optical data-processing system would achieve throughputs as high as 4×10^{15} bits per second. This high computing speed is due to the inherently parallel nature of processing in an imaging system and to the short processing time, which equals the time required by light to travel through the system.

Figure 1 depicts the overall optical configuration. Plane 1 represents the entrance pupil of a foreoptic system (for example, a camera lens) that focuses light from the object into an image through a field stop at plane 2. A lens system at plane 3 collimates the light from the image at plane 2 and images the pupil of plane 1 into a coherence interferometer at plane 4.

The coherence interferometer is a specially-shaped beam-splitting prism similar to a type that has been used in optical, astronomical, and atmospheric research for more than 10 years. Essentially, this interferometer enables the system to perform the two-dimensional white-light spatial-frequency Fourier transform of the image. It splits the light energy into two parts corresponding to

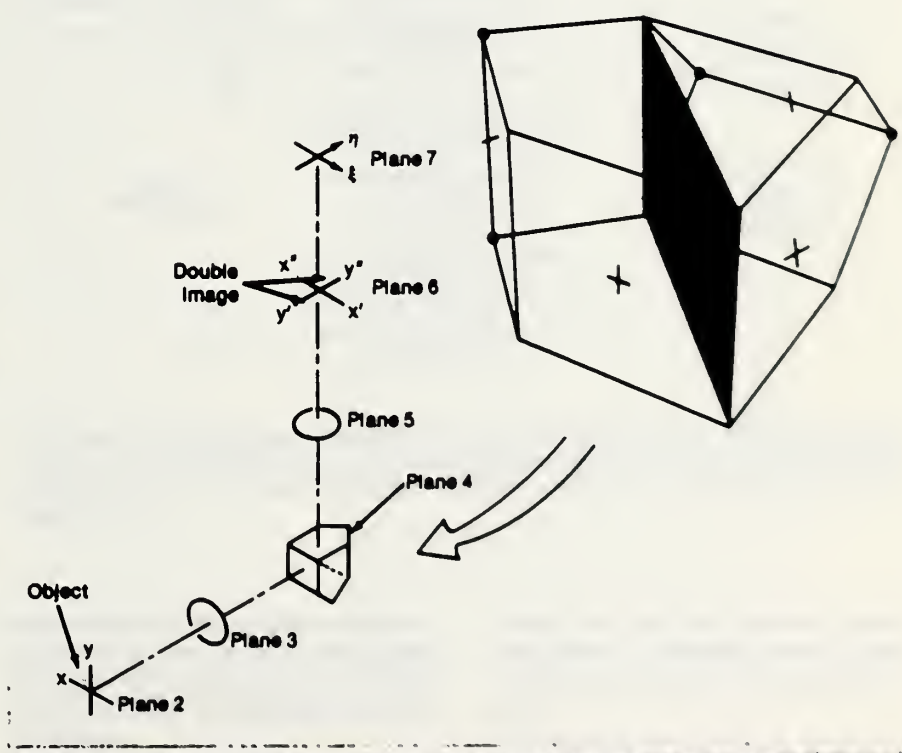

Figure 2. The Coherence Interferometer at plane 4 splits the light into parts that would form a double image at plane 6 if a projection screen were to be placed there.

images that are inverted with respect to each other and located at opposite points with respect to the optical center line (see Figure 2).

The lens at plane 5 relays the interferometer output to plane 6, where the double images are actually formed and could be seen if a screen were to be placed there. However, there is no screen at 6; instead, the light is allowed to travel to plane 7.

Although the white light from different points on each of the double images is not coherent, the light from the two points corresponding to the same point of origin on the object is coherent. Thus, the electromagnetic fields radiating from the two images are correlated and form white-light interference fringes at plane 7. The spatial dependence of light intensity at this plane includes a uniform component plus a component proportional to the cosine Fourier transform of the white-light scene at plane 2.

A programmable spatial amplitude or phase filter or both would be placed at plane 7 to modulate spatially the Fourier transform with the transform of a function to be convolved with the image data. An optical subsystem would re-transform the filter output, forming a final two-dimensional correlation signal on plane 8. A detector array of charge-coupled devices would receive this signal and pass it to image- or data-processing circuitry.

This work was done by James B. Breckinridge of Caltech for **NASA's Jet Propulsion Laboratory.**
NPO-16382 /TN

FOR ADDITIONAL INFORMATION: *Contact: Director, Technology Transfer Division, P.O. Box 8757, BWI Airport, MD. 21240; (301) 621-0100 Ext. 241*
REFER TO THE NUMBER LISTED AT THE END OF THE ARTICLE

NASA Tech Brief
National Aeronautics and Space Administration
Goddard Space Flight Center, Greenbelt, Maryland

Parallel Analog-to-Digital Image Processor

Compact circuitry performs conversions.

A proposed integrated-circuit network of many identical units would convert the analog outputs of imaging arrays of x-ray or infrared detectors to digital outputs. The converter would be located near the imaging detectors, within the cryogenic detector package. Because the converter output would be digital, it would lend itself well to multiplexing and to postprocessing for correction of the gain and offset errors peculiar to each picture element and its sampling and conversion circuits.

The conceptual processor (see figure) could include a primitive amplifier for the detector of each picture element. Alternatively, groups of detectors could be multiplexed to a smaller number of amplifiers to reduce the size of the processor. In either case, each amplified detector output is fed to an associated track-and-hold circuit, which charges a capacitor to a voltage representing the detector signal.

The analog-to-digital conversion is performed by using one digital-to-analog converter (D/A) common to all of the processors and external to the cryogenic chamber. A goal is to make each pixel converter as simple and small in integrated-circuit space as possible near the focal plane. Using high-speed silicon-gate CMOS technology operating at multimegacycle rates for digital counters, voltage-to-time conversions are performed for each detector or group of detectors. The sample is held as a voltage on a capacitor referenced to the most negative voltage in the range of the converter. Then the capacitor is ramped from the most positive voltage linearly downward using the D/A, and each pixel counter counts time until the pixel comparator stops the counting. These digital results are read out serially. A megahertz clock rate could perform 8-bit conversions in about 0.3 ms and 16-bit conversions in 75 ms. The ramp technique minimizes differential nonlinearity that is important to many detectors such as x-ray and infrared imaging.

Because such detectors have large voltage "read noise" offsets, previously estimated offset corrections can be preset into the counters by shifting offset values into the digital registers as readouts are being shifted out of the focal plane. The dynamic range required of the digital logic can then be reduced.

The combined offset and gain errors for each picture element and its following circuits can be measured in a calibration run, stored in digital memories, then applied as corrections to the raw converter outputs. Input offsets and adaptive control signals can also be fed directly into the detector array.

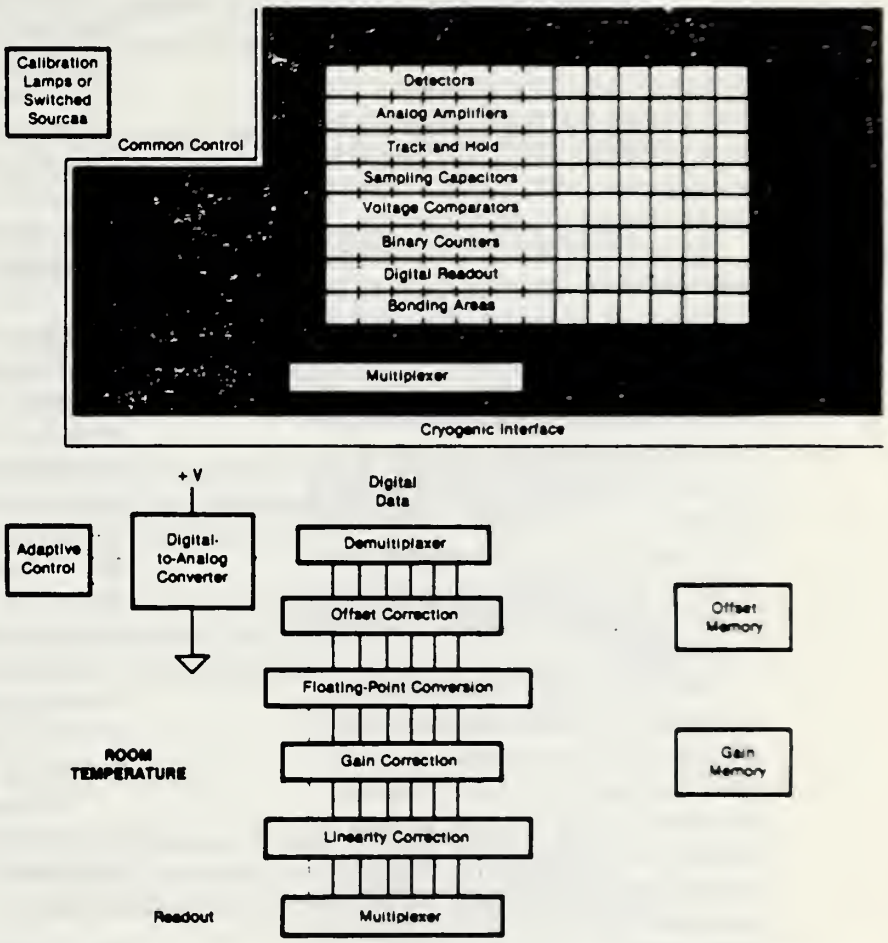

The Analog-to-Digital Image Processor is a massively parallel system for processing data from an array of photodetectors. The system could be built as a compact integrated circuit located near the focal plane. The buffer amplifier for each picture element can have a different offset.

This work was done by Donald C. Lokerson of **Goddard Space Flight Center**. *GSC-12898 /TN*

FOR ADDITIONAL INFORMATION: *Contact: Director, Technology Transfer Division, P.O. Box 8757, BWI Airport, MD. 21240; (301) 621-0100 Ext. 241*
REFER TO THE NUMBER LISTED AT THE END OF THE ARTICLE

Program Assesses Software Reliability During its Testing

With the rapid growth of computer software, a demand to produce software that is cost-effective and reliable has increased.

Researchers at the Naval Surface Weapons Center have developed a computer program that rapidly assesses a program's reliability during the testing phase and determines when a piece of software can be released for operational use.

The new interactive computer program called SMERFS, Statistical Modeling and Estimation of Reliability Functions for Software, allows a user to enter a set of data, modify it if necessary, fit an appropriate model, and determine the adequacy of the fitted model. SMERFS will run on any computer system that has a Fortran IV or V compiler, with some minor modifications. Two versions of the program are available for a VAX or Cyber computer system, with no modifications.

The computer program allows the user to perform a complete software reliability analysis using any of eight well-known models appearing in its documentation. The chosen model can then be used to estimate such parameters as the number of remaining software errors in the code, the expected number of errors in the next testing period, and the length of time to remove the remaining number of errors.

Studies have been undertaken to compare the performance behavior among the various models; however, no one model has demonstrated itself superior, and no one model can be advocated for all applications. The procedure includes selecting a candidate model, estimating the parameters of the model, testing the adequacy of the model, and then cycling back if necessary.

Data regarding past error discoveries have been used in many different models to estimate various measures of reliability. Reliability is measured by the total number of errors and expected time until the next error. By having a quantitative measure of a program's reliability, a software manager can best determine the allocation of testing personnel and just how much testing to employ before release to the user.

Three major approaches to estimating reliability are: error seeding/tagging, data domain, and time domain. The error seeding/tagging approach uses the concept of error introduction into software. Based upon the number of inserted errors and inherent errors found in the testing phase, the total number of errors still residing in the program can be estimated.

The data domain approach bases the reliability estimation on the number of successful execution runs out of the total number of runs attempted.

The time domain approach is what is captured in the SMERFS program, as all eight models model the error generation process.

For Additional Information:

Backup material on this effort is available from:

Navy Domestic Technology Fact Sheet
Reader Reply Service
Code E211
Naval Surface Weapons Center
Dahlgren, VA 22448-5000
(703) 663-8921

Refer to 120104/TN

Electrotechnology

629 Optical-Data Processing With Liquid-Crystal TV—Even in its present state of development, this miniature flat-screen television can be used for pattern recognition.

630 Small-Screen Displays—A literature search examines size, protocols, abbreviations, and vocabulary.

631 Better Radiation-Hardened Memory Chips Possible—Computer model predicts how much radiation can be withstood.

632 Tape Interconnect Materials and Processes for Military Electronic Packages

633 Millimeter-Wave Traveling-Wave-Tubes Circuits Produced at Reduced Costs

634 Designing High-Frequency Inductors—Procedures for both ferrite-core and Molypermalloy-core inductors are detailed.

635 CMOS Clock Synchronizer—A circuit synchronizes clock and gate signals within one-quarter of a clock cycle. (Licensing Opportunity)

636 Two-Layer, Full-Color Electroluminescent Display—A matrix-addressed, flat-panel display features increased resolution, brightness, and contrast. (Licensing Opportunity)

Testing & Instrumentation

637 Double-Referenced, Pulsed, Phase-Locked Loop—DRP2L2—The phase shift between two tone-burst signals is measured precisely. (Licensing Opportunity)

Other items of interest

622 Animal Electronics Make Cows Bionic Bovines

679 New Anisotropic Ceramic-Air Composites Improve the Strength and Operational Capability of Ceramic Electronic Devices

MANUFACTURING TECHNOLOGY NOTE

U.S. ARMY MATERIEL COMMAND

Deputy Chief of Staff for Manufacturing Technology, Alexandria, VA

Project Number: NONE

Filing Code: 62D007

Optical-Data Processing With Liquid-Crystal TV

Even in its present state of development, this miniature flat-screen television can be used for pattern recognition.

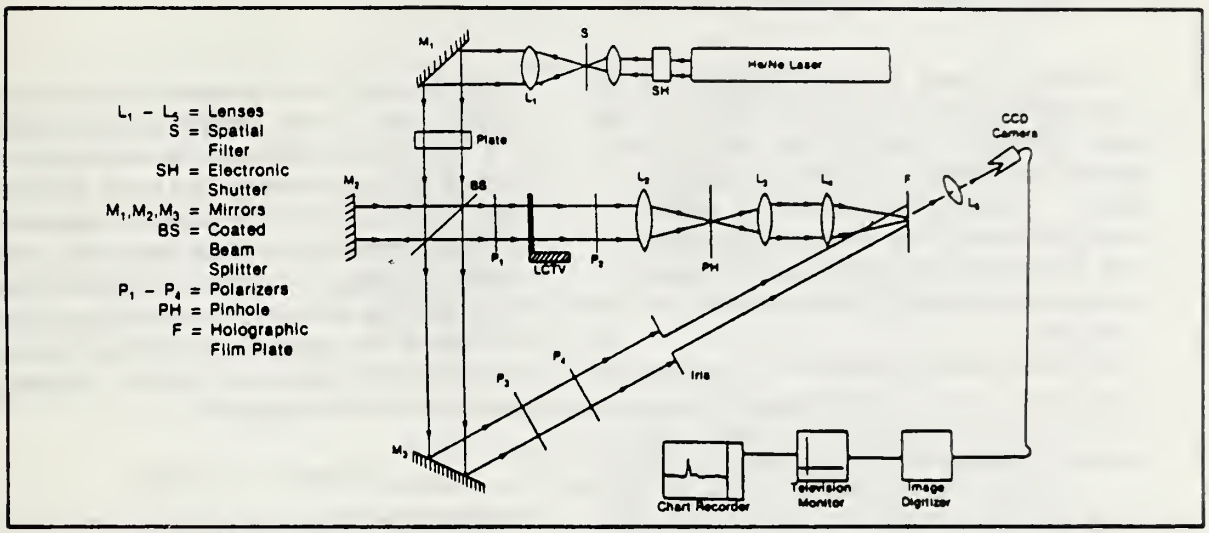

A **Liquid-crystal television** is incorporated in a standard Vander Lugt optical correlator. The pinhole helps to reduce the effects of the LCTV electrode grid structure on the image. The focal length and pinhole size are chosen to retain much of the higher frequencies in the image.

A commercially available flat-screen liquid-crystal television (LCTV) has been slightly modified and used as a spatial light modulator in a Vander Lugt-type optical correlator. The LCTV is inexpensive and small, costing about $100, with a screen measurement of 54 by 40.4 millimeters. It was used as a replacement for extremely expensive modulators normally employed in optical-data processing, such as liquid-crystal light valves and magneto-optic devices. The results of the experiment by the U.S. Army Missile Command show that the resolution, contrast, and speed of the LCTV in its present form are sufficient for basic real-time pattern recognition in certain applications.

The setup was the standard optical correlator used in many optical-data processing experiments, except for the addition of the LCTV (see figure). A prefiltering aperture was also included to remove the high spatial frequencies associated with the pixel grid structure of the LCTV.

The LCTV was modified by replacing original polarizers with external high-quality polarizers. The contrast of the resulting coherent image was greatly improved. The LCTV was addressed by a remote video camera through the video-input plug provided on the device. The standard television camera also allowed the option of radio-frequency addressing from an external transmitter. The LCTV may also be used as a monitor for most small computers. This option allows computer-generated images to be used for making Fourier-transform matched filters or for addressing such filters.

Project officer Don A. Gregory
(205) 876-2604 or AV 746-2604.

FOR ADDITIONAL INFORMATION:

You can learn more details about this technology by ordering the NTIS report:
Real-Time Pattern Recognition Using a Modified Liquid Crystal Television in a Coherent Optical Correlator.
Order number: AD-A168042/NAA
Price code: A02

Order from:
National Technical Information Service
5285 Port Royal Road
Springfield, VA 22161

This document was prepared under the sponsorship of the U.S. Government. Neither the United States Government nor any person acting on behalf of the United States Government assumes any liability resulting from the use of the information contained in this document, or warrants that such use will be free from privately owned rights.

MANUFACTURING TECHNOLOGY NOTE

U.S. ARMY MATERIEL COMMAND

Deputy Chief of Staff for Manufacturing Technology, Alexandria, VA

Project Number: NONE

Filing Code: 62B114

Small-Screen Displays

A literature search examines size, protocols, abbreviations, and vocabulary.

A report reviews literature pertinent to the human-performance aspects of small-screen displays. The report, prepared for the U.S. Army Human Engineering Laboratory, focuses on four topics: (1) display size, defined as number of characters per number of lines; (2) protocols, defined as ways users interact with a system to achieve their goals; (3) abbreviations; and (4) vocabulary.

For the purposes of the report, any screen displaying fewer than 80 characters per line and 24 lines per screen is considered a small screen. A representative sample of documentation pertaining to the use of small-screen displays on computers was obtained from academic and professional journals, computer-aided listing services, and contacts with human-factors consultants.

Overall, research pertaining to the relationship between human performance and the size of small-screen displays is sparse. Much of the material is very recent, indicating that the topic is under ongoing research that has not yet been published.

The literature review revealed a large number of articles about human performance and vocabulary. The research indicated that vocabulary is as broad a topic as protocols; as a result, vocabulary was investigated within several frameworks. Studies addressing command languages, menus, natural language, and icons contributed relevant but diverse results to the topic of vocabulary. There is a void in the research concerning vocabulary schemes for small-screen displays, indicating a need for further investigation.

FOR ADDITIONAL INFORMATION:

You can learn more details about this technology by ordering the NTIS report(s):
Human Performance Aspects of Small-Screen Displays:
A Literature Review Revealing the Lack of Specific Research.
Order number: AD-A170660/NAA
Price code: A04
Order from:
National Technical Information Service
5285 Port Royal Road
Springfield, VA 22161

This document was prepared under the sponsorship of the U.S. Government. Neither the United States Government nor any person acting on behalf of the United States Government assumes any liability resulting from the use of the information contained in this document, or warrants that such use will be free from privately owned rights.

Better Radiation-Hardened Memory Chips Possible

Computer model predicts how much radiation can be withstood.

Microelectronics experts at Sandia National Laboratories have developed a computer model that accurately predicts how much radiation their one-of-a-kind semiconductor memory chip can withstand in a variety of situations before losing its memory.

The chip, which can hold 16,000 bits (binary digits) of information, has a special kind of memory, called non-volatile. It does not require a continuous supply of electricity to retain information programmed into it.

The model, verified by several years of laboratory experiments, will help researchers at Sandia's Center for Radiation-Hardened Microelectronics (CRM) ensure the best possible design and fabrication of new, more advanced radiation-tolerant non-volatile memory chips.

Eliminates lengthy tests

It also frees researchers from having to rely on exhaustive laboratory tests, many lasting several years, to accurately characterize the way these devices react to radiation.

The model shows that CRM's SNOS (polySilicon-Nitride-Oxide-Silicon) semiconductor memory can retain stored information for at least 10 years despite a one-time 500-kilorad (500,000-rad) dose of penetrating radiation. That kind of dose could be received by a spacecraft flying through the Van Allen Belts, or by a satellite that orbits in the belts for about 5 years. A rad is a unit of radiation energy absorption. A whole body dose of about 1,000 rads is typically fatal to humans.

Sandia's 16K part—which measures about a quarter of an inch on a side—is the only non-volatile semiconductor memory capable of operating in highly-radioactive space and weapon environments. Most commercially available non-volatile memories can routinely store information for a decade; however, they would lose it immediately if exposed to even a few rads.

Non-volatile memory chips contain memory cells for each bit of information they hold; each cell consists of an access transistor and a memory transistor. Access transistors allow stored data to be read.

Writing data into a non-volatile memory requires supplying enough voltage (called the write voltage) to set each memory transistor into either the 1 or 0 logic state. Application of a positive voltage produces a 1 by injecting electrons into the transistor's memory layer, a thin silicon nitride insulating film, where they become

trapped. Negative voltage produces a 0 by injecting holes (positively charged void spaces) into the memory layer. It takes several memory transistors—some fixed in the 0 position and some in the 1 position—to store a meaningful piece of information, the letter A, for instance.

These charges do escape from the memory layer slowly over time. The retention period is proportional to the write voltage applied during programming and the length of that application, typically 0.1 to 100 milliseconds. However, exposing an unhardened non-volatile chip to radiation frees a charge almost immediately.

"The need for radiation-hardened non-volatile memories also is becoming more critical," says Bob Gregory, Sandia's Director of Microelectronics. "For example, as satellites become more autonomous, and hence more intelligent, designers need to put large stored computer programs into the spacecraft. This requires considerable use of non-volatile memories."

"This new computer model will help us to optimize process techniques and design geometries for new 16K chips and for a more sophisticated 256K radiation-tolerant non-volatile SNOS memory that we're developing, says Paul McWhorter, of Sandia's Non-Volatile IC Technology Division.

To use the computer model, CRM researchers determine what they call the emission and asymmetry constants for a chip's memory transistors. McWhorter defines emission constant as "the probability that a given electron or hole will escape from the memory layer of a transistor due to a 1-rad exposure." The asymmetry constant is the difference between the probabilities of the memory layer capturing unwanted radiation-induced electrons and holes.

Constants go into equation

"Once these constants are known, we insert them into an equation that a computer solves," McWhorter says. "Its solution tells us what kind of performance to expect following any dose of radiation to the part."

The CRM was established in 1981 for researchers to develop technologies and design capabilities for production of large-scale and very-large-scale integrated circuits capable of operating in high-radiation environments. The Center typically transfers those capabilities to private industry for commercial production.

Radiation hardening, a process perfected during the past 15 years at Sandia, involves fabricating integrated circuits in extremely clean surroundings and chemically and physically altering their electronic structure so that the degrading effects of radiation on the chips are slowed.

A key to development of the radiation-tolerant 16K non-volatile memory was Sandia's decision to use SNOS transistors instead of the typical floating gate variety. SNOS transistors use two insulator layers—one of silicon nitride (the memory layer) and one of silicon dioxide.

FOR ADDITIONAL INFORMATION

Public Information Division,
Code 3161,
Dept. of Energy,
Sandia National Laboratories,
Albuquerque, NM 87185-5800
(505) 844-4207.
Refer to announcement 22, No.1

Tape Interconnect Materials and Processes for Military Electronic Packages

Polymer films have been used for several years in consumer products such as calculators and watches to interconnect the chip to other internal components. However, the introduction of polymeric interconnect materials into military electronic packages and the ability of these materials to meet the test and reliability requirements of MIL-M-38510 have been a concern frequently expressed by tri-service VHSIC review teams.

In the recently completed NAVAIR Manufacturing Technology project A2002 "VHSIC Tape Interconnect Materials and Processes", IBM Federal Systems Division has shown the feasibility of using precision polymeric film decals for high lead count chip-to-package interconnects. In a program of low-volume fabrication and testing, it was proven that tape decal interconnects for 2.0 micron and 1.25 micron VHSIC chip technology could meet the requirements of MIL-M-38510.

Specific objectives of the Manufacturing Technology project were as follows:

1. To perform the materials development and testing necessary to select the optimum interconnect film for use in military hermetic packages. Some of the material properties investigated were film thermal resistance, solvent resistance and moisture absorption as a function of variations in the polymeric cure profile. Process-related properties were also investigated, such as the film's ability to withstand the metallization, pattern personalization, and package assembly processes. Of six films evaluated, a 1- to 2- mil PMDA/ODA Polyimide film was considered the overall optimum decal interconnect material for IBM's specific application.
2. With the resultant materials expertise, develop a materials guideline for widespread industry use, outlining alll acceptance/qualification criteria applicable to interconnect film. The Joint Electronic Device Engineering Committee (JEDEC JC13.0) will publish this guideline as "Test Method for Qualification and Acceptance of Circuit Support Films for Use in Microelectronic Applications."
3. Establish the fabrication, assembly and test processes for a decal flexible-film chip-to-package interconnection capable of meeting MIL-M-38510 requirements. Document these processes in a design specification. This design specification will cover materials, dimensions, mechanical/electrical requirements, assemblytechniques and quality assurance requirements.

This Manufacturing Technology project was sponsored by the Naval Air Systems Command and managed by the Solid State Electronics Division of the Naval Ocean Systems Center.

For Additional Information:

To discuss this effort further, contact:

Mr. Pat Reeves or Mr. W.D. McKeen
Naval Ocean Systems Center
San Diego, CA 92120
(619) 225-2752

Millimeter-Wave Traveling-Wave-Tubes Circuits Produced at Reduced Costs

A manufacturing technology program to establish the manufacturing methods and production capability to produce millimeter-wave TWT (traveling-wave tube) circuits at reduced costs using precision, computer numerical control, diamond turning machines was directed by the Naval Ocean Systems Center.

The goal was achieved and demonstrated with the successful manufacture of twenty prototype parts and three hundred pilot-line production parts.

Detailed inspection verified that part dimensional variations were less than the required ±70 microinches and part-to-part dimensional repeatability was 50 microinches or less. Final acceptability of these precision machined parts was demonstrated in VSWR (voltage standing-wave ratio) testing of RF (radio frequency) circuit sections.

Both the dimensional inspection and RF test results verified the usefulness of this diamond turning production method.

These parts were assembled into RF sections; subsequently the sections were incorporated into an operational traveling wave tube.

For Additional Information:

Backup material on this effort is available from:

Navy Domestic Technology Fact Sheet
Reader Reply Service
Code E211
Naval Surface Weapons Center
Dahlgren, VA 22448-5000
(703) 663-8921

Refer to 111202/TN

NASA Tech Brief
National Aeronautics and
Space Administration

Designing High-Frequency Inductors

Procedures for both ferrite-core and Molypermalloy-core inductors are detailed.

A report presents design procedures for two types of high-frequency inductors: those with iron or ferrite cores and lumped airgaps and those with Molypermalloy powder cores and distributed airgaps. These components, which carry no direct current, are widely used in ferroresonant power regulators, pulse-width-modulation inverters, and other power-processing equipment. They are designed more easily than are dc inductors, using procedures like those for designing transformers. With no dc-generated flux in the core, the design calculations are straightforward. Essentially, the high-frequency ac inductor is designed to support the applied voltage without saturating the core, then the airgap for the proper inductance is calculated.

The report lays the groundwork for the procedures by discussing the two major effects of the inductor airgaps; namely, the increases in the inductance and the power loss due to the fringing flux. For design purposes, the airgap length should be minimized to minimize the fringing flux, thereby maximizing the efficiency. To keep the gap small, the number of turns of wire is kept to a minimum. The number of turns is also minimized to operate the core at the highest possible magnetic-flux density without saturating the core or generating excessive power loss in the core.

The airgap, power handling, and other considerations are represented in the equations for inductor design. The report gives the equations and an 11-step procedure for designing an inductor with a lumper airgap.

Distributed-airgap inductors reduce the losses caused by fringing fluxes. The report presents a design procedure for a toroidal inductor of this type. This procedure is even simpler than that for a lumped-airgap type.

The report concludes with a comparison of the losses among three inductors designed to operate at 20 kHz with a 90-V square wave and a 1.4-A peak-to-peak triangular wave. Two of the inductors had lumped-airgap cores, and one had a distributed-airgap Molypermalloy-powder core. The temperature rise in the distributed-gap core was less than that of the other two.

This work was done by Colonel W. T. McLyman and Albert P. Wagner of Caltech for **NASA's Jet Propulsion Laboratory.**
"Designing High Frequency AC Inductors Using Ferrite and Molypermalloy Cores (MPP)," NPO-16553 /TN

FOR ADDITIONAL INFORMATION: ***Contact: Director, Technology Transfer Division, P.O. Box 8757, BWI Airport, MD. 21240; (301) 621-0100 Ext. 241***
REFER TO THE NUMBER LISTED AT THE END OF THE ARTICLE

NASA Tech Brief
National Aeronautics and Space Administration
Ames Research Center, Moffett Field, California

Licensing Opportunity

CMOS Clock Synchronizer

A circuit synchronizes clock and gate signals within one-quarter of a clock cycle.

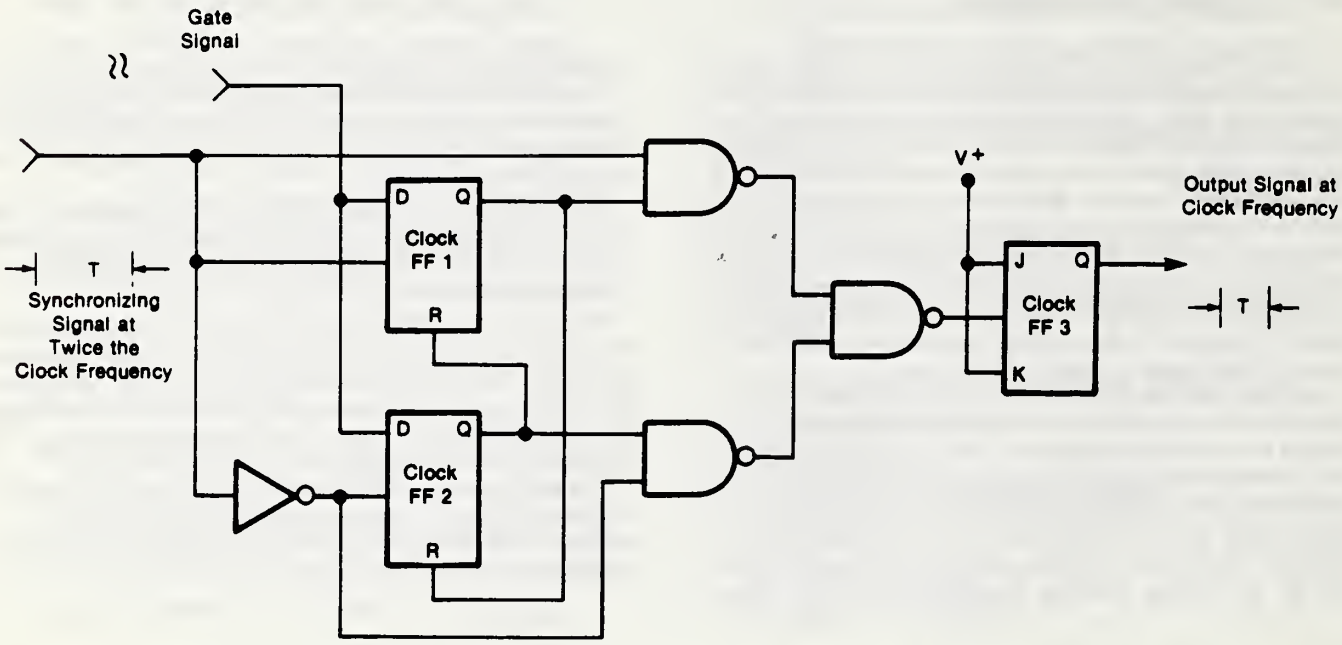

A **Clock Synchronizer** with one-quarter-cycle skew can be constructed from three flip-flops, three NAND gates, and an inverter. In addition to the gate signal to which the clock is to be synchronized, the circuit requires a square-wave input at twice the desired clock frequency.

A simple circuit develops a clock signal synchronized with an external gate signal, with a maximum skew of one-quarter of a clock cycle; yet it requires a synchronizing square wave of only twice the designated clock frequency. To effect the same maximum skew, previous circuits required synchronizing signals four times the clock frequency. The relatively low synchronizing frequency of complementary metal oxide/semiconductor (CMOS) circuits must be severely derated.

The circuit was originally developed for use in a dual-slope analog-to-digital converter. In such a converter, if the clock signal is simply gated without synchronization, the skew between the gate and clock signals can result in up to a 1-bit error in the converter output. With a one-quarter-cycle synchronization, the error from this source is reduced to one-quarter of a bit or less, provided that clock symmetry is good.

The new circuit (see figure) achieves its low skew by synchronizing an output clock with either the leading or the trailing edge of an input clock-signal pulse, whichever occurs first after the gate signal: the input clock signal is applied directly to flip flop FF_1 and, via an inverter, to FF_2. Thus either FF_1 is set by the next active edge of the input clock or FF_2 is set by the complement of the edge, whichever occurs first. The next active edge occurs within a one-half cycle of the synchronizing signal, which is one-quarter cycle of the designated clock signal.

The first FF to be set inhibits the other. Depending on the resulting settings of FF_1 and FF_2, the signal applied to the clock input of FF_3 is either the synchronizing signal or its complement. FF_3 acts as a divide-by-2 circuit to produce an output clock signal at one-half the synchronizing frequency.

This work was done by Robert B. Kepp of Martin Marietta Corp. for **Ames Research Center.**

Inquiries concerning rights for the commercial use of this invention should be addressed to the Patent Counsel, Ames Research Center Refer to ARC-11692 /TN

Ames Research Center
Technology Utilization Officer:
Laurance A. Milov
Mail Code 204-10
Moffett Field, CA 94035
(415) 694-5761
Patent Counsel:
Darrell G. Brekke
Mail Code 200-11
Moffett Field, CA 94035
(415) 694-5104

NASA Tech Brief
National Aeronautics and Space Administration
Langley Research Center, Hampton, Virginia

Licensing Opportunity

Two-Layer, Full-Color Electroluminescent Display

A matrix-addressed, flat-panel display features increased resolution, brightness, and contrast.

A full-color, matrix-addressed electroluminescent display uses three different color phosphors located in two separate, superimposed layers to provide higher brightness, better contrast ratio, and higher resolution than those of previous designs. This design can be used for such transparent, flat-panel display media as thin-film electroluminescent phosphors, liquid crystals, or light-emitting diodes.

Matrix-addressed, flat-panel displays are rapidly gaining acceptance as computer terminal displays and as instrument displays in automobiles and in aircraft cockpits. To compete with cathode-ray tubes in more than limited applications, flat-panel displays must be offered in full color. Full-color displays require the use and control of the three primary colors: red, blue, and green. The best available red, blue, and green phosphors for thin-film electroluminescence differ from each other in maximum brightness, the green phosphor being ten times brighter than the red. In a typical color display, the brightness of the display is limited by the brightness of the weakest color phosphor.

In this new design, the area of one of the phosphor dots is twice the area of either of the other two. If the dimmest phosphor is used for the large dot, the display can be twice as bright as in designs where all dots are of equal area. Additionally, the new two-layer design increases the resolution by 50 percent over that of single-layer designs, requires roughly one-third fewer interfaces, and creates less undesirable capacitance than do present three-layer designs.

The device is constructed by consecutive deposition of materials onto a transparent glass substrate to form the following layers (see figure):

- A transparent front column of electrodes,
- An insulating layer,
- An electroluminescent phosphor of color A,
- An insulating layer,

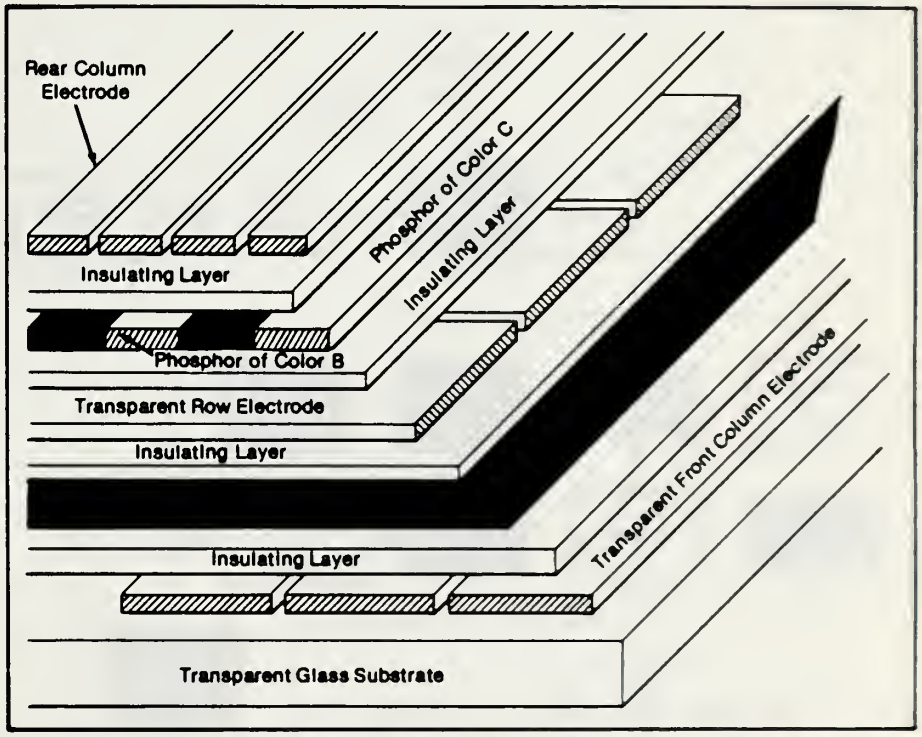

The Combination of Side-By-Side and Stacked-Layer Designs increases resolution and brightness in electroluminescent display panels.

- A transparent row of electrodes oriented perpendicularly to the column electrodes,
- A third insulating layer,
- Alternating side-by-side stripes of phosphors of color B and of color C oriented in parallel with the front column electrodes (the distance between centers of these stripes being one-half the distance between centers of the front column electrodes),
- A fourth insulating layer,
- A rear column of electrodes oriented in parallel with the phosphor stripes, with one electrode superimposed over each of these stripes, and

A passive layer or glass seal may be applied over the rear column of electrodes.

The design can be used with or without insulating layers between the electrodes and the display material. The layers of material deposited on the glass substrate may be deposited in reverse order, placing phosphors B and C in front of phosphor A as viewed from the glass substrate. The rear column electrodes may be reflective, transparent, or light absorbing. This combination of a partially side-by-side design with a partially stacked-layer design produces a flat-panel, full-color display that combines improved resolution, brightness, and contrast ratio with simplified fabrication.

This work was done by James B. Robertson of **Langley Research Center**. *No further documentation is available.*

This invention is owned by NASA, and a patent application has been filed. Inquiries concerning nonexclusive or exclusive license for its commercial development

should be addressed to the Patent Counsel, Langley Research Center Refer to LAR-13407 /TN

Langley Research Center
Technology Utilization Officer:
John Samos
Mail Stop 139A
Hampton, VA 23665
(804) 865-3281

Patent Counsel:
Howard J. Osborn
Mail Code 279
Hampton, VA 23665
(804) 865-3725

FOR ADDITIONAL INFORMATION: *Contact: Director, Technology Transfer Division, P.O. Box 8757, BWI Airport, MD. 21240; (301) 621-0100 Ext. 241*
REFER TO THE NUMBER LISTED AT THE END OF THE ARTICLE

NASA Tech Brief
National Aeronautics and Space Administration
Langley Research Center, Hampton, Virginia

Licensing Opportunity

Double-Referenced, Pulsed, Phase-Locked Loop — DRP^{2}L^2

The phase shift between two tone-burst signals is measured precisely.

The DRP^{2}L^2 system allows a precise measurement of the phase shift between two tone-burst signals initially derived from the same periodic source but delayed by different amounts through either path-length differences, propagation-velocity differences, or both. For example, the system can be used to measure accurately the phase shift encountered by an acoustic wave striking the front and back surfaces of a sample. With velocity known, the resulting measurement would be of sample thickness. With thickness known, the measurement would be of sound velocity. The technique applies to many sources of radiation and is not limited to acoustics.

The DRP^{2}L^2 has one leg similar in design to the pulsed, phase-locked loop, P^{2}L^2 (see figure). A voltage-controlled oscillator drives a gate/amplifier, which is turned on for several cycles by countdown-and-timing logic circuit 1. The gate/amplifier generates a tone burst exciting, for example, a first acoustic transducer. The sound wave propagates in the sample and is received at a second transducer, or as shown, at the first transducer.

The output of the second transducer is amplified/peak limited and split into two signals. One signal goes to phase detector 1, which receives its reference from the voltage-controlled oscillator through an electronically adjustable phase shifter. The signal from phase detector 1 goes through low-pass filter 1 to sample/hold module 1, which gets its logic signal from countdown-and-timing logic circuit 1. The output of sample/hold module 1 goes to integrator 1, the output of which is fed back to control the frequency of the oscillator.

If there is a propagation delay — for example, a water path between the sample and the second transducer — it will be included in the P^{2}L^2 phase measurement. That signal, called the sample front interface, is measured by phase-lock loop system 1. The signal from the sample back surface interface goes to phase detector 2, to low-pass filter 2, and to sample/hold module 2. This sample/hold module receives its logic pulse from countdown-and-timing logic circuit 2. The output of this sample/hold module is integrated and fed to the phase shifter.

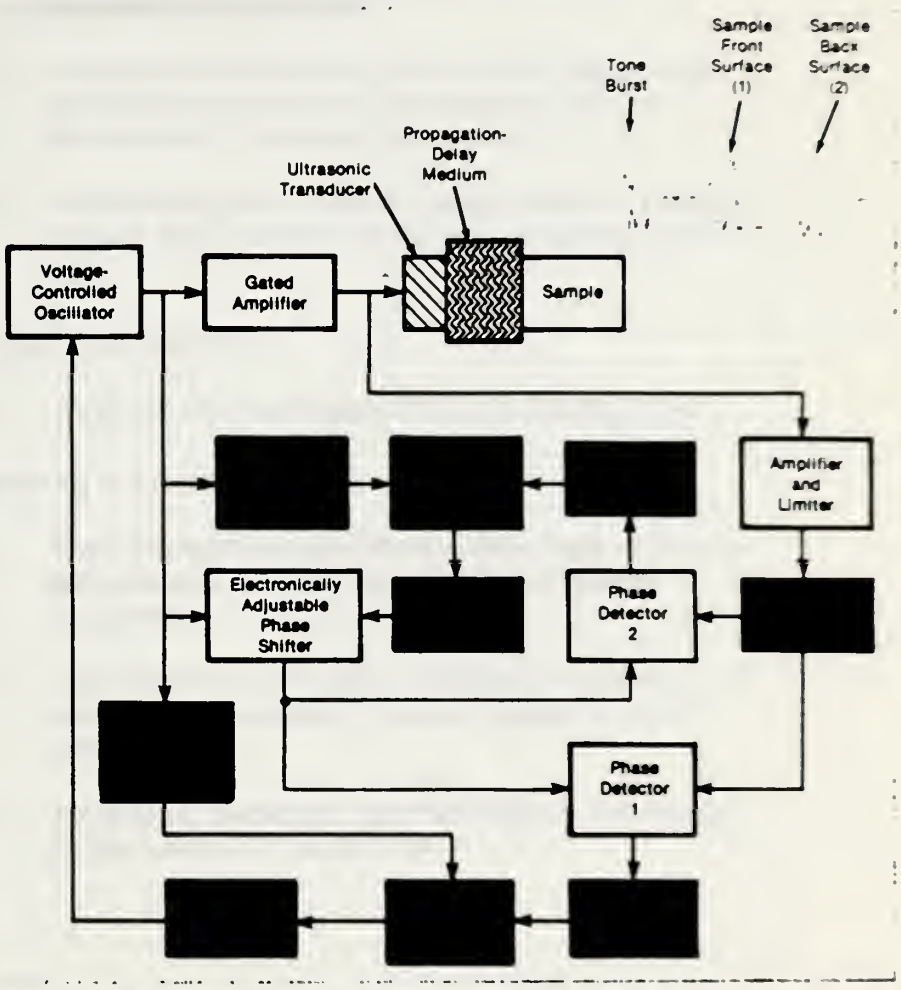

Loops 1 and 2 Share the Same Phase Shifter, thereby essentially eliminating the phase shift in the delay path.

Since both loops 1 and 2 are forced to quadrature and share the same phase shifter, a frequency representing a fixed number of waves or half-waves would exist in the sample. The effect of this would be to eliminate the phase shift in the water path. Countdown-and-timing logic circuits 1 and 2 ensure that each new tone burst occurs at a precise phase, that sufficient time has evolved to allow energy from the previous excitation to decay, and that the two sample/hold modules acquire their phase measurements at precise times.

The DRP^{2}L^2 system can use such other forms of radiation as electromagnetic waves (i.e., light or radio). The technique can be staged from one or both sides of a sample for accurate thickness or velocity measurements. Contour or shape measurements may be obtained by use of multiple transducer mountings. This system is insensitive to broad

changes in signal amplitude (a phase-only signal), is ideal for the high resolution through the statistical averaging that is inherent in frequency measurements, and is independent of unwanted delays caused by the effects of coupling-path lengths or propagation.

This work was done by Joseph S. Heyman and Francis D. Stone of **Langley Research Center.**

This invention is owned by NASA, and a patent application has been filed. Inquiries concerning nonexclusive or exclusive license for its commercial development should be addressed to the Patent Counsel, Langley Research Center Refer to LAR-13310 /TN

Langley Research Center
Technology Utilization Officer:
John Samos
Mail Stop 139A
Hampton, VA 23665
(804) 865-3281
Patent Counsel:
Howard J. Osborn
Mail Code 279
Hampton, VA 23665
(804) 865-3725

FOR ADDITIONAL INFORMATION: *Contact: Director, Technology Transfer Division, P.O. Box 8757, BWI Airport, MD. 21240; (301) 621-0100 Ext. 241*

REFER TO THE NUMBER LISTED AT THE END OF THE ARTICLE

Energy

638 Benefits of Replacing Residential Central Air Conditioning Systems

639 New Polymer Electrolyte for Batteries

640 Liquid-Crystal Thermal-Control Panels—Radiative temperature regulators would have no moving parts. (Licensing Opportunity)

641 Solar Cells With Reduced Contact Areas—Silicon cells are more efficient because less metal touches the semiconductor. (Licensing Opportunity)

642 More Efficient Solar Thermal-Energy Receiver—Thermal stresses and reradiation are reduced. (Licensing Opportunity)

Testing & Instrumentation

643 Monitoring the Heat Output of a Wood-Burning Stove

Other items of interest

670 Screening Mechanically-Defective Solar Cells—A flexure test eliminates failure-prone wafers before further processing.

712 One-Dimensional Simulation of Isotropic Radiation—Solar cells are tested for effects of radiation in a unidirectional beam.

718 Acceptance, Verification, and Performance Test Results for the Bedford CF Electric Van

energygram

BENEFITS OF REPLACING RESIDENTIAL CENTRAL AIR CONDITIONING SYSTEMS

The energy efficiency ratios (EERs) of marketed residential air conditioning equipment have increased recently. The benefits of replacing a unit having an EER of 6 with a unit having an EER of 10 in a prototypical two-story house were investigated for a house located in each of 32 cities in the United States. The U.S. Department of Energy building simulation model, DOE-2.1A, was used to predict the energy savings associated with this action. Using 1982 capital and electrical energy costs, simple payback periods were calculated to be as low as 5 years in the lower southern regions to about 10 to 15 years in the upper southern regions. If the existing air conditioning unit needs replacement, the simple payback period for the incremental cost of installing a high-efficiency unit is calculated to be about 2 to 5 years in these regions. Further savings would be realized if existing oversized units were replaced with properly sized, high-efficiency units.

When an existing residential air conditioning unit needs major repair or replacement, purchase of a high-efficiency unit is cost effective for householders in a large portion of the United States. In addition, electrical utilities would have a reduction of peak summer loads, thus leading to conservation of national fuel resources.

Additional information:

Office of Technology Applications
Information Service
Martin Marietta Energy Systems, Inc.
P.O. Box X
Oak Ridge, TN 37831
Telephone: (615) 574-4192; FTS 624-4192

H. A. McLain et al., *Benefits of Replacing Central Air Conditioning Systems*, ORNL/CON-113, Oak Ridge National Laboratory (April 1985).

H. A. McLain and D. Goldenberg, "Benefits of Replacing Residential Air Conditioning Systems," pp. E-226-E-237 in *Proceedings of the ACEEE Summer Study on Energy Efficiency in Buildings* (1984).

H. A. McLain et al., "Appropriate Conservation Measures for Single-Family Buildings in Hot, Humid Climates," pp. 44-52 in *Second Annual Symposium, Improving Building Energy Efficiency in Hot and Humid Climates*, Texas A&M University (1985).

NBS technology update

National Bureau of Standards
U.S. Department of Commerce
Gaithersburg, MD 20899

New Polymer Electrolyte for Batteries

NBS scientists have developed a new light-weight polymeric electrolyte material that has wide potential use in solid-state, high-energy density batteries for weapon systems, satellites, and consumer products that require a light-weight energy source. The polymeric electrolyte is based on a design of interpenetrating polymer networks (IPNs) with two co-continuous phases, like a sponge with holes. One phase is a cross-linked epoxy that provides strength and dimensional stability; the other is a low-molecular weight poly (ethylene oxide) with dissolved salt that gives high conductivity. Polymers that dissolve salts and conduct ions are an important class of materials because they are inert to lithium, the lightest metal that can be used in batteries, and they also can be fabricated in thin films for high-technology applications. The NBS research was partially funded by the Office of Naval Research. A patent application has been filed for the new polymeric electrolyte material.

FOR ADDITIONAL INFORMATION: To discuss this effort further, contact: Dr. George Davis, Room B320-Polymers Bldg., National Bureau of Standards, Gaithersberg, MD 20899; (301) 975-6725 or Dr. Barry Bauer, Room B210-Polymers Bldg., National Bureau of Standards, Gaithersberg, MD 20899; (301) 975-6849.

NASA Tech Brief
National Aeronautics and Space Administration
Marshall Space Flight Center, Alabama

Licensing Opportunity

Liquid-Crystal Thermal-Control Panels

Radiative temperature regulators would have no moving parts.

A conceptual temperature-regulating system proposed for spacecraft may be useful in the automatic or remotely controlled regulation of solar heating in buildings, provided that the cost can be reduced sufficiently. The system would consist of liquid-crystal panels that can be made to absorb or reflect sunlight.

A liquid-crystal panel is made absorbent or reflective by the application of a voltage. The voltage could be applied or removed according to the command from a thermostat, a photosensor, or a timer. To provide a controlled heating rate, the panel could be turned on and off according to a prescribed duty cycle.

Previously, panels with complicated mechanical linkages (reminiscent of venetian blinds) were used to alternate between absorption and reflection. Such panels are subject to breakage, wear, and jamming. Furthermore, they require considerable amounts of power. In contrast, the liquid-crystal panels have no moving parts and require very little power.

The liquid-crystal panels can be mounted on or near the surfaces to be heated or shielded from heating. They can be made with curved rear surfaces that conform to curved mounting surfaces. The panels can also be made in many small pieces in blankets that are unrolled like window shades over the areas to be heated or protected.

This work was done by Robert F. DeHaye, Teddy M. Edge, and William R. Feltner of **Marshall Space Flight Center**. *No further documentation is available.*

Inquiries concerning rights for the commercial use of this invention should be addressed to the Patent Counsel, Marshall Space Flight Center. Refer to MFS-28036 /TN

George C. Marshall Space Flight Center
Technology Utilization Officer:
Ismail Akbay
Code AT01
Marshall Space Flight Center, AL 35812
(205) 544-2223
Patent Counsel:
Leon D. Wofford, Jr.
Mail Code CC01
Marshall Space Flight Center, AL 35812
(205) 544-0014

FOR ADDITIONAL INFORMATION: *Contact: Director, Technology Transfer Division, P.O. Box 8757, BWI Airport, MD. 21240; (301) 621-0100 Ext. 241*
REFER TO THE NUMBER LISTED AT THE END OF THE ARTICLE

NASA Tech Brief
National Aeronautics and Space Administration

Licensing Opportunity

NASA's Jet Propulsion Laboratory, Pasadena, California

Solar Cells With Reduced Contact Areas

Silicon cells are more efficient because less metal touches the semiconductor.

The efficiency of silicon solar cells is increased to about 20 percent by the use of a smaller metal-contact area on silicon at the front and the back of each cell. The reduction in contact area reduces the surface recombination velocity under the contact and thus reduces the reverse saturation current and increases the open-circuit voltage.

In a conventional solar cell, 4 to 6 percent of the front surface is covered by contact metal, and the back is completely metallized. Even after passivation of the front surface with an oxide layer, the overall surface recombination velocity is on the order of 10^4 cm/s, the reverse saturation current density is 1.4×10^{-12} A/cm^2, and the open-circuit voltage is 618 mV.

In a high-efficiency cell, the contact area on the front surface is reduced to only 0.2 percent of the total and the back contact area to only 0.6 percent. As a result, the effective surface recombination velocity drops to or below 10^3 cm/s. With reduced contact area on back surface alone, the reverse saturation current density drops to 0.91×10^{-12} A/cm^2, and the open-circuit voltage rises to 628 mV.

A p/n junction is formed in the silicon wafer in the usual way, then a thermal oxide layer 100 Å thick is grown on the front and the back. An array of square "windows" is etched through the front oxide, and an array of circular "windows" is etched on the back side (see figure). Layers of titanium, palladium, and silver are evaporated into the "windows" and sintered, forming arrays of metal contacts on both surfaces. Metal fingers are deposited on the front oxide so that they form conductive paths for electrical output through metal in "windows." The front surface is provided with an antireflection coating. An aluminum layer is deposited on the back oxide where it forms an electrical connection to the back contact array and reflects light back into the silicon wafer. This is followed by metallization, using the titanium-palladium-silver for the back contact.

This work was done by Taher Daud, Gerald T. Crotty, Akaram H. Kachare, and Jeffrey T. Lewis of Caltech for **NASA's Jet Propulsion Laboratory.**

Inquiries concerning rights for the commercial use of this invention should be addressed to the Patent Counsel, NASA Resident Office-JPL. Refer to NPO-16762 /TN

Jet Propulsion Laboratory
Technology Utilization Manager:
Norman L. Chalfin
Mail Stop 201-110
4800 Oak Grove Drive
Pasadena, CA 91109
(818) 354-2240

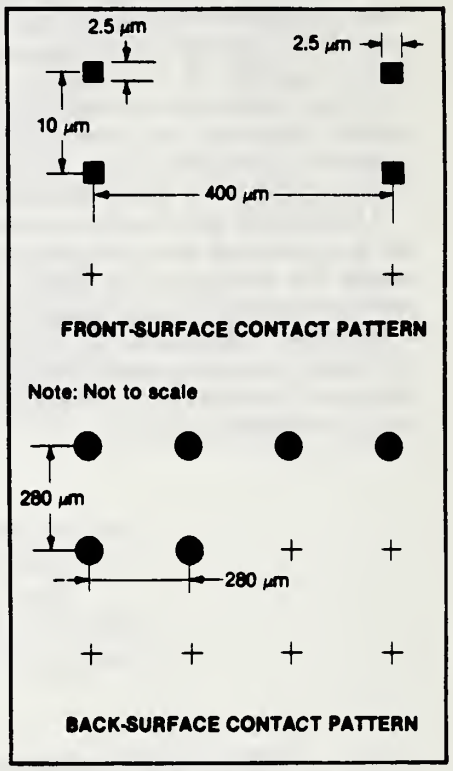

This Detail of Electrical-Contact Arrays shows how small a metal area touches the silicon wafer. The complete arrays are about 20 mm square.

FOR ADDITIONAL INFORMATION: *Contact: Director, Technology Transfer Division, P.O. Box 8757, BWI Airport, MD. 21240; (301) 621-0100 Ext. 241*
REFER TO THE NUMBER LISTED AT THE END OF THE ARTICLE

NASA Tech Brief
National Aeronautics and Space Administration
Lewis Research Center, Cleveland, Ohio

Licensing Opportunity

More Efficient Solar Thermal-Energy Receiver

Thermal stresses and reradiation are reduced.

An improved design for a solar thermal-energy receiver overcomes three major deficiencies of the solar dynamic receivers described in literature. These deficiencies are as follows:

1. Present receiver designs allow reradiation losses from the thermal-energy-storage material (TSM) during the shade period.
2. Most of the present receiver designs do not prevent the stressing of the TSM container due to expansion and contraction of the TSM as it freezes and melts.
3. When the solar energy enters such receivers, the rays can be easily reflected back out of the cavities, resulting in high reflection losses. To minimize these reflection losses, the rays must undergo several reflections from high-absorbtivity surfaces within the cavity.

In the proposed receiver (see Figure 1), solar energy is reflected by the surface of the concentrator into a small aperture. A working fluid, which can be liquid or gas, circulating through the receiver is heated by this energy and then ducted to a dynamic heat engine — for example, Brayton, Rankine, or Stirling — or to any other system requiring a high-temperature fluid.

The receiver, shown in Figure 2, is divided by an insulated partition into two chambers; a radiation section and a storage section. The radiation section receives the solar energy from the concentrator. The boiling ends of numerous heat pipes thermally connect the radiation section with the heat-storage section. The condensing end of each heat pipe delivers heat to the TSM, which is located coaxially around the heat pipes. Heat is passed through the TSM to the outer walls of the TSM container and into the working fluid. Fins on the outer wall of the container provide good heat transfer into the working fluid. The fins are not shown on the figure for clarity.

The improved receiver performance is attributed to three factors:

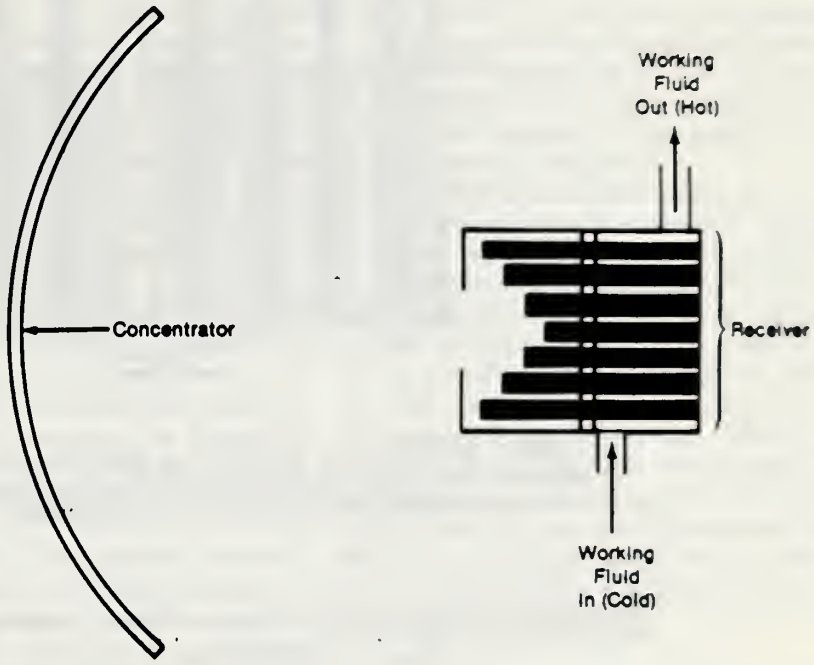

Figure 1. The Concentrator and Receiver are part of a solar-thermal-energy system.

1. It minimizes reflection losses: The heat pipes in the radiation section of the receiver are connected with webs. The webs conduct heat circumferentially around the receiver to maintain an even temperature distribution, provide a large heat-transfer surface, and cause the solar rays coming into the aperture to be reflected internally many times. Each of these reflections allows more of the solar energy to be absorbed, thereby minimizing the energy losses from the aperture.
2. It minimizes reradiation losses: Another feature is that the heat pipe can be constructed to pass heat in one direction only so that in the shade portion of the cycle the radiation section of the receiver is cold, thereby preventing heat from being lost by reradiation.
3. It minimizes thermal stresses in the thermal-storage-material container: Stresses in the TSM container are minimized by controlling the manner in which the TSM freezes and melts as the system goes through Sun and shade cycles.

The receiver can be used in a number of applications to produce thermal energy directly for use or to store thermal energy for subsequent use in a heat engine.

This work was done by Miles O. Dustin of **Lewis Research Center**.

Inquiries concerning rights for the commercial use of this invention should be addressed to the Patent Counsel, Lewis Research Center. Refer to LEW-14309 /TN

Lewis Research Center
Technology Utilization Officer
Daniel G. Soltis
Mail Stop 7-3
21000 Brookpark Road
Cleveland, OH 44135
(216) 433-5567
Patent Counsel
Gene E. Shook
Mail Code 60-2
21000 Brookpark Road
Cleveland, OH 44135
(216) 433-5753

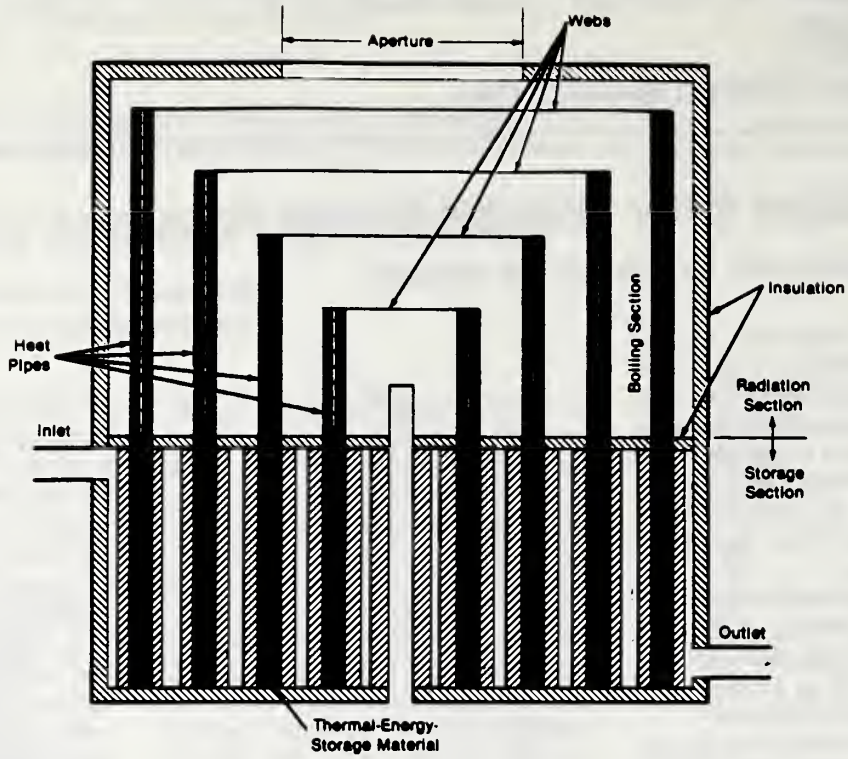

Figure 2. The Receiver is divided into a radiation section (top) and a storage section (bottom). Concentrated solar radiation falls on the boiling ends of heat pipes, which transmit the heat to the thermal-energy-storage medium.

FOR ADDITIONAL INFORMATION: *Contact: Director, Technology Transfer Division, P.O. Box 8757, BWI Airport, MD. 21240; (301) 621-0100 Ext. 241*

REFER TO THE NUMBER LISTED AT THE END OF THE ARTICLE

energygram

Monitoring the Heat Output of a Wood-Burning Stove

DOE/TIC/EG-86/107
OFFICE OF SCIENTIFIC AND TECHNICAL INFORMATION

This technical note was based on research conducted by Lawrence Berkeley Laboratory for the U.S. Department of Energy.

Lawrence Berkeley Laboratory

A technique has been developed to monitor the heat output of wood stoves that transfer their heat by radiation and natural convection. It is possible to determine the energy-exchange rate directly from the surface temperature and the temperature of the surroundings. The method is a simplification of general engineering models of radiation and natural convection for wood stoves.

General engineering models of heat transfer are used to develop a model that predicts heat output of a stove from measurements of surface temperature with the stove surface area as input. The predicted heat outputs are then compared with the actual heat outputs as measured by a calorimeter room.

The predictions involve several potential monitoring schemes: (1) separate temperature measurements for each surface of the stove, (2) an average temperature measurement for all stove surfaces, and (3) a single surface temperature measurement. The accuracies of the predictions are characterized by their geometric bias and scatter as well as their predictions of the total energy delivered.

Predictions made from average temperature measurements are found to be as accurate as those based on individual temperature measurements, whereas single-temperature measurements cause an additional 5% uncertainty in predictions. For both the average temperature and individual temperature predictions, the bias is between 2 and 24%, with 16% as the typical scatter. The trend in the bias is underprediction. The individual temperature predictions of total energy delivered were 8% low on average, whereas the predictions based on the average temperature were 3% low on average.

FOR ADDITIONAL INFORMATION

Monitoring the Heat Output of a Wood Stove, Energy and Buildings, *8: 79-80 (1985).*

DOE report(s):
A One-Channel Monitor for Wood Stove Heat Output: Project Report for the Hood River Conservation Program, presented at the 1984 American Society for an Energy Efficient Economy Summer Study, Santa Cruz, CA, August 14-22, 1984.
Report number: LBL-16924/NAB
Order number: DE85012547/NAB
Price: $9.95

Order DOE report(s) from:
National Technical Information Service
5285 Port Royal Road
Springfield, VA 22161

For additional information, contact:
M. P. Modera
Lawrence Berkeley Laboratory
Building 90, Room 3074
Berkeley, CA 94720
Telephone No.: (415) 486-4678

Engineering

644 Predicting the Impulse of Blast Waves—A computer code predicts potentially hazardous effects with acceptable accuracy.

645 The POP Pipe-Joining System—Tests evaluate the suitability of the system for gap or river crossings.

646 Zirconia-Bonded Zirconia Fiber Insulation Structures

647 Energy-Absorbing Passenger Seat for Aircraft—Tests show probability of passenger survival to be high.

648 Improved Heat-Transfer Calculations for Hypersonic Flow—The Lewis number is corrected for extremely high airspeeds.

649 Multiple-Scale Turbulence Model—The turbulence in complex, recirculating flows is not in spectral equilibrium.

Testing & Instrumentation

650 Propeller Flows Studied Using Doppler Velocimetry

651 Depth Gauge for Liquids Under High Pressure—An ultrasonic transducer is protected from high pressure and is easy to connect. (Licensing Opportunity)

652 Measuring Room Area or Volume Electronically—Results would be obtained rapidly with minimal effort.

653 Measuring Fluid Velocities With Glowing Particles—Particle trajectories are recorded photographically. (Licensing Opportunity)

654 Taking Impressions of Hidden Cavity Walls—A device for field checks makes casts of internal contours.

655 Environmental Testing of Glass-Fiber/Epoxy Pressure Vessels—Strength diminishes during long exposure to the environment.

656 Identifying Vibration Parameters In Large Structures—An analytical method separately examines low-frequency and high-frequency behavior.

MANUFACTURING TECHNOLOGY NOTE

U.S. ARMY MATERIEL COMMAND

Deputy Chief of Staff for Manufacturing Technology, Alexandria, VA

Project Number: 1L161102AH43 Filing Code: 79E018

Predicting the Impulse of Blast Waves

A computer code predicts potentially hazardous effects with acceptable accuracy.

A study has provided an improved scheme for predicting the impulse of blastwaves exiting guns and shock tubes. The scheme uses the Euler finite-difference code DAWNA, which calculates the blastwave field along the boreline of a gun. The code employs shock fitting, takes into account the decay rate of the energy efflux quantity, and executes much faster than a numerical axisymmetric scheme.

The results of the computer simulation by the U.S. Army Ballistic Research Laboratory show that the impulse increases with the decay time of the energy efflux. Comparisons of experimental data with simulation results show a similar dependence of the impulse on the decay time of the energy efflux (see figure). It appears that the barrel exhaust time is a significant parameter for improving the correlation of the impulse data.

Although the simulation is limited to the boreline direction, this is not a major impediment, since the scaling approach allows application of the results to all polar angles. The numerical simulation also allows for isolation from turbulence and other phenomena in the blast-flow.

Thus, the impulse given to nearby structures by guns or shock tubes can now be more accurately predicted in a range of distances where possible injury can result to personnel and equipment. The relationship is not yet applicable, however, to very large distances from the gun or shock tube.

Project officer Kevin S. Fansler
(301) 278-3677 or AV 283-3677.

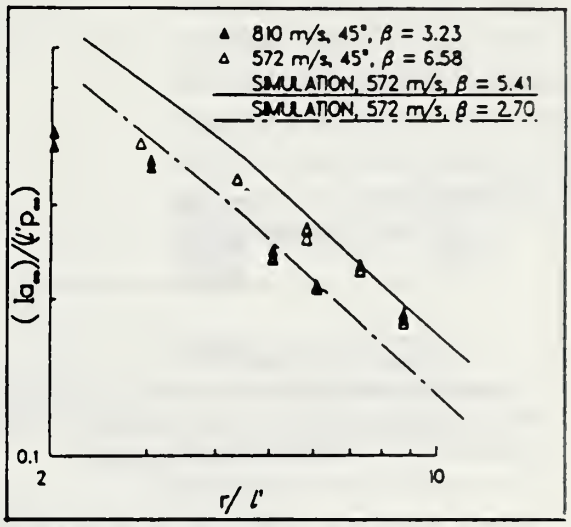

Simulated and Experimental Values for the impulse from a shock tube agree well, considering that the simulation is based on a gross simplification of the muzzle blastflow. The vertical scale represents normalized impulse, and the horizontal scale represents normalized distance from the muzzle. Although the emptying times are smaller for the simulation, impulse values are higher. The simulated curves also show a steeper decline of impulse with distance.

FOR ADDITIONAL INFORMATION:

You can learn more details about this technology by ordering the NTIS report(s):
Dependence of Free-Field Impulse on the Decay Time of Energy Efflux for a Jet Flow.
Order number: AD-A165365/NAA
Price code: A03

Order from:
National Technical Information Service
5285 Port Royal Road
Springfield, VA 22161

This document was prepared under the sponsorship of the U.S. Government. Neither the United States Government nor any person acting on behalf of the United States Government assumes any liability resulting from the use of the information contained in this document, or warrants that such use will be free from privately owned rights.

MANUFACTURING TECHNOLOGY NOTE

U.S. ARMY MATERIEL COMMAND

Deputy Chief of Staff for Manufacturing Technology, Alexandria, VA

Project Number: NONE

Filing Code: 60B004

The POP Pipe-Joining System

Tests evaluate the suitability of the system for gap or river crossings.

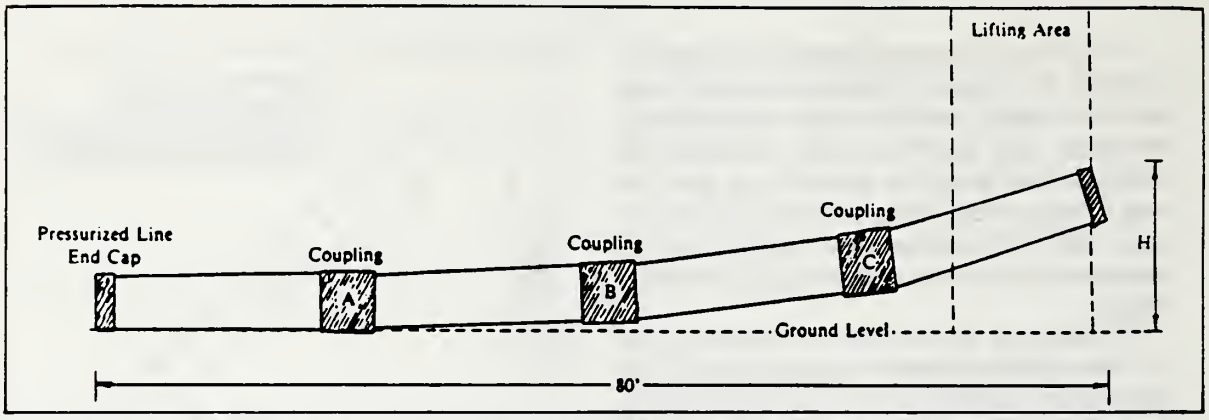

In the **Natural Bending Test**, one end of a coupled pipe assembly is raised by a crane until at least two couplings are off the ground and the assembly has assumed an unrestrained, natural bend. The assembly is filled with water, capped, and pressurized to 650 lb/in. (4.6 MPa) gauge.

Tests have evaluated the Pipeline Outfit, Petroleum (POP), a commercial pipe-joining system consisting of a hydraulic joining press that swages a plain pipe section into a special coupling. In the evaluation by the U.S. Army Belvoir Research, Development, and Engineering Center, the joined piping was subjected to hydrostatic pressure tests, natural bending tests, tensile pull tests, and flexure tests.

The tests showed that, although an aluminum press fitted with 5-in. (12.5-cm) hydraulic cylinders successfully joined aluminum pipes with wall thicknesses of 0.109- and 0.150-in. (2.77- and 3.81-mm), a steel frame with 7-inch (18-cm) cylinders is needed to join aluminum pipe having 0.188-in. (4.78-mm) wall thickness; the aluminum frame will not withstand the forces generated by the larger cylinders. A Neutra Rust DL coating (or equivalent) was found superior to an epoxy coating because it is easier to use, requires less field work, and provides the proper sealing characteristics.

For simple, straight hydrostatic applications, the Series 800 (or equivalent) positive seal coupling is satisfactory. However, if the coupling is subjected to bending and pulling, its performance may be marginal. Hydrostatic burst pressure in a system of pipe and positive seal couplings, with no bending or tensile loading, is limited by the yield strength of the pipe wall, not by the pipe-coupling connection.

Sharp pipe ends tend to peel the coating from the inside wall of the couplings during insertion. Therefore, the pipe ends should be lightly filed to round the outside edge and remove burrs.

Partial insertion of the pipe into the coupling does not mean a weaker joint. Contrarily, given a constant force from the hydraulic cylinders, the joint with partial insertion might be tighter because the insertion motion has been stopped by the interference between the pipe and coupling taper.

Project officer Frederick O. Balling
(703) 664-5781 or AV 354-5781.

FOR ADDITIONAL INFORMATION:

You can learn more details about this technology by ordering the NTIS report(s):
Test Report for the Evaluation of the Pipeline Outfit, Petroleum (POP).
Order number: AD-A170867/NAA
Price code: A03
Order from:
National Technical Information Service
5285 Port Royal Road
Springfield, VA 22161

This document was prepared under the sponsorship of the U.S. Government. Neither the United States Government nor any person acting on behalf of the United States Government assumes any liability resulting from the use of the information contained in this document, or warrants that such use will be free from privately owned rights.

ZIRCONIA-BONDED ZIRCONIA FIBER INSULATION STRUCTURES

Zirconia-bonded zirconia fiber insulation structures are a class of lightweight, monolithic insulators that have been developed for use at temperatures greater than 2000°C (3600°F) in all types of furnace atmospheres. The insulation structures contain 80 to 85 vol % porosity and have bulk densities below 1.0 g/cc (60 pcf). These insulators are self-supporting and have low thermal mass for fast cycle times in furnace operations.

Such structures are produced using filtration molding techniques. Disks, cylinders, frustra, and a variety of other geometric shapes are produced with wall thicknesses of up to 2.5 cm (1 in.). Fibers in the structures are deposited in orientations that produce maximum resistance to conductive heat flow through the walls of the structures.

Process furnaces equipped with these zirconia fiber insulating structures can be operated at sustained temperatures above 2000°C, as compared with the 1700°C-upper limit of existing oxide-fiber-lined furnaces. This will enable industrial processing of new alloys and ceramic materials that contain higher concentrations of refractory elements. The zirconia structures can also serve as substrates for production of high-density ceramic composites.

Additional information:

Office of Technology Applications
Information Service
Martin Marietta Energy Systems, Inc.
P.O. Box X
Oak Ridge, TN 37831
Telephone: (615) 574-4192; FTS 624-4192

G. E. Wrenn, Jr., et al., *Zirconia-Bonded Zirconia Fiber Insulation Structures*, Y/DV-378, Oak Ridge Y-12 Plant (July 1984).

NASA Tech Brief
National Aeronautics and Space Administration
Langley Research Center, Hampton, Virginia

Energy-Absorbing Passenger Seat for Aircraft

Tests show probability of passenger survival to be high.

The development of an energy-absorbing passenger seat, designed to minimize injury in a commercial-aircraft crash, was part of a joint FAA/NASA controlled-impact flight test of a transport-category commercial aircraft. After developmental tests were successfully completed at NASA's Langley Research Center, the seat assembly was flight-tested on a Boeing 720B aircraft at NASA's Dryden Flight Research Facility.

A commercially available triple-passenger seat was selected for conversion to an energy-absorbing seat assembly. The design goal was to protect the passengers, simulated by three 165-lb (75-kg) anthropomorphic dummies, against a vertical impact velocity of 21 ft/s (6.4 m/s) and a longitudinal velocity of 21 ft/s (6.4 m/s). To limit acceleration, the seat was modified so that it would collapse or "stroke" under high load. To accomplish seat stroking, split-sleeve-type bearings were attached to the upper ends of the rear legs, and a combination nylon-bearing-block/steel-yoke unit was installed on the upper ends of the forward legs. All bearings encircled the seat-frame tubes to allow rotation.

Conventional aircraft bolts were used as hinge pins to permit the rotation of both the forward and rear legs at the lower seat/rail-attachment ends. Two graphite/epoxy energy-absorbing tubes that crush as the seat moves down and forward were used. The tube assemblies, designed to crush as axial columns during the aircraft-impact shock pulse, were installed diagonally between the forward and rear seat legs.

The figure depicts a cross section of the modified seat. To overcome a local bending problem encountered at the ends of the graphite/epoxy tubes, an axially-aligning pivot attachment was added to each end of the tubes. As the seat stroked forward and downward, the pivot-attachment mechanism caused the tubes to crush uniformly in an axial compressive mode, turning them literally into granular dust.

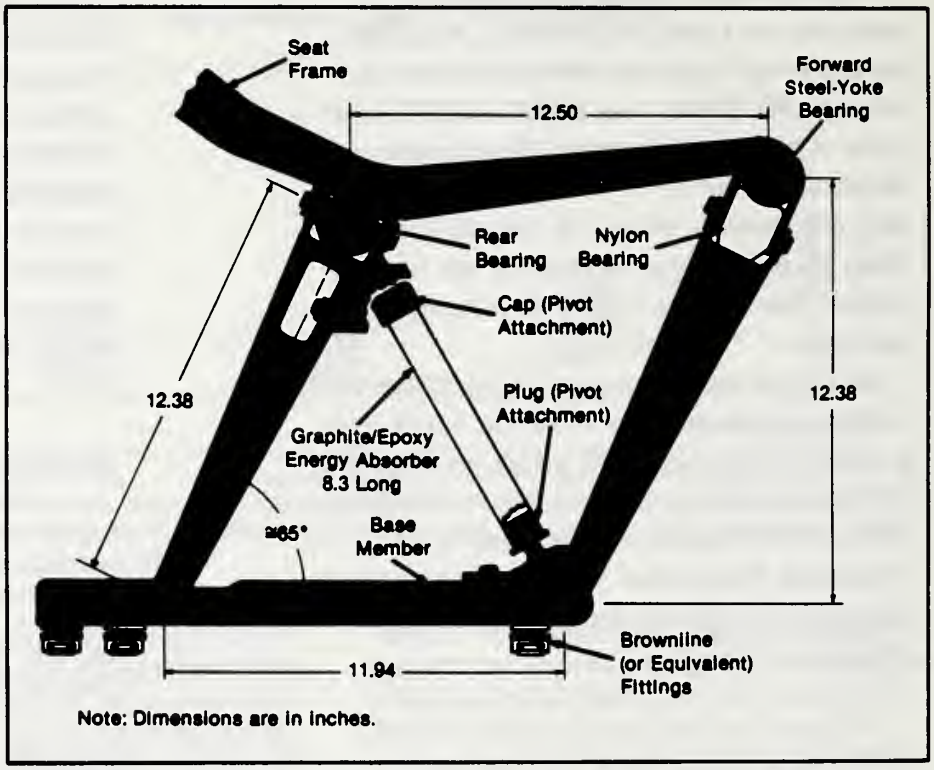

The **Modified Seat Mechanism** collapses under a heavy load to absorb impact energy and thereby protect the passenger.

The seat assembly was installed in the Langley Research Center Dynamic Impact Facility, and a series of dynamic drop tests were successfully conducted to simulate the vertical and forward shock-pulse characteristics. In the subsequent flight test at Dryden Flight Research Facility, a highly instrumented B-720, remotely controlled from the ground by pilots in a simulated cockpit, was crashed on a specially prepared, gravel-covered impact site to provide various crash data in addition to the information desired on the seats. The aircraft was crashed in an air-to-ground, gear-up mode at 150 kn (77 m/s) and a 4° glide slope. The results of the simulation tests indicate the probability of passenger survival to be high. This proposed seat mechanism could very well mitigate passenger injuries by reducing impact forces in a crash.

This work was done by Charles P. Eichelberger and Emilio Alfaro-Bou of **Langley Research Center** *and Edwin L. Fasanella of Kentron International, Inc.*
LAR-13385 /TN

FOR ADDITIONAL INFORMATION: *Contact: Director, Technology Transfer Division, P.O. Box 8757, BWI Airport, MD. 21240; (301) 621-0100 Ext. 241*
REFER TO THE NUMBER LISTED AT THE END OF THE ARTICLE

NASA Tech Brief
National Aeronautics and Space Administration
Lyndon B. Johnson Space Center, Houston, Texas

Improved Heat-Transfer Calculations for Hypersonic Flow

The Lewis number is corrected for extremely high airspeeds.

An algorithm calculates an improved, variable value of the Lewis number, a factor in the equation for the heat-transfer coefficient at the stagnation point of a body in hypersonic flow (mach numbers of approximately 25). In the past, a constant value of 1 had been used for the Lewis number. The new algorithm improves the accuracy of calculations of the heat generated by hot air acting on a moving body.

Input data for the algorithm are the stagnation-point density, temperature, and pressure; the stagnation-point wall temperature; the viscosity at the wall; the Prandtl number at the wall; and the total enthalpy. The steps in the algorithm are as follows:

- Calculate the stagnation-point compressibility from the stagnation-point density, temperature, and pressure;
- Find the weight percentages of the various air components;
- Using the weight percentages, find the dissociation enthalpy;
- Calculate the collision cross sections at the wall and average them;
- Calculate the improved Lewis number from a formula that relates this quantity with the previously calculated quantities; and
- Insert the improved Lewis number in the equation for the stagnation-point heat-transfer coefficient.

This work was done by Samuel N. Greenschlag of Rockwell International Corp. for **Johnson Space Center**.
MSC-20756 /TN

FOR ADDITIONAL INFORMATION: *Contact: Director, Technology Transfer Division, P.O. Box 8757, BWI Airport, MD. 21240; (301) 621-0100 Ext. 241*
REFER TO THE NUMBER LISTED AT THE END OF THE ARTICLE

NASA Tech Brief
National Aeronautics and
Space Administration

Multiple-Scale Turbulence Model

The turbulence in complex, recirculating flows is not in spectral equilibrium.

A report discusses a mathematical fluid-flow model that includes multiple turbulence scales. The model was developed for the numerical prediction of confined, recirculating flows. Based on multiple-time-scale concepts introduced in a previous study, the model takes into account that the turbulence in recirculating flow is not in spectral equilibrium and that the different energy-transfer rates for eddies of different spatial scales should be treated separately.

First, the fluctuating parts of the velocity are decomposed into components defined in terms of the turbulent-kinetic-energy densities of large- and small-scale eddies. The principal feature of the multiple-scale model is that the kinetic-energy spectrum of turbulence is divided roughly into three regions: large-scale energy production, intermediate energy transfer, and small-scale dissipation eddies.

The partition of the energy spectrum allows the energy transfer of large-scale eddies to be related directly to the mean strain. For sufficiently small eddies, the model includes an assumption regarding the isotropy of fluctuations. This justifies the use of a triple-velocity correlation function (of large- and small-scale fluctuation components) that was indicated, in another previous study, to act as an energy-transfer rate from one fluctuating field to another.

Invoking the same justification, an energy-dissipation term representing the eddies of smallest scale is derived from a double-velocity correlation function that includes the small-scale-eddy velocity components alone. Thus, the energy-transfer rates of the small eddies are treated as though they were due to the actions of the small eddies alone and are mathematically decoupled from the mean flow field.

The model equations include gradient-type transport equations in which the spectral-energy and energy-transfer densities are the transported quantities, the effective fluid velocity is the mean (nonfluctuating component of the total) fluid velocity, and the energy-generation source terms include an effective eddy viscosity and other coefficients.

The partition between the energy-production and transfer regions of the spectrum is characterized by the coefficients, which have yet to be determined. Some preliminary coefficient values have been assigned by calibration against a simple homogeneous-flow experiment, by inference from limiting single-turbulence-scale model results and by requiring that the spectral-energy and energy-transfer densities remain positive throughout time in the simulations.

This work was done by C. P. Chen of **Marshall Space Flight Center**. *Further information may be found in NASA CR-178536 [N86-12551/NSP], "Multiple-Scale Turbulence Closure Modeling of Confined Recirculating Flows."*

Copies may be purchased from the National Technical Information Service, Springfield, Virginia 22161, [A02]
MFS-27141 /TN

FOR ADDITIONAL INFORMATION: *Contact: Director, Technology Transfer Division, P.O. Box 8757, BWI Airport, MD. 21240; (301) 621-0100 Ext. 241*
REFER TO THE NUMBER LISTED AT THE END OF THE ARTICLE

Propeller Flows Studied Using Doppler Velocimetry

David Taylor Naval Ship R&D Center (DTNSRDC) is investigating detailed model propeller flows, using laser Doppler velocimetry (LDV) and flow visualization to improve propeller designs.

The advent of LDV permits detailed velocity measurements about operating model propellers. This nonobtrusive technique enables one to measure velocity within the blade boundary layers along the edges of the blade and through the blade's tip vortex.

The LDV studies are supplemented with more routine blade surface flow visualization techniques to identify laminar and turbulent regions on the blade and to note the occurrence of flow separation.

The LDV measurements are correlated with the propeller boundary layer and potential flow computation models to verify propeller performance predictions. With proper consideration of Reynolds number effects, propeller performance can be predicted at full-scale conditions.

For Additional Information:

Backup material on this effort is available from:

Navy Domestic Technology Fact Sheet
Reader Reply Service
Code E211
Naval Surface Weapons Center
Dahlgren, VA 22448-5000
(703) 663-8921

Refer to 111203/TN

Blade flow measurement using LDV.

Blade surface flow visualization.

NASA Tech Brief
National Aeronautics and Space Administration
Langley Research Center, Hampton, Virginia

Licensing Opportunity

Depth Gauge for Liquids Under High Pressure

An ultrasonic transducer is protected from high pressure and is easy to connect.

A continuous reading of the depth of a liquid in a vessel at pressures exceeding 5,000 psi (34 MN/m^2) is obtained from ultrasonic waves emitted from a transducer that is mounted in a modified high-pressure plug. A flat-bottom hole is drilled into the plug, leaving enough wall to meet the pressure-vessel code. An ultrasonic transducer is rigidly bonded to the inner end of the hole. The plug is inserted into the pressure-vessel wall in a way that leaves the transducer exposed to the atmosphere (see figure). This protects the transducer from high pressure and makes it easier to connect supporting electronic devices.

In operation, the transducer excites the plug flange into vibration, sending an ultrasonic pulse through the liquid to the liquid/gas interface where the pulse is reflected. The returning pulse is intercepted by the transducer and transmitted to the supporting electronics that compute the liquid depth.

The prototype device was used in a high-temperature-structures tunnel that has cooling water pressurized to 6,000 psi (41 MN/m^2). A 7/16-in. (11-mm) hole was drilled into a 3/4-in. (19-mm) high-pressure plug, leaving at least a 1/8-in. (3-mm) wall at the inner end of the hole. A piezoelectric element having a fundamental vibration frequency of 10 MHz was bonded to the inner end of the hole. The combined piezoelectric element and plug vibrate at 258 kHz.

This new configuration transmits the ultrasonic vibration directly into the liquid, enhancing signal strength, accuracy, and range, yet the piezoelectric element is protected from the high-pressure liquid.

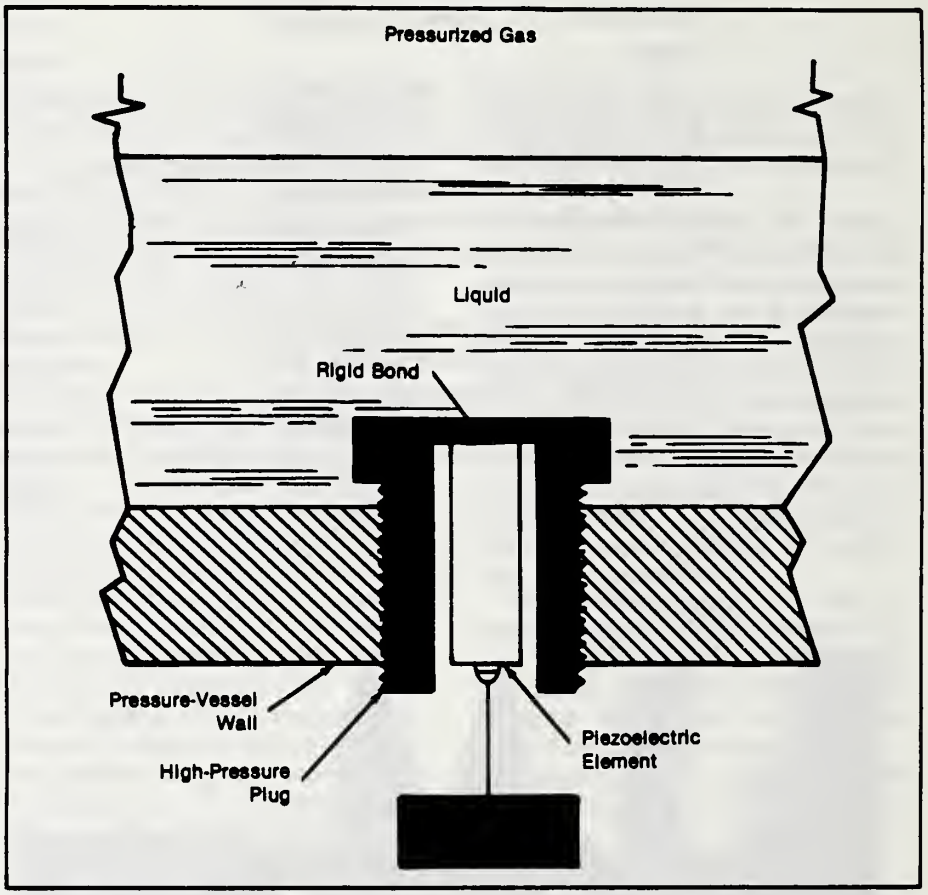

The **Piezoelectric Element** is mounted in a hole drilled in a high-pressure plug. The transducer is used to measure the depth of the liquid when the pressure in the vessel is high.

This work was done by Allan J. Zuckerwar of **Langley Research Center** *and David S. Mazel of Old Dominion University. No further documentation is available.*

This invention is owned by NASA, and a patent application has been filed. Inquiries concerning nonexclusive or exclusive license for its commercial development should be addressed to the Patent Counsel, Langley Research Center Refer to LAR-13300 /TN

Langley Research Center
Technology Utilization Officer:
John Samos
Mail Stop 139A
Hampton, VA 23665
(804) 865-3281
Patent Counsel:
Howard J. Osborn
Mail Code 279
Hampton, VA 23665
(804) 865-3725

NASA Tech Brief
National Aeronautics and Space Administration
NASA's Jet Propulsion Laboratory, Pasadena, California

Measuring Room Area or Volume Electronically

Results would be obtained rapidly with minimal effort.

A conceptual portable ranging instrument would measure the floor area or the volume of a room. The instrument would be advantageous where it is too difficult or time consuming to take linear measurements with tapes or rulers; for example, where a room is very large, where measurements have to be taken at dangerous locations, or where heavy objects have to be moved for access to the walls.

The instrument would include a pulsed, scanning radar, laser ranger (lidar), or sonar device capable of transmitting a beam sufficiently narrow for high angular resolution. For an area measurement, the instrument would be placed at a point in the room and set to take distance measurements to the walls in a horizontal plane, at all angular positions separated by small increments related to the angular resolution. If the angular increment is 360° ÷ M, then the area, A, is computed from the distance measurements by the formula

$$A = (\pi/M) \sum_{k=1}^{M} d_k^2$$

where d_k is the distance to the wall as measured at the kth angular position.

The volume would be measured in a similar manner, except that the instrument would have to scan vertically as well as horizontally, with the beam aimed at the walls, floor, and ceiling. In a spherical coordinate system with a vertical polar axis, the azimuthal (changing-longitude) scan would consist of measurements at intervals of 360° ÷ M, while the polar-angle (change-latitude) interval would be 180° ÷ N. Then the volume, V, of the room would be given by

$$V = (4\pi/3MN) \sum_{k=1}^{M} \sum_{l=1}^{N} d_{kl}^3 \sin \theta_l$$

where d_{kl} is the distance to the wall, floor, or ceiling as measured at the kth longitude and the lth latitude and θ_l in the lth polar angle (colatitude).

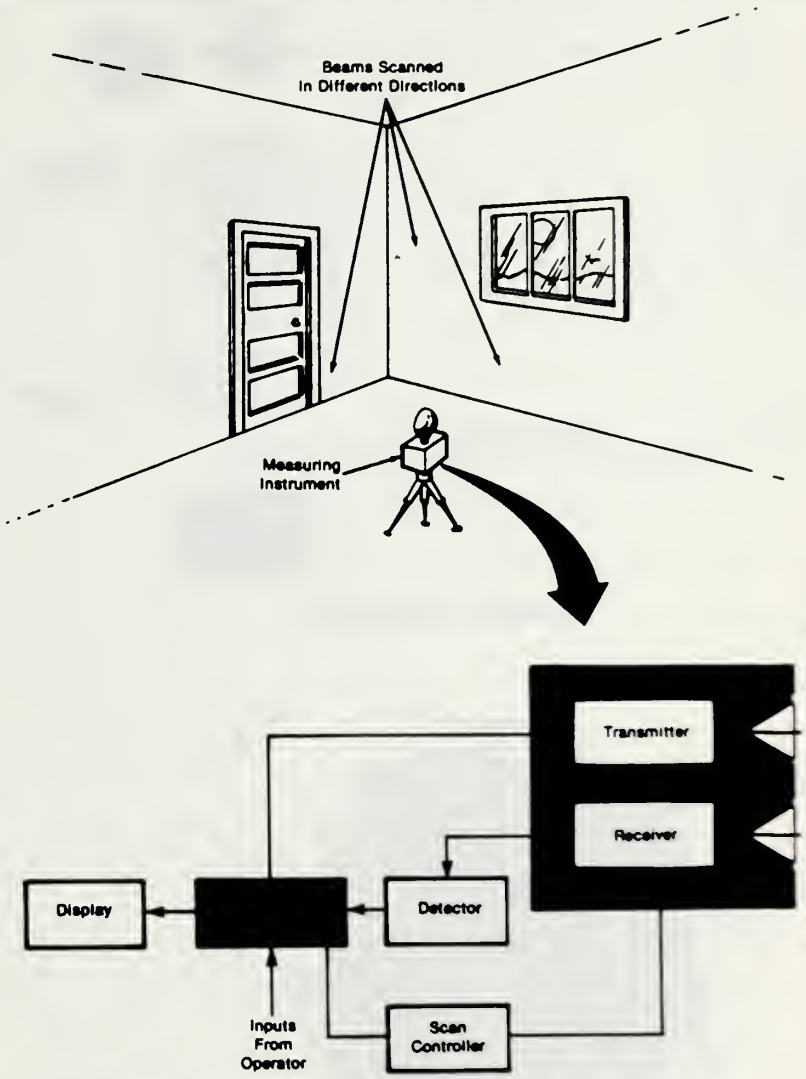

The Area- and Volume-Measuring Instrument could be hand-held or mounted on a tripod. The instrument would rapidly measure the distances to the walls, ceiling, or floor at many viewing angles and automatically compute the area or volume of the room.

The instrument is illustrated schematically in the figure. It should be possible to make the device small enough to be held by the operator. The unit would be powered by a battery. The rangefinder portion would be controlled by the microprocessor and very-large-scale-integrated control circuits. Operator inputs might include starting and stopping commands, scanning rate, angular resolution, and units of linear, area, or volume measurement. The program for the microprocessor might be contained in a plug-in read-only memory. A different memory could be plugged in to take a different kind of measurement.

To obtain an accurate area measurement, the scanning plane has to be level. The device could be placed on a tripod and leveled mechanically. The operator could also take several readings at different orientations, retaining the lowest reading. One of the computer programs could be set up to retain the lowest of several readings automatically.

For an accurate area reading, it is also necessary to place the instrument above any furniture or other large object in the room. Areas and volumes hidden from the beam by columns, pipes, or other obstructions will not be included in the measurements. The instrument might be programmed to recognize obstructions of small angular extent (for example, one angular interval) by ignoring distance measurements much shorter than those of adjacent angular positions and instead interpolating from the adjacent to the ignored values.

This work was done by Michael J. Kavaya of Caltech for **NASA's Jet Propulsion Laboratory**. *NPO-16629 /TN*

FOR ADDITIONAL INFORMATION: *Contact: Director, Technology Transfer Division, P.O. Box 8757, BWI Airport, MD. 21240; (301) 621-0100 Ext. 241*

REFER TO THE NUMBER LISTED AT THE END OF THE ARTICLE

NASA Tech Brief
National Aeronautics and Space Administration
NASA's Jet Propulsion Laboratory, Pasadena, California

Licensing Opportunity

Measuring Fluid Velocities With Glowing Particles

Particle trajectories are recorded photographically.

The directions and magnitudes of velocities in an unsteady liquid flow are measured with the aid of a fluorescent- and phosphorescent-tracing technique. The method is accurate and proceeds automatically, requiring minimal labor.

Small, uniformly sized particles of mass density close to that of the fluid are introduced into the flow. The particles have previously been coated with a fluorescent/phosphorescent material. A brief pulse of light is flashed on the flow. The particles fluoresce for about 10^{-5} s as the dye re-emits the absorbed light through electronic transitions. After the fluorescence has subsided, the dye continues to give off a less-intense phosphorescent glow for about 0.4 s. The light is flashed once more so that the particles fluoresce brightly again, then glow phosphorescently again.

The flow, meanwhile, is photographed in a continuous exposure. A particle path appears as a bright spot followed by a narrow streak and another bright spot and streak. This represents the initial fluorescence, the afterglow, and the initial fluorescence from the second flash followed by a second afterglow. The direction of a particle can be inferred from the intensity gradient on the tail.

The speed of the particle can be calculated from the length of its path between bright spots, because the elapsed time between light flashes is known accurately. The velocity of a particle is essentially the same as that of the flowing liquid immediately surrounding it, and the photograph of the many particle paths thus gives a picture of the velocity distribution in the liquid.

The photographic image is examined by a computer that generates an analysis of the flow. Previous attempts at computerized image analysis were unsuccessful, because the particles were photographed by reflected light. The particle paths on film had uniform brightnesses from beginning to end, and the computer had no way of determining the directions

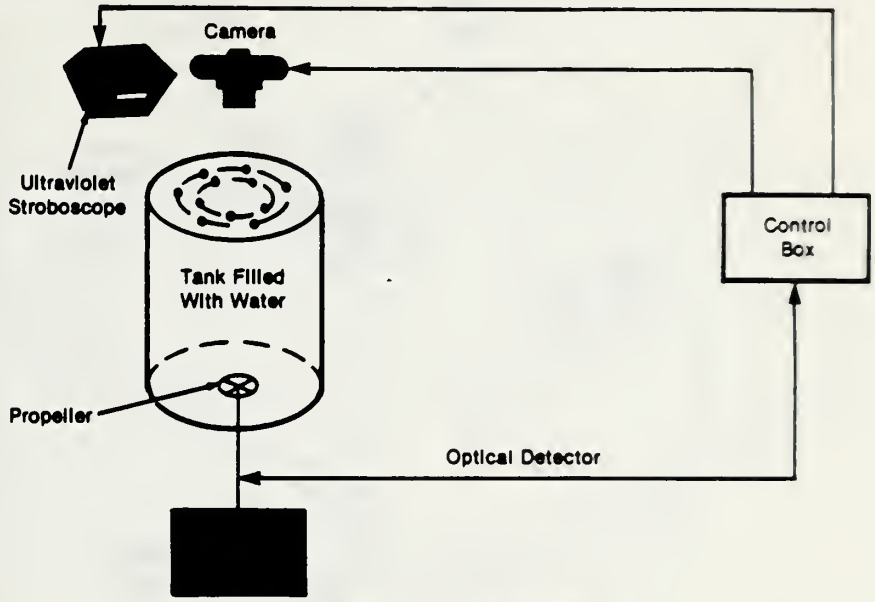

EXPERIMENTAL APPARATUS

PHOTOGRAPHIC NEGATIVE AFTER DOUBLE PULSE

A **Camera Views Glowing Particles** in a water vortex. The photograph shows tandem dot-and-tail pairs created on film by each pair of illumination pulses.

of particle movement. An operator had to decide the direction of each trace individually. The double dot/tail structure eliminates the directional ambiguity so that the direction can readily be determined automatically by the image-analyzing computer.

This work was done by Morteza Gharib, Miguel A. Hernan, Andre H. Yavrouian, and Virendra Sarohia of Caltech for **NASA's Jet Propulsion Laboratory**.

Inquiries concerning rights for the commercial use of this invention should be addressed to the Patent Counsel, NASA Resident Office-JPL. Refer to NPO-16653 /TN

Jet Propulsion Laboratory
Technology Utilization Manager:
Norman L. Chalfin
Mail Stop 201-110
4800 Oak Grove Drive
Pasadena, CA 91109
(818) 354-2240

FOR ADDITIONAL INFORMATION: *Contact: Director, Technology Transfer Division, P.O. Box 8757, BWI Airport, MD. 21240; (301) 621-0100 Ext. 241*

REFER TO THE NUMBER LISTED AT THE END OF THE ARTICLE

NASA Tech Brief
National Aeronautics and Space Administration
Marshall Space Flight Center, Alabama

Taking Impressions of Hidden Cavity Walls

A device for field checks makes casts of internal contours.

A lightweight, portable internal-molding device makes it possible to measure the radii of, or otherwise examine the contours of, passageways in hidden or complicated cavities. With the device, measurements can be made in the field, without returning assemblies to a shop or laboratory for inspection.

An acrylic molding head is wrapped with a polytetrafluoroethylene tube encapsulated by a surgical tube. The head is inserted in the cavity. When air at 40 lb/in.^{2} (280 kPa) pressure is applied to the head, the surgical tube expands and forms an airtight seal around the periphery of the cavity. The polytetrafluorethylene tube is held in place by a retaining ring that also controls the expansion of the surgical tube. As the surgical tube expands, it raises the head, forcing a molding compound (Citrocon or equivalent) into the cavity. The head is then rotated 180° and the procedure repeated to make a mold of the bottom part of the cavity.

After the head is removed from the cavity, the dimensions of the molded impression can be measured. A nylon string is extruded into the cavity along with the molding compound so that the casting can be easily retrieved if it breaks away from the head during its extraction from the cavity.

This work was done by Dick Burley and Walter Mayer of Rockwell International Corp. for **Marshall Space Flight Center.** *No further documentation is available.*

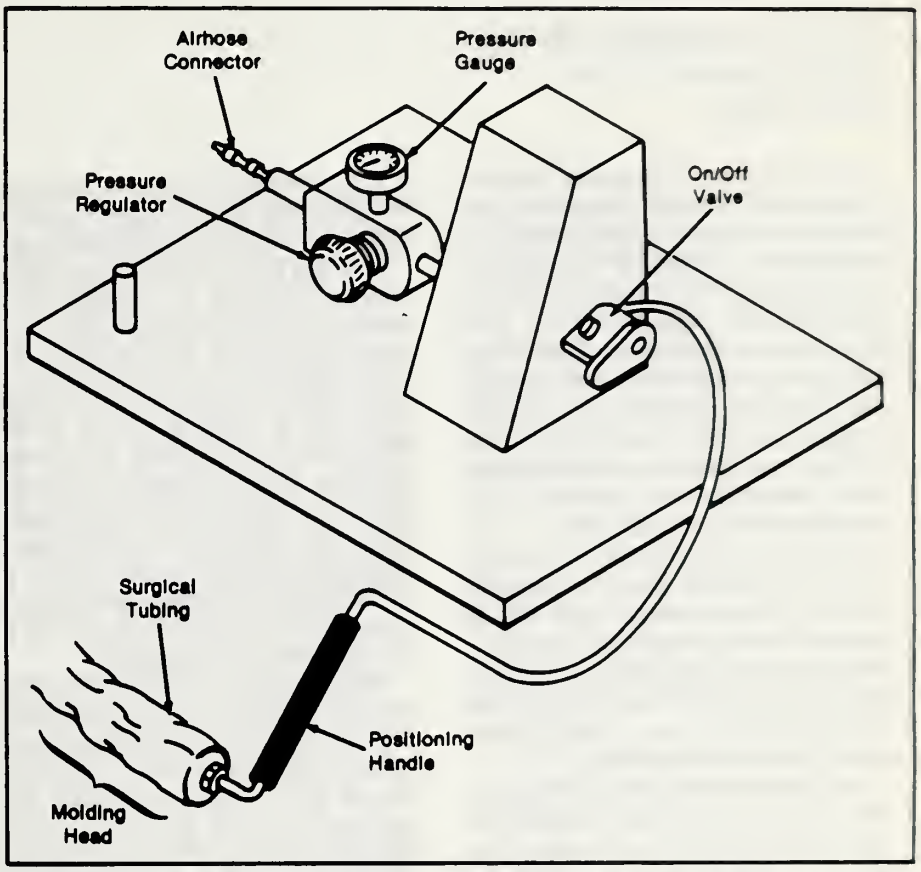

The Molding Head Expands when compressed air is applied. Inflatable tubes around the head perform a dual sealing and aligning function.

Inquiries concerning rights for the commercial use of this invention should be addressed to the Patent Counsel, Marshall Space Flight Center. Refer to MFS-29135 /TN

George C. Marshall Space Flight Center
Technology Utilization Officer:
Ismail Akbay
Code AT01
Marshall Space Flight Center, AL 35812
(205) 544-2223
Patent Counsel:
Leon D. Wofford, Jr.
Mail Code CC01
Marshall Space Flight Center, AL 35812
(205) 544-0014

NASA Tech Brief
National Aeronautics and
Space Administration

Environmental Testing of Glass-Fiber/Epoxy Pressure Vessels

Strength diminishes during long exposure to the environment.

A pair of reports discusses long-term environmental tests of glass-fiber/epoxy composite pressure vessels. Some of the hardest data to obtain on materials and structures are the long-term effects of environmental exposure. Since such data were necessary for accurate design of long-life structures such as pressure vessels, NASA Lewis Research Center built an outdoor test stand in 1973. This test stand maintains a system under constant pressure loading without the frequent intervention of personnel.

Accumulators were used to maintain a constant pressure (within 10 percent). The accumulator pressure and outside temperature were recorded twice daily. Automated data recording and pressure-limit warning systems were incorporated to minimize the number of man-hours required to monitor the system.

With this test equipment in place, a test program was started in January of 1984 to determine the environmental effects on glass-fiber/epoxy composite pressure vessels incorporating aluminum liners. The first pressure vessels put into test were designed by Martin Marietta/Denver Division (MM) and by Structural Composites Industries (SCI) as a part of a NASA L. B. Johnson Space Center program to develop a lightweight emergency breathing system such as those used by firemen. Both designs were filament wound with 20 end S-2 glass filaments. The SCI pressure vessels used a Dow Chemical epoxy (DER-332) while MM used a Shell epoxy (50:50 blend of Epon 828 and Epon 1031). Both the SCI and MM resins used an anhydride curing agent, which required an elevated-temperature cure.

The test environment was continuous outdoor exposure in Cleveland, Ohio. Some vessels were held under a constant pressure of 4,500 psi (31 MPa), some were pressure cycled 1,000 times from 200 to 4,500 psi (1.4 to 31 MPa) every year (in addition to constant pressure during the balance of the year), and, for control, some were not pressurized. The 4,500-psi (31-MPa) pressure was approximately 50 percent of the ultimate vessel capability and resulted in a composite stress of 31 percent of the ultimate composite capability.

Vessels of each type were removed from the test rack at scheduled intervals and subjected to a single-cycle-to-failure pressurization (burst test). All of the original group of pressure vessels (36 in all) were unpainted, and those that were exposed for more than 24 months showed significant visual effects of the exposure in addition to a reduction in the residual burst strength. This was true regardless of test conditions although the vessels that were subjected to pressure cycling tended to be most significantly affected.

There was considerable data scatter with a worst-case extrapolation indicating a 65-percent reduction in burst strength over a 10-year period for the unpainted pressure vessels. These data are not significantly different from those developed by other investigators in a benign laboratory environment, where it was found that one glass-fiber/epoxy sample in 100 would fail in a 10-year period due to a sustained load of 33 percent of the original ultimate.

However, to demonstrate the effectiveness of coatings in protecting the fiberglass structures and in reducing environmental degradation, a second series of glass-fiber/epoxy pressure vessels was placed on the test rack in 1980. To date, these vessels have not shown any degradation in residual burst strength. The test program on these bottles is expected to run into the 21st century.

Conclusions that can be drawn at this time are that the exposure of unpainted glass-fiber/epoxy composites to the varying environment of Cleveland, Ohio will result in a degradation of the ultimate strength of the material. The environmental effects are variable, and structural effects do not correlate with visual surface effects. The worst case degradation is on the order of what would be expected in a benign laboratory environment, but paints or ultraviolet-protective coatings can be expected to minimize any loss of strength.

This work was done by James R. Faddoul of **Lewis Research Center**. *Further information may found in:*

NASA TM-87058 [N85-30034/NSP], [A04] "Ten Year-Environmental Test of Glass Fiber/Epoxy Pressure Vessels" and NASA CR-165320 [N81-25492/NSP], [A02] "Survey of Long-Term Durability of Fiberglass-Reinforced Plastic Structures."

Copies may be purchased from the National Technical Information Service, Springfield, Virgina 22161.

LEW-14371/TN

FOR ADDITIONAL INFORMATION: *Contact: Director, Technology Transfer Division, P.O. Box 8757, BWI Airport, MD. 21240; (301) 621-0100 Ext. 241*

REFER TO THE NUMBER LISTED AT THE END OF THE ARTICLE

NASA Tech Brief
National Aeronautics and
Space Administration

Identifying Vibration Parameters in Large Structures

An analytical method separately examines low-frequency and high-frequency behavior.

A report discusses techniques for identifying rigid-body parameters, flexible-body parameters, and quasi-static disturbances in large structures. The techniques are being developed to aid in planning the space station. Although this effort has been directed towards the space station dynamic model and environment, the proposed methodology for systems identification is generic enough to allow application to arbitrarily large space structures and spacecraft configurations.

The space station will consist of five pressurized modules and supporting framework. A transverse truss on a vertical keel supports four solar panels, rotatable so that they can follow the Sun. Farther down on the keel is a pair of radiator panels that are also rotatable. At the base of the keel is a docking facility for the Space Shuttle. The structure configuration and attitude will be controlled by control-moment gyroscopes, magnetic torquers, and reaction-control thrusters.

The parameter-identification problem can be separated into low-frequency (0 to 0.01 Hz) and high-frequency (above 0.01 Hz) parts. The low-frequency disturbances come from attitude-control-system, aerodynamic, and gravity-gradient torques. These disturbances provide adequate excitation for the identification of such rigid-body parameters as the location of the center of mass and the inertia tensor and for such quasi-static parameters as the average atmospheric density, diurnal bulge, peak density, phase lag, and center of pressure. The high-frequency disturbances come from crew movements, thruster firing, and Space Shuttle docking. These disturbances can be used to identify the parameters associated with flexible-body dynamics.

The rigid-body parameters and the quasi-static parameters can be identified from accelerometer readings. The algorithm that processes the readings is based on a formulation of the rotation and vibration problems that is linear in the parameters sought. Using dynamic excitations, one can identify the flexible-body parameters by a maximum-likelihood estimation. This requires the solution of a nonlinear parameter-optimization problem. At present, this type of solution is restricted to non-real-time processing.

The techniques have been used to identify modal frequencies in a 15 degree-of-freedom space station model. This case study revealed problems arising from modes that are not excited, modes that are excited but not enough to ensure good identification, and modes that are not resolvable with the chosen sensor configuration. The solution can be made easier by resorting to a large number of sensors and to intentional excitation at prescribed locations around the structure. Whether the advantages of these provisions outweigh their cost remains to be determined.

This work was done by David S. Bayard, (Fred) Y. Hadaegh, and Che-Hang Charles Ih of Caltech for **NASA's Jet Propulsion Laboratory**.

"On-orbit Parameter and Disturbance Identification for Space Station,"
NPO-16770 /TN

FOR ADDITIONAL INFORMATION: *Contact: Director, Technology Transfer Division, P.O. Box 8757, BWI Airport, MD. 21240; (301) 621-0100 Ext. 241*
REFER TO THE NUMBER LISTED AT THE END OF THE ARTICLE

Environmental Science & Technology

657 Process Eliminates 99% of NOx from Exhaust in Lab Tests

658 Geotextiles for Drainage, Gas Venting, and Erosion Control at Hazardous Waste Sites

659 Waste Characterization and Analysis Activities in Support of the INEL Solidification Development Program

Testing & Instrumentation

660 Air Monitoring Device Developed—New meter measures light scattered by particulates.

Other items of interest

695 Underground Channels Mapped by Radar

Process Eliminates 99% of NOx from Exhaust in Lab Tests

Scientists at the Combustion Research Facility in Livermore, CA, have discovered a new chemical process for eliminating an important class of noxious pollutants, the nitrogen oxides (NOx), from exhaust gases. Sandia National Laboratories operates the facility for the U.S. Department of Energy (DOE).

The process is capable of completely removing NOx from the products of combustion, according to Sandia Livermore scientists Robert A. Perry and Dennis L. Siebers. They say that it "potentially could play a major role in controlling NOx emissions from most combustion devices."

"Nitrogen oxides are major contributors to photochemical smog and are directly implicated in the occurrence of acid rain, particularly in the western United States," explains Perry.

In the newly identified process, a common, nontoxic chemical already in widespread use as a chlorine stabilizer for swimming pool water is inserted into the exhaust stream, and the exhaust gases pass over it. Tests show the process converts the exhaust's nitrogen oxides—the progenitors of smog—into molecular nitrogen and other gases. "If you didn't have NOx, you wouldn't have photochemical smog," says Perry.

Process named RAPRENOx

The new process, invented by Perry, a Sandia chemist, is named rapid reduction of nitrogen oxides (RAPRENOx) and is reported in the December 18 issue of the British journal Nature. In a series of laboratory tests, it has been shown to remove more than 99 percent of the nitrogen oxides present in the exhaust of a small diesel engine. Pollution-control devices based on this invention would use a relatively inexpensive, nontoxic solid as the starting material.

"Potential applications for RAPRENOx range from diesel engines, where it is difficult to meet newly mandated federal particulate and NOx standards, to stationary power plants that burn coal," says Dan L. Hartley, former director of the Combustion Research Facility (CRF), who on November 1 became Sandia's Vice President for Energy Programs. RAPRENOx may also have applications in industrial processes, says Peter L. Mattern, new director of the CRF, although they have not yet been demonstrated.

Sandia spokesmen emphasize that the RAPRENOx concept has been investigated only in the laboratory, in order to prove scientific theory. Further confirma-

tory testing is in progress. However, the technology—including engineering research, the development of chemical devices that could be fitted to commercial engines, and studies of performance under actual driving conditions—does not yet exist. It is anticipated that product-oriented research and development will be carried out in the private industrial sector.

Will be developed commercially

To facilitate this process, the DOE has formally waived its title to the invention in favor of Perry, who plans to leave Sandia and form a company to bring the invention to commercial fruition. The Federal Government, however, retains the right to use the invention, without paying any license fees.

If RAPRENOx is successfully commercialized, it could have an important and positive effect on transportation and heavy industry by providing a practical means to meet federal pollution guidelines. NO_2 is a precursor molecule in the production of photochemical smog. Sunlight splits the nitrogen oxide molecule into nitric oxide plus an oxygen atom. The oxygen atom reacts with oxygen in air to produce ozone, one of the major ingredients in smog.

In the RAPRENOx process, exhaust gas is used to heat cyanuric acid, $C_3N_3(OH)_3$, a harmless compound commonly used as a swimming-pool-water chlorine stabilizer. Heating causes the cyanuric acid to sublime and transform into isocyanic acid, HNCO. The isocyanic acid then mixes with the exhaust gases, reacts with nitrogen oxides, and generates nitrogen, carbon dioxide, carbon monoxide, and water.

The feasibility of applying the RAPRENOx process to exhaust gases to reduce NOx has been explored in an engine experiment using the exhaust gases of a single-cylinder diesel engine. In these initial experiments, nitrogen oxide levels were reduced by at least 99 percent.

An added benefit of the new discovery, according to Mattern, is that it effectively decouples the control of NOx and the particulates (soot) that form during the combustion process in diesel engines. Techniques to reduce NOx tend to increase soot formation; similarly, reducing soot increases the NOx. Now it may be possible to control soot in the engine during combustion and then use the RAPRENOx process outside the engine to control the resulting higher NOx.

Works at lower temperatures

One major advantage of the technique over existing chemical additive technologies is the ability of the process to occur at lower temperatures, less than 600°C. Extensive research, technological development, and testing lie ahead before all the experiments can be confirmed and RAPRENOx can be made publicly available.

The Combustion Research Facility of Sandia National Laboratories is a national facility for studying fundamental problems in energy-related combustion. Staff and visiting scientists from around the world use state-of-the-art laser-diagnostic and computational tools to carry out a vigorous combustion research program.

FOR ADDITIONAL INFORMATI

Public Information Division,
Code 3161,
Dept. of Energy,
Sandia National Laboratories,
Albuquerque, NM 87185-5800
(505) 844-4207.
Refer to announcement 22, No.1

United States
Environmental Protection
Agency

Hazardous Waste Engineering
Research Laboratory
Cincinnati OH 45268

Research and Development

EPA

Project Summary

Geotextiles for Drainage, Gas Venting, and Erosion Control at Hazardous Waste Sites

Geotextiles (engineering fabrics) have proven to be effective materials for solving numerous drainage and stability problems in geotechnical engineering, and they can be used to solve similar problems in the containment and disposal of solid and hazardous waste. "Geotextile" is defined as any permeable synthetic textile product used in geotechnical engineering.

Important mechanical, hydraulic, and endurance properties of fabrics are discussed. Tensile strength and elongation as measured by the grab tensile test; tearing resistance as measured by the trapezoidal tear test; and puncture resistance as measured by the U.S. Army Corps of Engineers puncture test are emphasized as being the most important mechanical properties. Tests for other mechanical properties such as creep susceptibility, tear resistance, frictional and pull-out resistance with soil, and seam strength are also reviewed.

The important hydraulic properties of fabrics are their ability to allow free passage of fluids, to retain soil particles (piping resistance) and to resist clogging. The equivalent opening size (EOS) and gradient ratio tests used to evaluate these qualities are discussed, as well as possible causes of the long-term reduction of fabric hydraulic flow capacity.

Fabric resistance to ultraviolet light and chemicals and to biological degradation is considered .

Applications of geotextiles to (1) landfill cover drains, leachate collection systems, and ground-water control systems; (2) gas venting; and (3) protection of landfill covers and waste disposal sites from surface erosion are addressed in detail. In each of these applications, design considerations, fabric requirements, and construction techniques are discussed. Model specifications for fabrics in the various applications are given. For drainage systems and erosion control, criteria for selecting fabrics based on the fabric's piping and clogging resistance are presented. Strength requirements based on the severity of the construction environment and long-term chemical/biological degradation are addressed.

Introduction

The use of geotextiles (engineering fabrics) has grown from 12.5 million m^2 (15 million yd^2) in 1977 to 115 million m^2 (138 million yd^2) in 1983 in the United States and Canada alone. In spite of this rapidly expanding use of geotextiles, their use and performance in applications related to waste containment and disposal has rarely been documented in the open literature. The information in this report draws on the experiences of the geotechnical field to provide guidance for the use of geotextiles in land waste disposal activities.

A geotextile is defined as any permeable synthetic textile product used in geotechnical engineering. Related products such as plastic grids (geogrids) or composite products such as drainage panels are also

Design of Filters and Drainage Systems

Rules for designing filters and drainage systems using sand and gravel are well established and have been used successfully for many years. When substituted for granular filters in these applications, geotextiles must fulfill the same requirements imposed on granular filters: the fabric must prevent piping of the soil to be drained while remaining sufficiently permeable over the life of the project to prevent the buildup of hydrostatic pressures. There have been numerous approaches to developing filter criteria for geotextiles. At least in the United States, most hydraulic criteria for geotextiles are based in whole or in part on tests and criteria originally proposed by the U.S. Army Corps of Engineers.

Recommended geotextile selection criteria for filtration and drainage applications in hazardous waste landfills are given in the main report and include mechanical, hydraulic, and environmental requirements.

Gas Venting

Thick geotextiles with significant in-place permeability have been used as a venting layer beneath impermeable synthetic membrane liners at liquid impoundments for over a decade. In landfills, gases generated by decomposition of organic matter or volatilization of chemicals can lead to undesirable gas migration with

consequent dangers of explosions and poisoning of people and vegetation. Geotextiles with sufficient gas transmissivity can relieve this problem.

Erosion Control

In landfill cover protection, erosion most commonly occurs in sheet form when vegetative cover is inadequate or in localized areas where rainwater runoff concentrates in surface depressions, swales, and ditches. Removal of cover soils leads to exposure of synthetic membrane covers with consequent deterioration of the cover from ultraviolet light or mechanical damage. Layers of stones or rip-rap (broken rock) can prevent surface erosion on cover slopes or areas of concentrated runoff but these stones must be supported and protected from sinking into the underlying soils. Traditionally, a bedding layer of sand or gravel has been used, but a properly selected geotextile can be substituted for the sand and gravel bedding layer. Generally, fine sands, silty sands, and silts are most susceptible to erosion and are in most need of protection.

In drainage ditches and culvert outlets, fabric should be selected and placed as landfill covers. In cases where erosion potential is less severe, specialized mat-like geotextile related products may be installed as a supplemental root anchor to maintain vegetative cover. This should only be used where vegetative cover can be established to provide adequate permanent protection. Where stone is used in conjunction with geotextiles to line ditches and protect culvert outlets, proper preparation of the soil surface and proper alignment of fabric panels are essential.

The full report was submitted in fulfillment of Interagency Agreement No. AD-96-F-1-400-1 by the U.S. Army Engineer Waterways Experiment Station under sponsorship of the U.S. Environmental Protection Agency.

Raymond C. Horz is with the U.S. Army Engineer Waterways Experiment Station, Vicksburg, MS 39180.
***Jamet M. Houthoofd** is the EPA Project Officer (see below).*
The complete report, entitled "Geotextiles for Drainage, Gas Venting, and Erosion Control at Hazardous Waste Sites," (Order No. PB 87-129 557/AS; Cost: $18.95, subject to change) will be available only from:
National Technical Information Service
5285 Port Royal Road
Springfield, VA 22161
Telephone: 703-487-4650
The EPA Project Officer can be contacted at:
Hazardous Waste Engineering Research Laboratory
U.S. Environmental Protection Agency
Cincinnati, OH 45268

energygram

Waste Characterization and Analysis Activities in Support of the INEL Solidification Development Program

DOE/TIC/EG-86/126
OFFICE OF SCIENTIFIC AND TECHNICAL INFORMATION

This technical note was based on research conducted by Idaho National Engineering Laboratory for the U.S. Department of Energy.

INEL
Idaho National Engineering Laboratory

EG&G Idaho, Inc., has initiated a program to develop safe, efficient, cost-effective solidification treatment methods for disposal of some of the hazardous and mixed wastes generated at the facility. An integral part of the solidification program is the identification and evaluation of waste streams. The results of the waste characterization and analysis activity conducted in support of the solidification development are presented in this report.

The waste identification, characterization, and treatment options evaluation activities discussed were conducted in support of the solidification development program. The identification portion of the study resulted in a listing of the hazardous and radioactive mixed wastes generated at Idaho National Engineering Laboratory (INEL). Each of the wastes was characterized as to the nature of the hazard it presents [extraction procedure (EP) toxic, corrosive, ignitable, etc.]. The next phase of the waste characterization was the evaluation of treatment options for each waste.

In general, EP toxic wastes were determined to be candidates for solidification processing. Corrosive wastes were also included as solidification candidates because detailed analysis may show EP toxic constituents in excess of the limits in the wastes after neutralization.

Solidification processing is the best method of disposition available for EP toxic or corrosive wastes with metal contents in excess of the limits. Solidification processing provides a stable waste form for disposal by chemically binding the metals to the cement matrix. This prevents the metals from leaching out of the solidified waste monolith and thus enables the waste form to pass leach tests. Once the solidified waste has passed the leach tests, it can be disposed of as a nonhazardous or low-level waste, depending on its radioactivity.

The report deals with a wide spectrum of wastes generated at INEL. Apart from radioactive components of the mixed wastes, most of the materials discussed in this report are commonly found in industry, and the information presented is of immediate value to waste disposal organizations and regulatory authorities as a comprehensive reference.

FOR ADDITIONAL INFORMATION

DOE report(s):
Waste Characterization and Analysis Activities Conducted in Support of the Solidification Development Program at the Idaho National Engineering Laboratory.
Report number EGG-WM-7175/NAB
Order number DE86011046/NAB
Price: $16.95

Order from:
National Technical Information Service
5285 Port Royal Road
Springfield, VA 22161

For additional information contact
J. M. Welch
EG&G Idaho, Inc.
P.O. Box 1625
Idaho Falls, ID 83415
Telephone No. (208) 526-8318

or

A. M. Boehmer
EG&G Idaho, Inc.
P.O. Box 1625
Idaho Falls, ID 83415
Telephone No. (208) 526-8060

NAVY
Domestic Technology Transfer Fact Sheet

Air Monitoring Device Developed
New meter measures light scattered by particulates.

A Naval Research Laboratory (NRL) scientist has developed a compact and inexpensive device for effectively monitoring particulates, such as in smoke, dust, pollution, fog, and clouds.

The device, a forward scatter meter, should prove to be a valuable sensor aboard Navy ships for measuring the optical quality of the atmosphere in the far infrared. The meter should also be useful in private industry as a method for monitoring various particulates, such as in pollution from smokestacks.

The meter measures the light scattered by the suspended particulates out of a light beam and into the near-forward direction. This scattered light is proportional to the volume or mass of the particulate matter.

Even though the light beam is generated with a helium neon laser operating at a visible wavelength, the scattered light can also be scaled to the far infrared to give a useful estimate of the infrared attenuation due to the particulates. This capability will be useful aboard Navy ships where infrared systems are used for navigation and landings on aircraft carriers during nighttime and poor visibility conditions. The meter will allow sailors to better judge the transparency of the atmosphere in the infrared, a factor that is sometimes crucial for safe landings.

The new meter is an improvement over the current Navy practice of estimating infrared transparency in the vicinity of ships from existing meteorological conditions. The meter, which has passed extensive testing, is being incorporated into a new naval environmental sensing package which will be installed in the Fleet in the near future.

For Additional Information:

Backup material on this effort is available from:

Navy Domestic Technology Fact Sheet
Reader Reply Service
Code E211
Naval Surface Weapons Center
Dahlgren, VA 22448-5000
(703) 663-8921

Refer to 120101/TN

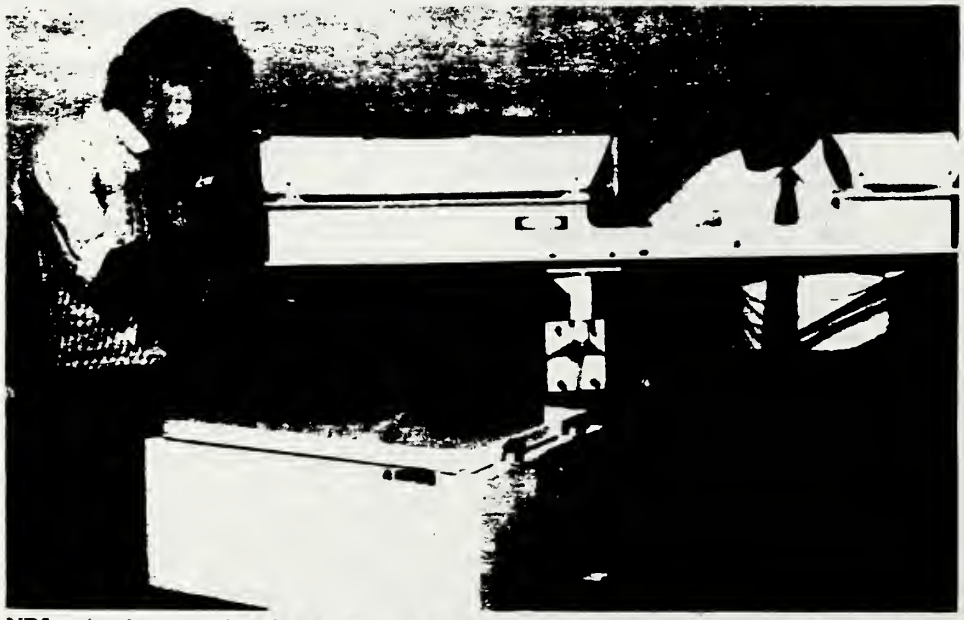

NRL scientists examine the device. The device monitors the quality of the atmosphere.

Manufacturing, Machinery, & Tools

661 Low-Loss Coherent Fiber-Optic Arrays—Multifibers can be made from fused silica glass.

662 Robot Carts Given Flexibility with New Software

663 Part Geometry Data Used to Direct Robot Deburring

664 Cleaner Vacuum-Bag Curing—An improvement upon recommended procedures saves time and expense. (Licensing Opportunity)

665 Hot-Air-Pulse Generator—Mixer blades interrupt airflow for rapid testing of insulating materials.

666 Remotely Adjustable Hydraulic Pump—Outlet pressure can be adjusted to match varying loads. (Licensing Opportunity)

667 Local Data Processing for a Robot Hand—Integrated-circuit microcomputers process signals among sensors, external controls, and the end-effector motor.

668 Simplified Explosive Joining of Tubes to Fittings—A ribbon explosive and mild detonating fuse allow the use of a smaller charge. (Licensing Opportunity)

Software

669 NASA Test File—Comparisons among different computer-aided design systems are facilitated.

Testing & Instrumentation

670 Screening Mechanically-Defective Solar Cells—A flexure test eliminates failure-prone wafers before further processing.

671 Eddy-Current Detection of Weak Bolt Heads—An electronic test identifies flawed units that pass hardness tests.

672 Eddy-Current Detection of Cracks in Tubes—A nondestructive device tests narrow, sharply-bent metal tubes.

673 Measuring Hole Elongation in Bolted Joints—The measurement does not affect joint parameters. (Licensing Opportunity)

Other items of interest

633 Millimeter-Wave Traveling-Wave-Tubes Circuits Produced at Reduced Costs

677 Rubber-Processing Studies—Processing of natural rubber and styrene/butadiene was studied.

682 Fast-Response Heating of Silicon Melts—Heating would be confined to a small mass near the growing crystal.

MANUFACTURING TECHNOLOGY NOTE

U.S. ARMY MATERIEL COMMAND

Deputy Chief of Staff for Manufacturing Technology, Alexandria, VA

Project Number: NONE

Filing Code: 48C087

Low-Loss Coherent Fiber-Optic Arrays

Multifibers can be made from fused silica glass.

A study has demonstrated the feasibility of fabricating coherent fiber-optic bundles from fused silica by producing 36-element 60-micron-square multifiber, the basic building block for coherent fiber-optic bundles. Such bundles have application in advanced electro-optic imaging systems. However, conventional silicate-glass fiber-optics is limited in these applications by high light attenuation coefficients (up to 2000 dB/km). Fused silica fiber, with its low attenuation (1 to 50 dB/km), offers substantial improvement.

The study, which was done for the U.S. Army Ballistic Research Laboratory, showed that the mechanics of multifiber drawing is a straightforward extension of the technology previously developed for mixed silicate glasses. The study also identified the preform requirements for both mechanical and optical performance of the multifiber. The preferred preform consists of a germanium-doped fused silica core with a pure fused silica optical cladding and has an outside diameter-to corediameter ratio of 1.4.

The drawing of multifiber comprises three steps:

1. Drawing cane
2. Laying up the cane into an array, and
3. Drawing the array into multifiber.

The cane is drawn from the preform down to a diameter of 1.5 millimeter in 1-meter lengths. The cane is assembled in a 6- by 6-element square array. The individual cane elements fuse together in the hot zone of the draw furnace to form a solid square fiber. The resulting 60-micron multifiber has 36 8-micron optical cores held together in a matrix of low-index cladding material. The secret to drawing good-quality square multifiber is to find a combination of draw speed and temperature that permits consolidation of the elements without distortion.

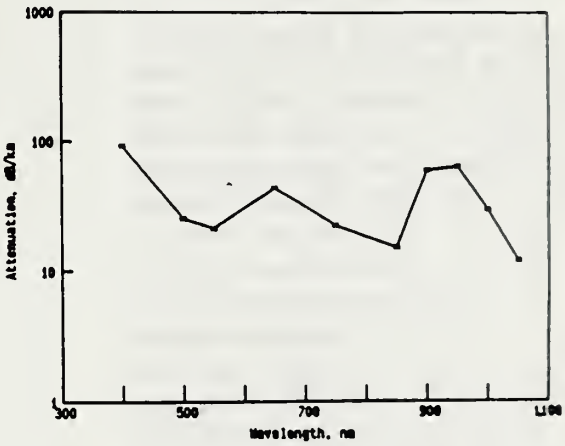

Attenuation is plotted against wavelength for a 100-micron fused-silica monofiber. The fiber exhibits attenuation through the visible and near-infrared region of about 20 to 40 dB/km.

FOR ADDITIONAL INFORMATION:

You can learn more details about this technology by ordering the NTIS reports:

Feasibility of Making Coherent Fiber-Optic Arrays from Fused Silica.
Order number: AD-A170873/NAA
Price code: A02

Order from:
National Technical Information Service
5285 Port Royal Road
Springfield, VA 22161

This document was prepared under the sponsorship of the U.S. Government. Neither the United States Government nor any person acting on behalf of the United States Government assumes any liability resulting from the use of the information contained in this document, or warrants that such use will be free from privately owned rights.

Robot Carts Given Flexibility with New Software

New software incorporated into a commercial AGV system by NBS engineers provide a high degree of flexibility and ease in establishing new movement and load patterns.

The robot carts transport trays of raw materials, part blanks, tools and finished parts in and out of storage units and between AMRF workstations. The carts are able to load and unload from both sides and to leave their guide-wire track for as much as ten feet to perform "patterned" movements.

The two robot carts are part of the newly completed Material Handling Workstation. This system was first demonstrated during the September 1986 test run of the facility and further refined for the December test run. It controls the movement and storage of all materials and finished parts throughout the AMRF.

Remote programming, an NBS modification to the orignal cart architecture, allows changes in the cart programs to be made quickly and easily. Message sets, written as regular text files and run on an ordinary personal computer provide instructions which the carts can follow. Prior to this modification, fixed behavior patterns had to be programmed into ROMs in the computer of the cart.

An added capability of the carts permits them to automatically dispatch themselves to a recharging station when their batteries are low.

In addition to the two robot carts moving about the facility, components of the Material Handling Workstation are located throughout the AMRF. The workstation has an automated storage and retrieval system consisting of six Kardex Industiever 8000 units. Each unit holds 34 trays. A smaller Kardex system for material buffering is located at the Horizontal Workstation, and roller tables to receive and load trays are located at the other workstations.

For Additional Information:

To discuss this effort further, contact:

Carl Wenger
AMRF Project Manager
Building 220—Room B-246
National Bureau of Standards
Gaithersburg, MD 20899
(301) 975-3553

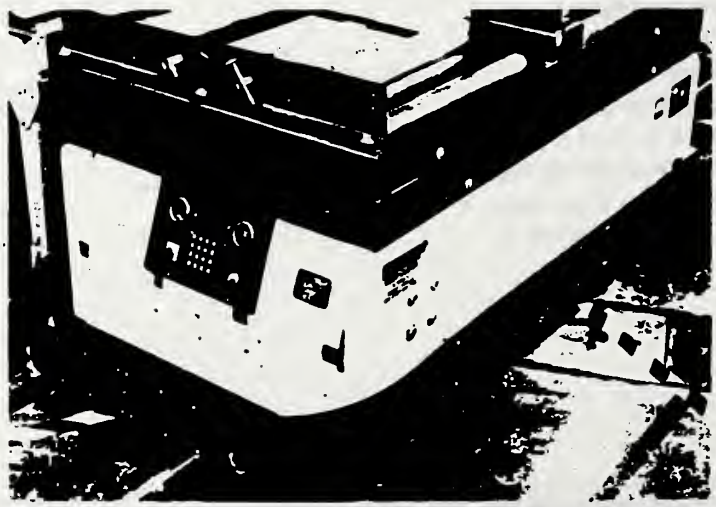

ROBOT CART OF THE AMRF AS IT EXCHANGES A TRAY-LOAD OF FINISHED PARTS FOR A TRAY-LOAD OF BLANKS. THIS CART CAN LEAVE ITS GUIDE WIRE FOR EXTENDED COMPLEX MANEUVERS.

Part Geometry Data Used to Direct Robot Deburring

Part description data from the AMRF Geometry Modeling database is being used to generate a robot path for deburring parts at the AMRF's Cleaning and Deburring Workstation. Once an operator selects the sequence of edges to be deburred, the computer automatically generates commands which define the robot's path.

Robots used in automated deburring generally do repeatable, high-quality work but require substantial teaching by a programmer. The programmer must move the robot from point-to-point along the edge to be deburred while the robot's controller records the measurements necessary and the movements required to follow the edge to be deburred. This training process must be repeated for each edge selected.

In contrast, researchers at the Cleaning and Deburring Workstation select edges from a CAD-based visual representation of the part by clicking a "mouse". The workstation controller uses parts data from the CAD system to determine the set of steps to carry out the task. This set of steps is called the process plan.

The workstation controller coordinates the movements of the workstations's two robots, a Unimate 2000 and a Puma 760. While the Unimate 2000 is picking up the part and placing it in the vise, the Puma is acquiring the proper tool. The Puma controller determines joint angles and movements required to carry out the process plan.

The complete deburring process, from edge selection to finished part, takes only minutes. New edges can be selected easily from the workstation's computer screen using the geometry model. Researchers are currently blending with this CAD-directed approach their recent success using sensors to help the robot locate edges and "feel" its path along an edge. By applying the results of studies of parameters such as part material, contact force, feed rate, tool speed and cutter type, researchers are working to increase the accuracy of the robot in following edges.

For Additional Information:

To discuss this effort further, contact:

Rick Norcross
AMRF Project Manager
Building 220—Room B-127
National Bureau of Standards
Gaithersburg, MD 20899
(301) 975-3440

NASA Tech Brief
National Aeronautics and Space Administration
Marshall Space Flight Center, Alabama

Licensing Opportunity

Cleaner Vacuum-Bag Curing

An improvement upon recommended procedures saves time and expense.

A caul plate used in vacuum-bag curing can become more easily reusable by a simple extra step in setting up the bag. Ordinarily, a caul, which covers and protects a laminated composite panel during curing, is coated with resin when removed from the bag. Removing the coating is nearly impossible; it is more economical to discard the caul, even though a new plate must then be prepared for the next cure. Moreover, the resin on the caul also sticks to the composite panel and delays removal of the panel.

The problem is eliminated by covering the face and edges of the caul plate with adhesive-backed polytetrafluoroethylene sheet (see figure). (Interestingly, documents spelling out the procedure for vacuum-bag curing recommend a polytetrafluoroethylene cover for the lower press platen but not for the caul plate.) The added polytetrafluoroethylene sheet has a smooth surface, to which the resin will not adhere. This enables the caul plate to be reused and shortens the time needed to remove the panel from the curing assembly. The extra step in no way detracts from the properties of the cured panel.

This work was done by Johnny M. Clemons, Benjamin G. Penn, Frank E. Ledbetter, III, and Julia G. Daniels of **Marshall Space Flight Center**. *No further documentation is available.*

Inquiries concerning rights for the commercial use of this invention should be addressed to the Patent Counsel, Marshall Space Flight Center Refer to MFS-28071 /TN

George C. Marshall Space Flight Center
Technology Utilization Officer:
Ismail Akbay
Code AT01
Marshall Space Flight Center, AL 35812
(205) 544-2223
Patent Counsel:
Leon D. Wofford, Jr.
Mail Code CC01
Marshall Space Flight Center, AL 35812
(205) 544-0014

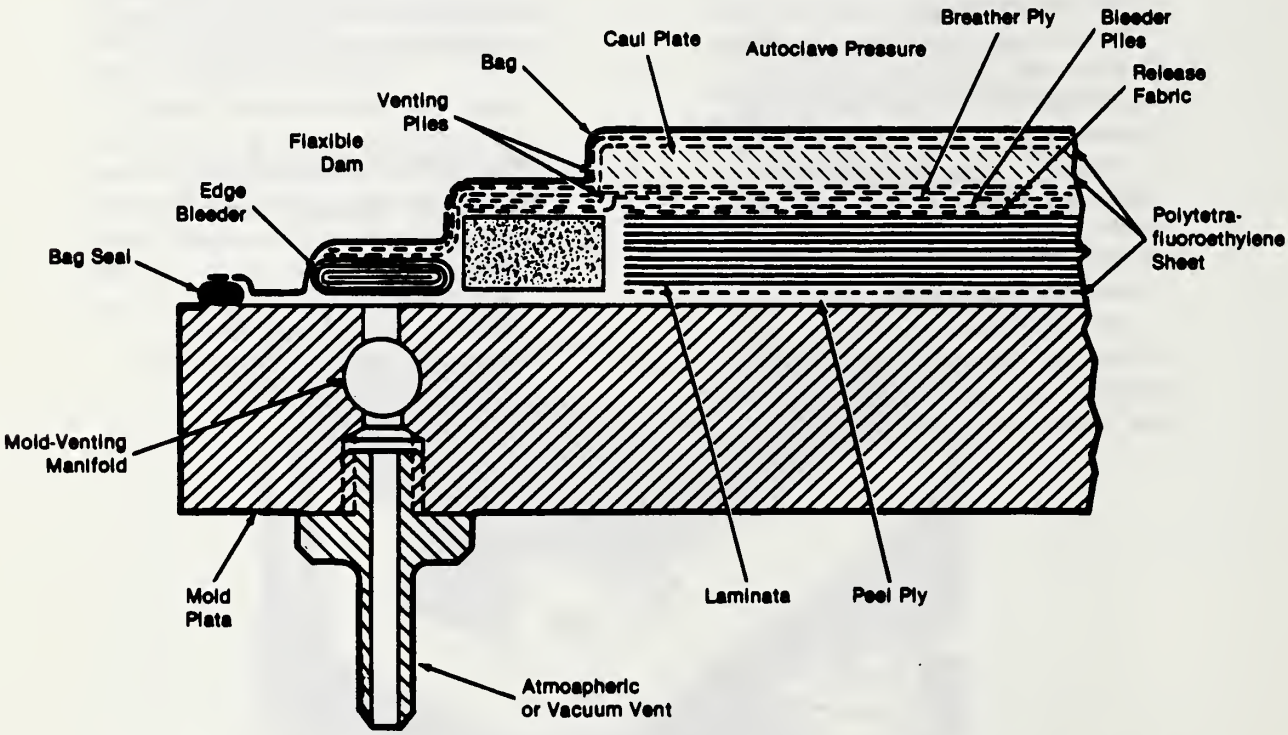

Autoclave Molding in a vacuum bag is cleaner if an adhesive-backed covering (color) is placed around the caul plate as well as on the mold plate. The covering is easy to remove after curing and leaves the caul plate free of resin deposits.

FOR ADDITIONAL INFORMATION: *Contact: Director, Technology Transfer Division, P.O. Box 8757, BWI Airport, MD. 21240; (301) 621-0100 Ext. 241*
REFER TO THE NUMBER LISTED AT THE END OF THE ARTICLE

NASA Tech Brief
National Aeronautics and
Space Administration
Lyndon B. Johnson Space Center, Houston, Texas

Hot-Air-Pulse Generator

Mixer blades interrupt airflow for rapid testing of insulating materials.

A device for producing periodic blasts of heated air can be used for rapid testing of flexible insulating materials. The device can be used to compare materials and to select candidates for more detailed testing in wind tunnels.

An electric paint mixer is positioned so that its propeller is at the outlet of a hot-air-jet nozzle (see Figure 1). The propeller blades are flattened and oriented perpendicularly to the jet; they thus interrupt the jet when they pass the orifice. Between interruptions, the hot air strikes the surface of the specimen.

The propeller speed is adjusted with the aid of a stroboscope. The pulse rate can be varied up to 85 Hz. The strobe is then set to a slightly different frequency so that the effects of the pulsating jet on the tested article can be observed. Figure 2 shows some nozzle parameters used in typical test setups.

This work was done by Mark C. Ammerman of Rockwell International Corp. for **Johnson Space Center**. *No further documentation is available.*
MSC-20768 /TN

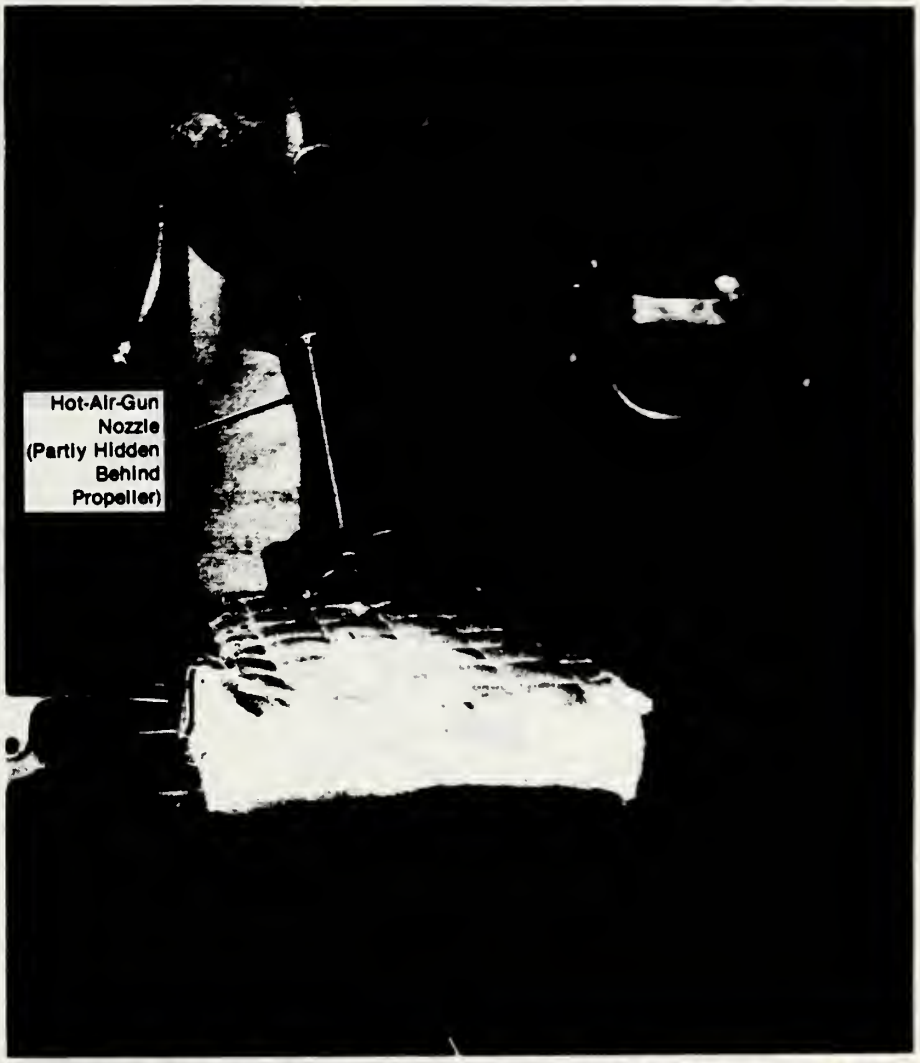

Figure 1. A **Bat of Flexible Insulation** is tested in the air-pulse apparatus. The orifice of the hot-air jet is periodically obstructed by the propeller of the mixer.

Note: Dimensions are in inches (millimeters)

	W	H
1/4 (6.4) O.D. Nozzle	0.30 (7.6)	0.06 (1.5)
3/16 (4.8) O.D. Nozzle	0.22 (5.6)	0.06 (1.5)
1/2 (12.7) O.D. Nozzle	0.70 (17.8)	0.05 (1.3)

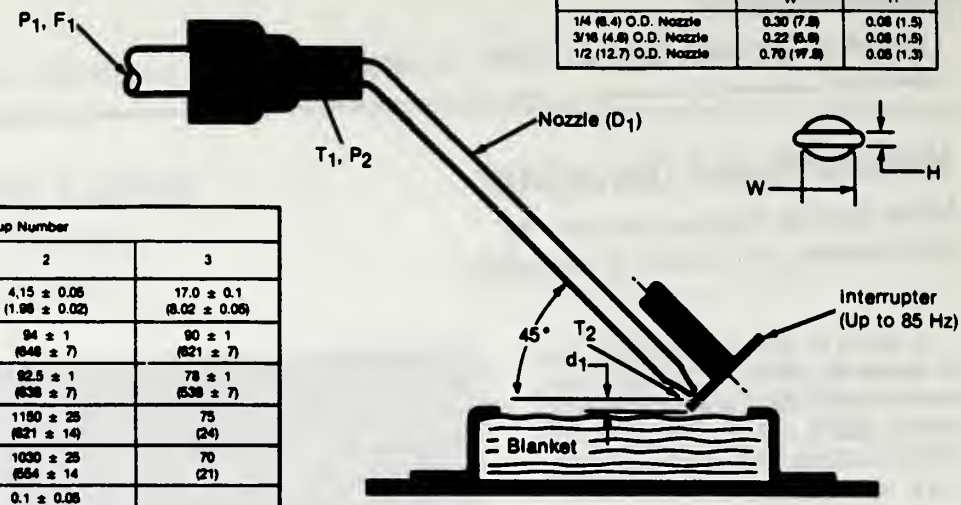

Parameter	Setup Number 1	2	3
F_1	4.5 ± 0.1 (2.1 ± 0.05)	4.15 ± 0.05 (1.96 ± 0.02)	17.0 ± 0.1 (8.02 ± 0.05)
P_1	45 ± 2 (310 ± 14)	94 ± 1 (648 ± 7)	90 ± 1 (621 ± 7)
P_2	42 ± 2 (290 ± 14)	92.5 ± 1 (638 ± 7)	78 ± 1 (538 ± 7)
T_1	1150 ± 50 (621 ± 28)	1150 ± 25 (621 ± 14)	75 (24)
T_2	1050 ± 50 (566 ± 28)	1030 ± 25 (554 ± 14	70 (21)
d_1	1/16 (1.5) (FIXED) 0.05 (1.3) TO 0.2 (5.1) 1-Hz Oscillation	0.1 ± 0.05 (FIXED) 0.05 (1.3 TO 0.2 (5.1) 1-Hz Oscillation	0.46 (11.7)
D_1	1/4 (6.4)	3/16 (4.8)	1/2 (12.7)
W	0.30 (7.6)	0.22 (5.6)	0.7 (17.8)
H	0.06 (1.5)	0.06 (1.5)	0.05 (1.3)
V	1,150 (514)	1,150 (648)	800 (358)
ν	0.079 (0.54)	0.129 (0.89)	?

Definitions

F_1 = Gas Flow Rate, scfm (l/s)
P_1 = Line Pressure, psi (kPa)
P_2 = Nozzle Inlet Pressure, psi (kPa)
T_1 = Nozzle Inlet Temperature °F(°C)
T_2 = Nozzle Exit Temperature °F(°C)
d_1 = Nozzle Distance From Blanket
D_1 = Nozzle O.D.
V = Nozzle Exit Velocity, mi/h (m/s)
ν = Theoretical Surface Shear, psi (kPa)

Figure 2. Some Nozzle Parameters were determined for typical test setups.

FOR ADDITIONAL INFORMATION: *Contact: Director, Technology Transfer Division, P.O. Box 8757, BWI Airport, MD. 21240; (301) 621-0100 Ext. 241*

REFER TO THE NUMBER LISTED AT THE END OF THE ARTICLE

NASA Tech Brief
National Aeronautics and Space Administration
Lyndon B. Johnson Space Center, Houston, Texas

Licensing Opportunity

Remotely Adjustable Hydraulic Pump

Outlet pressure can be adjusted to match varying loads.

The outlet pressure of a hydraulic pump can be adjusted remotely while the pump is operating. The pump can be used in aircraft and robots, for example, where hydraulic actuators are repeatedly turned on and off, changing the pump load frequently and over a wide range. The pump pressure can be reset as often as necessary to ensure adequate — but not excessive — pressure.

The pump pressure does not have to be preset for the worst case — all actuators operating simultaneously, a condition that may prevail only briefly. It therefore does not demand as much energy from its motor drive. Moreover, it is not necessary to reduce the high worst-case pressure for its regulation mechanism, and its internal leakage is less. The remotely controllable pump is therefore more efficient than are conventional pumps.

The pump is a variable-displacement, pressure-compensated type. It contains a hydraulically-operated pressure-regulation mechanism and an electrically-operated pressure-adjustment mechanism.

Pistons in a motor-driven barrel slide on an inclined plate as the barrel rotates (see figure). Following the plate surface, the pistons reciprocate in bores in the barrel with each revolution. As they reciprocate, the pistons draw in hydraulic fluid at low pressure from an inlet port and expel it at high pressure from an outlet port.

Hydraulic feedback maintains the outlet pressure at a nearly constant value by altering the angle of the inclined plate as necessary. A small passage connects the pump-outlet port with a spool bore inside the regulator. There the pressure acts on the right side of a control land on the sliding spool, opposing the compensator-spring pressure acting on the left side of the spool.

If the pressure at the pump outlet drops, the compensator spring forces the spool to the right. The rightward movement of the control land uncovers a control port and reduces the pressure on the control piston. The control piston moves upward. The inclined plate is forced by a tilting spring to follow the piston, so that the angle of the inclined plate increases. The displacement of the pump is thereby increased, and its outlet pressure rises.

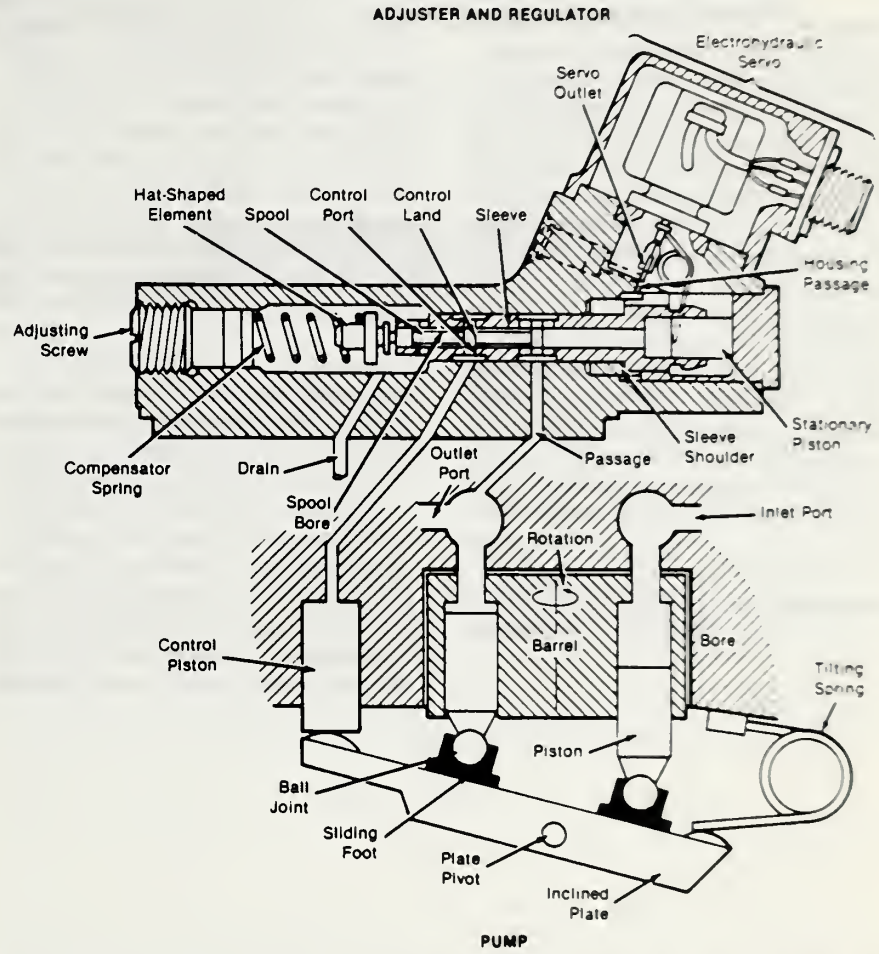

The Electrohydraulic Servo Has Positioned the Sleeve in its leftmost position, thereby adjusting the outlet pressure to the maximum value. The sleeve is in an equilibrium position, with the control land covering the control port. For the lowest pressure setting, the sleeve would be shifted toward the right by increased pressure on the sleeve shoulder from the servovalve.

As the pressure in the spool bore simultaneously rises, it returns the control land to its original position, closing the port once more and returning the system to equilibrium. For overpressure at the pump outlet, the regulator works in reverse, decreasing the tilt angle and reducing the outlet pressure.

Meanwhile, the pressure-adjusting

mechanism is an electrohydraulic servovalve. It continuously supplies hydraulic fluid at the pump-outlet pressure through a passage in the housing to a shoulder on the sleeve that forms the spool bore. To change the outlet pressure, an operator or an automatic controller changes the electric current to the servomotor. This changes the output pressure of the servo and the pressure on the sleeve shoulder, thereby shifting the sleeve with respect to the compensating spring.

To increase the outlet-pressure setting, the operator decreases the servocurrent. The servo decreases the pressure on the shoulder and thereby allows the outlet pressure between the stationary piston and the sleeve to push the sleeve to the left. This moves the control port to the left. The outlet pressure on the spool must then compress the compensator spring farther to move the control land past the control port. Thus, the control piston will not push the inclined plate down to decrease the pump displacement until a higher outlet pressure is reached. In a similar but opposite manner, the outlet-pressure setting is reduced when the servocurrent is increased.

This work was done by Herbert H. Kouns and Loren D. Gardner of Abex Corp. for **Johnson Space Center**.

Title to this invention has been waived under the provisions of the National Aeronautics and Space Act [42 U.S.C 2457 (f)], to the Abex Corp. Inquiries concerning licenses for its commercial development should be addressed to:

Abex Corp.
P.O. Box 10268
Stamford, CT 06904-2268

Refer to MSC-21007,

Lyndon B. Johnson Space Center
Technology Utilization Officer:
Dean C. Glenn
Mail Code EA4
Houston, TX 77058
(713) 483-3809
Patent Counsel:
Edward K. Fein
Mail Code AL3
Houston, TX 77058
(713) 483-4871

FOR ADDITIONAL INFORMATION: *Contact: Director, Technology Transfer Division, P.O. Box 8757, BWI Airport, MD. 21240; (301) 621-0100 Ext. 241*

REFER TO THE NUMBER LISTED AT THE END OF THE ARTICLE

NASA Tech Brief
National Aeronautics and
Space Administration
NASA's Jet Propulsion Laboratory, Pasadena, California

Local Data Processing for a Robot Hand

Integrated-circuit microcomputers process signals among sensors, external controls, and the end-effector motor.

A multiple-microprocessor system within the end effector of a remote manipulator accepts data from sensors in the end effector, communicates with the external control system, and controls the end-effector motor. The external system includes a central control computer (which interacts with the operator) and a display.

The electronic system in the end effector (see figure) is based on a distributed-microcomputer architecture, using high-level, multifunctional, monolithic integrated circuits. The architecture minimizes the chip count. A single-chip data-acquisition system accepts the analog signals from sensors, amplifies them, samples and holds them, and finally converts them to digital form. A pair of single-chip microcomputers equipped with input/output ports for serial data constitutes the heart of the communication subsystem. A third microcomputer chip controls the hand motor and turns the sensors on and off.

The chips are on three printed-circuit cards — one disk-shaped to fit behind the end-effector motor and the others annular to fit around the motor. Seven sliprings at the wrist connect the hand electronics with the rest of the manipulator system. Four sliprings carry power at 24 Vdc and 50 Vac. One ring is for bidirectional sensor data-communication. One is for bidirectional control-data communication. The remaining ring is for the system ground.

The communication microprocessor and the motor-control microprocessor constitute the end-effector subsystem. In addition to accepting serial input and providing serial output, the communication chip checks for transmission errors.

External commands from the central computer pass through the communication chip to the motor-control chip. These commands specify the final position of the claws on the end effector, the maximum-allowable claw closing speed, and the desired claw-gripping force. The motor-control chip uses sensor data and closed-loop feedback from the force, position, and speed sensors to ensure that the end effector follows the commands accurately. Once every millisecond, the chip calculates the proper width of the power pulses, which are then sent to the motor.

The chip in the sensor subsystem includes a 16-channel commercial data-acquisition system. A separate multiplexer provides access to the proximity-detector readings and feeds them to the data-acquisition chip, allowing it to accommodate a total of 27 analog channels of torque, proximity, force, and position data. It sends the sensor readings as 12-parallel-bit data to the external control system.

This work was done by Antal K. Bejczy of Caltech for **NASA's Jet Propulsion Laboratory**. *NPO-16695 /TN*

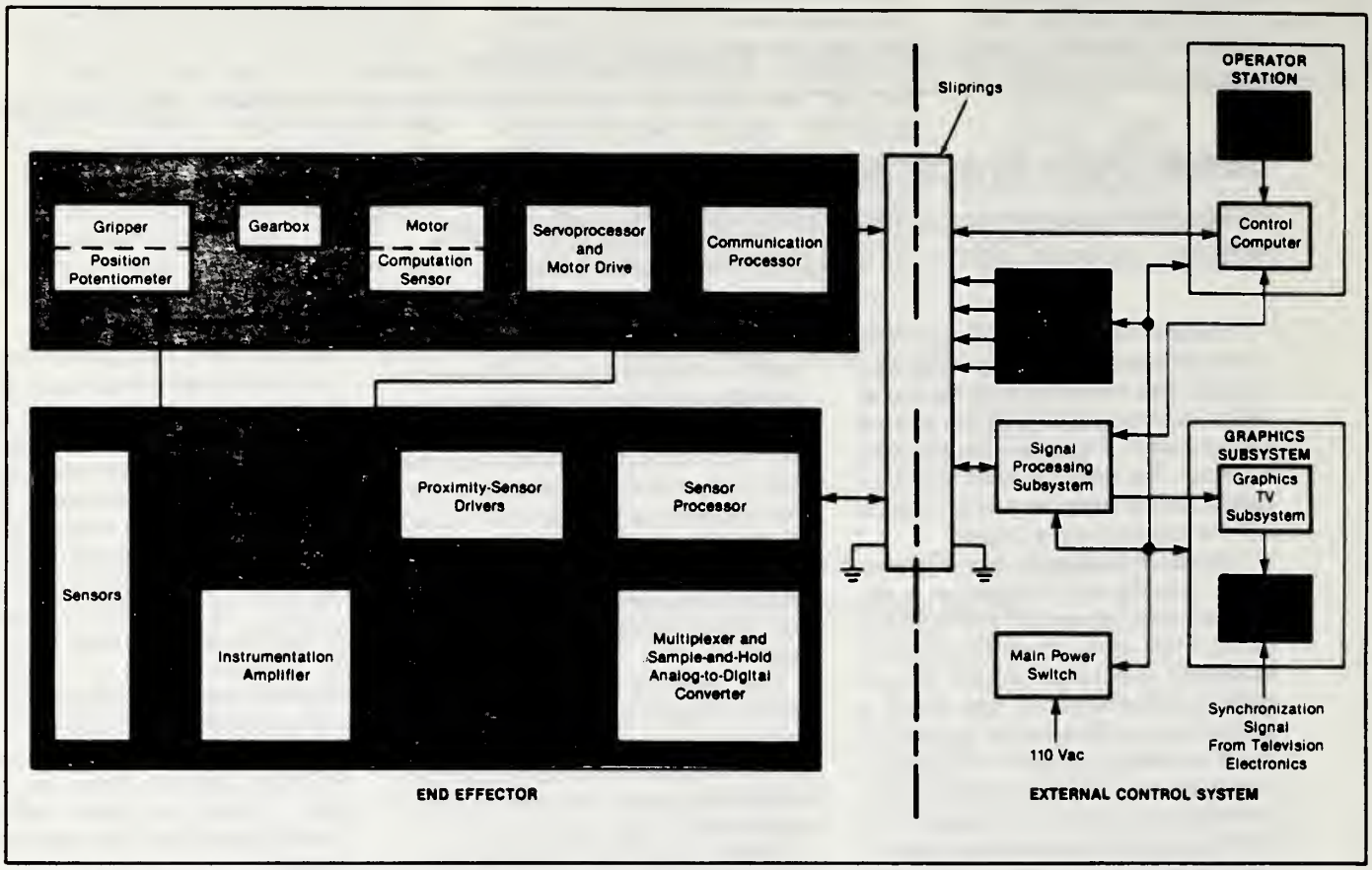

The **Local Data-Processing System in the End Effector** (left) relieves the external control system (right) of some of its computational load and minimizes data communication load with the external higher level controller.

FOR ADDITIONAL INFORMATION: *Contact: Director, Technology Transfer Division, P.O. Box 8757, BWI Airport, MD. 21240; (301) 621-0100 Ext. 241*

REFER TO THE NUMBER LISTED AT THE END OF THE ARTICLE

NASA Tech Brief
National Aeronautics and Space Administration
Langley Research Center, Hampton, Virginia

Licensing Opportunity

Simplified Explosive Joining of Tubes to Fittings

A ribbon explosive and mild detonating fuse allow the use of a smaller charge.

This technique simplifies tube-to-fitting joining, as compared to fusion welding, and provides an improvement on the standard procedures used to join tubes explosively to tube fittings. A special tool is inserted into the tube to be joined. This tool allows a strip of ribbon explosive to be placed right at the joint.

The state-of-the-art explosive joining of tubing has relied on the loading of a granulated explosive into the tube by means of a short plug. The use of the special tool with a ribbon explosive and a mild detonating fuse (MDF) and tube initiator requires much less explosive to achieve a metallurgical bond, thereby reducing collateral damage to the tube itself. The bond can be enhanced by machining a V-shaped notch into the fitting prior to joining. The joint thus created exhibits parent-material properties and is hermetically sealed.

The tool and process can be used when tube diameters are 0.20 inch (5.1 millimeters) and higher. The 0.20-inch lower limit is based on the physical restrictions imposed by the diameter of the initiator and the minimum diameter to which the ribbon explosive can be wrapped without causing the breakup of the explosive load. The initiator uses an open-ended steel cylinder (booster sleeve) loaded with explosive, allowing the insertion of an MDF in each end. To enhance safety, this process uses only secondary explosives; i.e., those explosives that require an explosive input, not a flame, for initiation. Therefore, complete assembly of the tool with maximum safety is possible before a blasting cap is introduced to effect initiation.

Larger diameter tubes can accommodate an electrical blasting cap to simplify the initiation system, where safety procedures can be enhanced.

The tool and process can be modified to join a tube within a cylindrical interface for repair or strengthening.

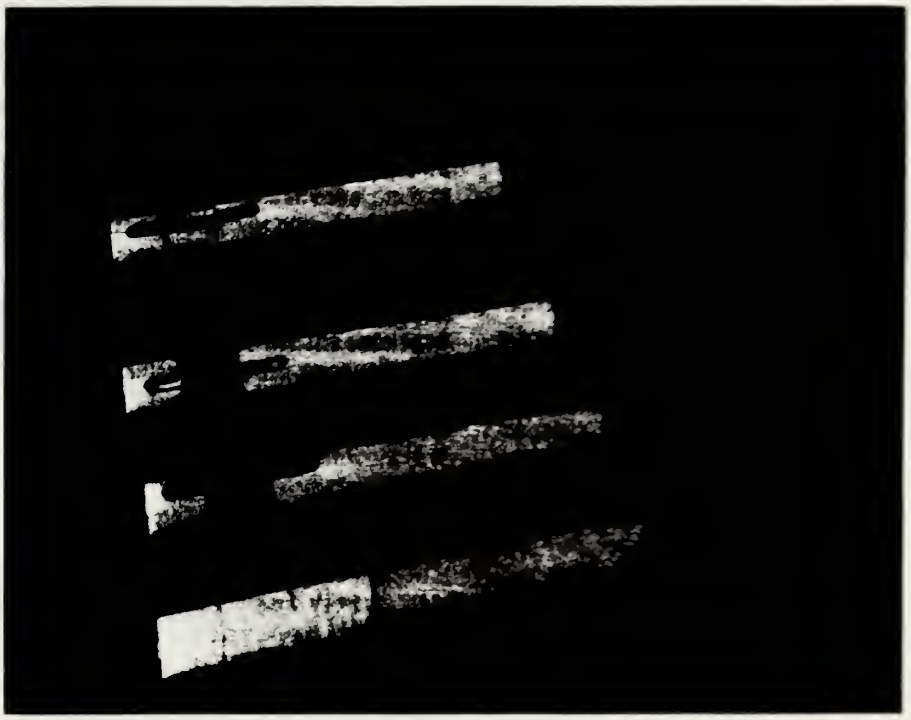

The **Components of the Joining Tool** and process are, from the top: the tube and MDF initiator, tool, ribbon explosive, ribbon explosive on tool, and assembled tool wrapped with polytetrafluoroethylene tape or heat-shrink tubing (used to size the tube exactly).

Also, the tool with two ribbon explosives and two initiators could be inserted into an internal tube configured to provide the necessary explosive-joining interface. In this way, any number of joints can be made with any number of tubes.

The assembled tool is storable, and the process is amenable to automation. The assembly of the components, insertion of the tool into the weld site, and the joining operation could be mechanized without human contact. This technique is being considered for assembly of tubes into a heat exchanger in the Space Shuttle main engine. It could also be used to assemble components in nuclear reactors or in other environments hostile to humans.

This work was done by Laurence J. Bement of **Langley Research Center** *and James W. Bailey, Ronnie Perry, and Marvin S. Finch of Kentron International, Inc.*

This invention is owned by NASA, and a patent application has been filed. Inquiries concerning nonexclusive or exclusive license for its commercial development should be addressed to the Patent Counsel, Langley Research Center. Refer to LAR-13309 /TN

Langley Research Center
Technology Utilization Officer
John Samos
Mail Stop 139A
Hampton, VA 23665
(804) 865-3281
Patent Counsel:
Howard J. Osborn
Mail Code 279
Hampton, VA 23665
(804) 865-3725

FOR ADDITIONAL INFORMATION: *Contact: Director, Technology Transfer Division, P.O. Box 8757, BWI Airport, MD. 21240; (301) 621-0100 Ext. 241*
REFER TO THE NUMBER LISTED AT THE END OF THE ARTICLE

NASA Test File

Comparisons among different computer-aided design systems are facilitated.

The Test File is a data file containing computer-aided design (CAD) data formatted according to the National Bureau of Standards Initial Graphic Exchange Specification (IGES). This file was created for the purpose of conducting NASA tests to determine to what extent dissimilar CAD systems can exchange data using the IGES standard formats and IGES translators.

The IGES Test File is used to test IGES translators by converting the IGES format data to and from the native internal format of the CAD system. The file contains 28 different IGES entitles, which were chosen because they define the geometric, annotation, and display-formatting information that is important in CAD information transfer. The documentation contains a procedure for using the file to test IGES translators, along with sample output of the scaled, rotated, and translated entities. It has been verified by an independent company that the file does indeed conform to Version 2.0 of the IGES standard.

These data are in ASCII code and are machine-independent. The file was created in 1985.

This program was written by Scott Gordon of **Goddard Space Flight Center.** *GSC-12988 /TN*

FOR ADDITIONAL INFORMATION

CONTACT:

COSMIC®
112 Barrow Hall
University of Georgia
Athens, GA 30602
(404) 542-3265

NASA Tech Brief
National Aeronautics and
Space Administration

Screening Mechanically-Defective Solar Cells

A flexure test eliminates failure-prone wafers before further processing.

The probability of cracking of silicon solar cells can be substantially reduced by mechanical proof testing of silicon wafers before further processing, according to a report. The report is based on a study that demonstrated that weak wafers can be eliminated by subjecting all the wafers in a manufacturing batch to a biaxial-flexure test.

The test is performed after the wafers have been chemically polished but before junctions are formed in them. Wafers that are likely to crack in service or during processing break as soon as they are flexed in a test jig. Those wafers having no internal flaws that would eventually cause mechanical failure withstand the flexure test.

The study showed that the biaxial-flexure test does not induce additional damage in otherwise good wafers; that is, if a wafer is sound, the testing does not create flaws that would later weaken the specimen.

The experimental results were analyzed statistically. The biaxial-strength distribution of silicon wafers that failed from surface flaws was found to correspond to a Weibull equation. The critical flaw sizes were found to be 4.6, 3.1, and 2.1 μm for proof-testing stress levels of 215, 260, and 310 MPa, respectively.

This work was done by Chern P. Chen and Martin H. Leipold of Caltech for **NASA's Jet Propulsion Laboratory.** *"Stress Rate and Proof Testing of Silicon Wafers," NPO-16573/TN*

FOR ADDITIONAL INFORMATION: *Contact: Director, Technology Transfer Division, P.O. Box 8757, BWI Airport, MD. 21240; (301) 621-0100 Ext. 241*
REFER TO THE NUMBER LISTED AT THE END OF THE ARTICLE

NASA Tech Brief
National Aeronautics and
Space Administration
Marshall Space Flight Center, Alabama

Eddy-Current Detection of Weak Bolt Heads

An electronic test identifies flawed units that pass hardness tests.

An eddy-current test detects weakness in the head-to-shank junctions of ¼-28 cup-washer lock bolts. The test was developed for alloy A286 steel bolts in the Space Shuttle main engine fuel turbopump. Some of the bolts were failing in tension tests, even though they had passed hardness tests designed to measure strength.

A complex process is required to increase the tensile strength of the steel to 2×10^5 lb/in.^{2} (1.4 GPa), compared with the normal fully heat-treated value of 1.4×10^5 lb/in.^{2} (0.97 GPa). This process sometimes leaves relatively weak regions in the bolt head, even though a Rockwell C hardness test on the shank end yields the minimum allowable value of 39 or more. The shape of the head prevents hardness tests from being made there. The eddy-current test examines the full volume of the head, including the head-to-shank transition and thus can nondestructively screen out potentially defective units.

Since alloy A286 is a precipitation-heat-treatable austenitic nickel/chromium steel, it is readily inspectable by eddy currents. This inspection is possible because as the strength of the alloy is increased by heat treatment or cold working, its electrical conductivity decreases. A region of higher conductivity in the head, as indicated on the eddy-current meter, is therefore a weaker region.

Calibration standards, special induction coils, and a procedure have been prepared for the eddy-current test. The test can be performed by unskilled people with a minimum of training. The test sorts bolts at a rate of 20 per minute. It rejects a small percent of marginally strong bolts but does not accept any weak bolts. The test can be adapted to any other alloys, the mechanical properties of which are improved by solution heat treatment and aging or by cold working or by both.

This work was done by Carmen P. Messina of Rockwell International Corp. for **Marshall Space Flight Center**. *No further documentation is available.*
MFS-29092 /TN

FOR ADDITIONAL INFORMATION: *Contact: Director, Technology Transfer Division, P.O. Box 8757, BWI Airport, MD. 21240; (301) 621-0100 Ext. 241*
REFER TO THE NUMBER LISTED AT THE END OF THE ARTICLE

NASA Tech Brief
National Aeronautics and Space Administration
Marshall Space Flight Center, Alabama

Eddy-Current Detection of Cracks in Tubes

A nondestructive device tests narrow, sharply-bent metal tubes.

An eddy-current probe detects incipient cracks inside small metal tubes. The probe was developed for coolant tubes in the Space Shuttle main engine nozzle. The tubes are bent sharply just before they are assembled in the engine. Previously, the tubes were inspected for post-bend cracks by destructive metallographic examinations of samples in a batch. If only a few samples were found defective, the entire batch had to be scrapped. Since the value of the tubes is significant at this stage of fabrication — more than $250 each — a substantial investment is lost when a batch is discarded. If half of the tubes are good and can be used instead of being scrapped, an estimated saving of $125,000 would be realized on an engine. The new probe makes it possible to distinguish the good bent tubes from the cracked ones.

The probe consists of an eddy-current generating and detecting coil or pair of coils on which a pair of centering bars is mounted (see figure). The magnitudes and phases of the eddy currents induced in a tube as it passes between the bars indicates the depths of cracks; the current amplitudes and phases are displayed on an oscilloscope.

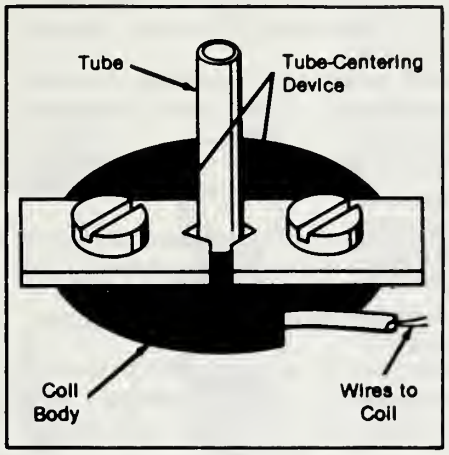

A Tube-Centering Device consisting of a pair of opposed bars ensures that a tube is centered on the eddy-current coil. The probe can be moved along the length of a bent tube to inspect repeatably for cracks.

The probe is thin and can therefore accommodate small-radius bends in tubes. The diameter of the coil and the distance between the centering bars can be changed to suit a variety of tube diameters. Instead of a single coil, a pair of coils can be used for differential current measurements. The coil-excitation frequency can be adjusted to give adequate penetration for a particular tube alloy and wall thickness. The probe is compatible with tubes of many different cross sections — oval, flattened, square, rectangular, or irregular.

Besides its Space Shuttle application, the probe could be adapted for inspecting formed tubes in petrochemical, automotive, nuclear, and medical equipment. Its tube-centering feature makes it useful in testing straight tubes as well.

This work was done by R. G. Parent and D. D. Kettering of Rockwell International Corp. of **Marshall Space Flight Center**. *MFS-29081/TN*

FOR ADDITIONAL INFORMATION: *Contact: Director, Technology Transfer Division, P.O. Box 8757, BWI Airport, MD. 21240; (301) 621-0100 Ext. 241*
REFER TO THE NUMBER LISTED AT THE END OF THE ARTICLE

NASA Tech Brief
National Aeronautics and Space Administration
Langley Research Center, Hampton, Virginia

Licensing Opportunity

Measuring Hole Elongation in Bolted Joints

The measurement does not affect joint parameters.

The verification of analytical and strength-prediction methods for bolted composite joints is based generally on data obtained experimentally from double-lap-joint specimens. In mechanically fastened joints, the stresses are maximal at the fastener holes. The ability to measure accurately hole elongations without affecting the joint parameters would provide a better understanding of the elastic and plastic behavior of the joint material leading to failure. The effective determination of the failure mechanisms in mechanically fastened joints is required for the design of more-efficient, lightweight composite joints.

A double-lap-joint-testing assembly for measuring hole elongation without affecting joint parameters is shown in the figure. The bodies of the linear variable-differential transformers (LVDT's) are rigidly attached to the stud. The movable cores of the LVDT's are in contact with the reference angles, which are securely bonded to the test specimen below the spacer washers. The center of the reference-angle area bonded to the specimen is one reference point, and the top of the stud in contact with the hole is the other reference point.

As the hole elongates under tensile loading, the distance between the stud and the reference angle increases because of the stress concentrations around the hole. The cores of the LVDT's move with the reference angles, and the change in distance between the two reference points is reflected in the output voltages of the LVDT's.

With increasing load, displacements caused by bending and bearing stresses within the stud will be measured along with the hole elongations. However, these stud displacements would, in many cases, be negligible with high-strength, hardened-steel studs. In cases where stud displacements must be taken into account, the magnitudes of elastic displacements could be analytically determined and subtracted from the measured displacements, yielding only the hole elongations.

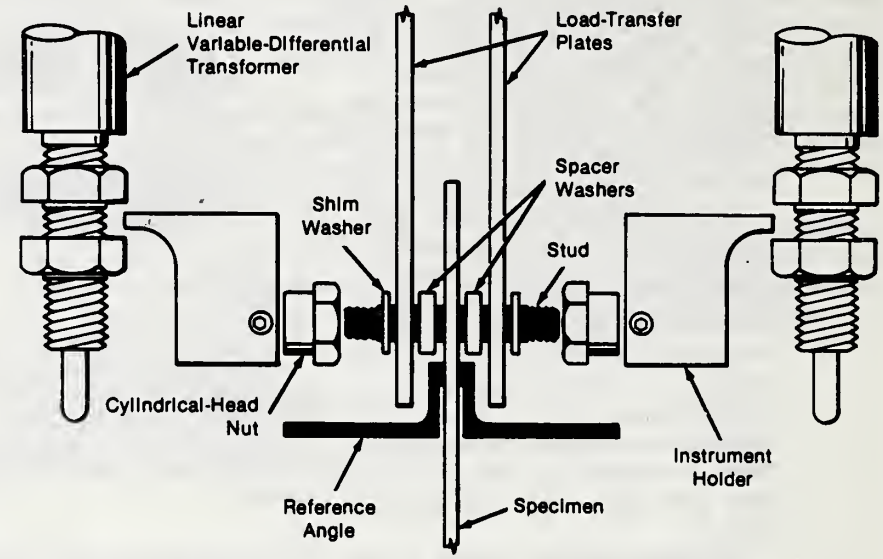

This **Double-Lap-Joint-Testing Assembly** is used to measure the elongations of holes in specimens.

This measurement technique offers a direct comparison between the displacements occurring at each outer-hole surface since the measuring instruments are equidistant from the specimen surfaces, and the reference angles are mounted opposite each other. Within the elastic limit of the specimen material, specimen bending or unequal loading through the load-transfer plates can be detected by comparing the displacement-versus-load responses. The technique is suitable for different bolt diameters, washer sizes (clamping areas), clamping forces (bolt torque), and joint materials, and for some multifastener arrangements.

This work was done by Gregory R. Wichorek of **Langley Research Center**. *No further documentation is available.*

Inquiries concerning rights for the commercial use of this invention should be addressed to the Patent Counsel, Langley Research Center Refer to LAR-13453. /TN

Langley Research Center
Technology Utilization Officer:
John Samos
Mail Stop 139A
Hampton, VA 23665
(804) 865-3281
Patent Counsel:
Howard J. Osborn
Mail Code 279
Hampton, VA 23665
(804) 865-3725

FOR ADDITIONAL INFORMATION: *Contact: Director, Technology Transfer Division, P.O. Box 8757, BWI Airport, MD. 21240; (301) 621-0100 Ext. 241*
REFER TO THE NUMBER LISTED AT THE END OF THE ARTICLE

Materials

674 Hot Isostatic Pressing of Sintered Ceramics—A model of the process has been developed and analyzed.

675 Self-Propagating High-Temperature Synthesis—A new method of preparing ceramics offers many advantages.

676 Properties of Sintered Beta Silicon Carbide at High Temperature—Commerically produced material is compared with earlier samples made in the laboratory.

677 Rubber-Processing Studies—Processing of natural rubber and styrene/butadiene was studied.

678 Hypersonic Plane Material—Basic tests on aluminum-lithium alloys will be conducted.

679 New Anisotropic Ceramic-Air Composites Improve the Strength and Operational Capability of Ceramic Electronic Devices

680 Fracture Analysis of Welded Type 304 Stainless Steel Pipe

681 Microstructure and Aging of Powder-Metallurgy Al Alloys—Peak hardness is achieved at lower aging temperatures than with standard ingot-metallurgy alloys.

682 Fast-Response Heating of Silicon Melts—Heating would be confined to a small mass near the growing crystal.

683 Evaluation of GaAs Fracture Mechanics—These data can aid the design of solar cells.

684 Radiation Effects on Polymer Properties—Tables present lowest doses for which effects are noticeable.

685 Fire-Retardant, Decorative Inks—The effectiveness of fire-retardant additives is evaluated. (Licensing Opportunity)

686 Polyimide Pregregs With Improved Tack—Drape and tack are improved without loss of strength.

Testing & Instrumentation

687 Mechanical Tests of Coated Carbon/Carbon Composite—The duplex coating performs its function despite nonuniformity, cracks, and debonding.

688 Damping Capacity Measurements for Characterization of Degradation in Advanced Materials

689 Furnace for Tensile Testing of Flexible Ceramics—Ceramic cloth and thread are tested quickly at temperatures up to 1,250°C. (Licensing Opportunity)

Other items of interest

646 Zirconia-Bonded Zirconia Fiber Insulation Structures

United States
Department of
Agriculture

Research Technology
Agricultural Research Service

Fabric Treatment Process Improves Thermal and Physical Properties

The POLYTHERM process produces fabrics that adjust to hot and cold temperatures and have enhanced properties

A new process, called Polytherm, can impart improved performance characteristics to a wide variety of fabrics. It gives textiles several useful performance features such as thermal heating or cooling properties, excellent oily soil release, reduced pilling, anti-static protection, durable press qualities and increased moisture absorption.

The Polytherm fabrics are prepared by binding polyethylene glycol polymers to the material using a "pad-dry-cure" manufacturing process. The Polytherm addition will typically increase the fabric base weight by 25-60%. Thus, the treated products are considerably heavier than the starting material. It is applicable to any textile fiber or fabric including cotton, cotton/polyester blends, worsted wool, polyester, nylon, rayon, acrylic, and fiberglass.

Polytherm properties can be imparted to the fabrics using polyethylene glycol having a molecular weight custom designed for each particular application. Laboratory studies of Polytherm materials indicate that treated fabrics will release heat at cool temperatures giving a warming effect and absorb heat at warmer temperatures giving a cooling effect; the precise temperatures at which these effects occur depends on the molecular weight of the polymer.

The Department of Agriculture is interested in either establishing cooperative research and development agreements or licensing the process to U.S. companies.

FOR ADDITIONAL INFORMATION:

A special technology opportunity package is available describing the properties of the new licensable fabric treatment process called Polytherm. The package provides samples of treated fabric, a full technical description, a technical contact point at the Agricultural Research Service for consultation, and a videotape showing the process and fabric properties.

To order the POLYTHERM FABRIC TREATMENT technology package, ask for PB87-181186/NAC from the National Technical information Service, Springfield, VA 22161; (703) 487-4650. The cost of the package is $325.

Questions not detailed in the information package may be addressed to Dr. Richard Parry, Assistant to the Administrator, USDA-ARS, Beltsville, MD 20705: (301) 344-2734.

Potential POLYTHERM Applications

Application	*Properties* Thermal	Soil Release	Reduced Pilling	Antistatic	Durable Press	Moisture/Water Absorption/Retention
I. APPAREL						
Men's Wear						
Work clothing	x	x	x	x	x	x
Shirts--dress, sport	x	x	x		x	
Underwear-T-shirts, shorts, etc.	x		x	x	x	
Socks	x	x	x	x		x
Athletic wear	x					x
Jeans	x	x	x		x	
Sweaters (wool,	x			x		
acrylic)	x					
Women's wear						
Work clothing	x	x	x	x	x	x
Blouse & dress wear	x	x	x	x	x	
Lingerie	x	x		x		
Sweaters	x		x		x	
Overcoat Lining	x					
Gloves	x					
II. HOME FURNISHINGS						
Blankets	x					
Mattress Pads	x	x				x
Sheets (Flat, flannel)	x	x	x	x	x	
Towels						x
Draperies	x			x		
Upholstery	x					
Wall covering	x					
Carpets	x	x				
Bath rugs	x	x				x
III. INDUSTRIAL/ GENERAL						
Interlinings	x					
Woven & nonwoven						
Wipes (woven and nonwoven)						x
Tents						x
Medical dressings	x					x

MANUFACTURING TECHNOLOGY NOTE

U.S. ARMY MATERIEL COMMAND

Deputy Chief of Staff for Manufacturing Technology, Alexandria, VA

Project Number: NONE

Filing Code: 71D046

Hot Isostatic Pressing of Sintered Ceramics

A model of the process has been developed and analyzed.

A study has investigated the final-stage densification of undoped Al_2O_3, MgO-doped Al_2O_3, and composites of magnesium aluminosilicate glass and Al_2O_3 by hot isostatic pressing of unencapsulated, closed-porosity samples. The material systems are representative of those ceramics that can be densified by solid-state diffusion and solution-precipitation mechanisms.

In the study for the U.S. Army Research Office, experiments examined the following:

- The effects of dihedral angle, effective stress, grain size distribution, and pore/grain size ratio on pore stability during hot isostatic pressing of pure and MgO-doped alumina. Models were developed to explain the influence of these parameters. However, 100-percent densification was not achieved because porous heterogeneities exceeded the critical pore/grain size ratio of 2.3.
- The effects of dihedral angle, effective stress, grain size, volume percent liquid, gas diffusion, and liquid redistribution during hot isostatic pressing of alumina-glass composites. Models for pressureless and pressure-enhanced solution precipitation were derived to incorporate the effective stress. Experiments at various pressures agreed well with the models and showed that densification is limited by the interface reaction for short hot isostatic pressing times — less than 1 hour.

Longer hot isostatic pressing experiments resulted in dedensification as a result of pressure-enhanced gas diffusion into the glass matrix. Models were derived to predict the effect of gas diffusion on densification. Macropores — pores with about 100-μm diameters — can be closed by pressure-driven liquid redistribution at greater than 98 percent relative density. Depending on the matrix grain size, the macropores can be filled completely by a liquid or a liquid-particle mixture.

FOR ADDITIONAL INFORMATION:

You can learn more details about this technology by ordering the NTIS report(s):
Hot Isostatic Pressing of Sintered Ceramics.
Order number: AD-A169467/NAA
Price code: A02
Order from:
National Technical Information Service
5285 Port Royal Road
Springfield, VA 22161

This document was prepared under the sponsorship of the U.S. Government. Neither the United States Government nor any person acting on behalf of the United States Government assumes any liability resulting from the use of the information contained in this document, or warrants that such use will be free from privately owned rights.

MANUFACTURING TECHNOLOGY NOTE

U.S. ARMY MATERIEL COMMAND

Deputy Chief of Staff for Manufacturing Technology, Alexandria, VA

Project Number: 1L161102AH42 Filing Code: 71D045

Self-Propagating High-Temperature Synthesis

A new method of preparing ceramics offers many advantages.

A report describes self-propagating high-temperature synthesis (SHS), a promising new method for processing ceramics. The process uses the heat generated by an exothermic reaction between precursor components to densify the resulting reaction products. The report was prepared by the U.S. Army Materials Technology Laboratory.

The heat generated can produce temperatures in excess of 2,500 °C. Since the heat is self-generated, high-temperature furnaces are not required. Processing times are in seconds or minutes instead of hours or days as in conventional processes. In addition, the products of SHS tend to be of higher purity than the starting materials, since the high temperatures vaporize the volatile contaminants. Furthermore, ordinarily intractable borides and carbides can be made.

Generally, powders of the reactants are mixed for the proper stoichiometric ratio and then pelletized at room temperature (see figure). The reaction is initiated at an outer surface by a short, intense burst of energy (spark, laser, or heat, for example). A reaction wave then propagates through the pellet. Complete reaction occurs within a matter of seconds. Many reactions can be carried out in air, but since an inert atmosphere eliminates surface oxidation, most reactions are carried out in controlled environments.

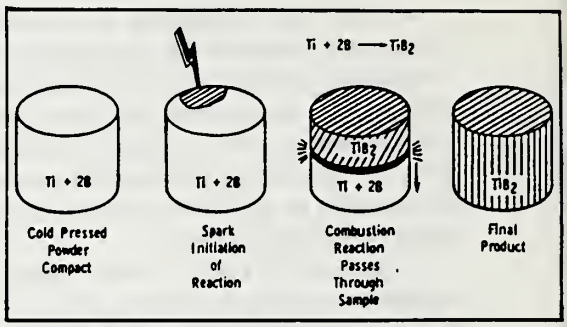

The **SHS Reaction Starts** with a pellet of pressed powder — here titanium and boron. A spark initiates the reaction, which proceeds through the pellet, yielding titanium boride ceramic.

Project officer James W. McCauley (617) 923-3463 or AV 955-3463.

FOR ADDITIONAL INFORMATION:

You can learn more details about this technology by ordering the NTIS report(s):
Self-Propagating High-Temperature Synthesis (SHS): Current Status and Future Prospects.
Order number: AD-A169588/NAA
Price code: A02
Order from:
National Technical Information Service
5285 Port Royal Road
Springfield, VA 22161

This document was prepared under the sponsorship of the U.S. Government. Neither the United States Government nor any person acting on behalf of the United States Government assumes any liability resulting from the use of the information contained in this document, or warrants that such use will be free from privately owned rights.

MANUFACTURING TECHNOLOGY NOTE

U.S. ARMY MATERIEL COMMAND

Deputy Chief of Staff for Manufacturing Technology, Alexandria, VA

Project Number: NONE

Filing Code: 71F106

Properties of Sintered Beta Silicon Carbide at High Temperatures

Commercially produced material is compared with earlier samples made in the laboratory.

A program has evaluated the mechanical properties of sintered beta silicon carbide at room and elevated temperatures. The program, conducted by the U.S. Army Materials Technology Laboratory, was designed to verify the properties of the commercial form of the material.

Earlier studies have suggested that the laboratory hot-pressed and sintered beta silicon carbide materials have excellent high-temperature properties up to 1,500 °C, including strength retention and resistance to creep and slow crack growth. These properties, coupled with the complex shape capabilities of sintering, suggest that the commercial beta silicon carbide is a promising heat-engine-grade ceramic.

Twelve specimens were tested by the stepped-temperature stress rupture procedure (see figure). Seven specimens failed at various points during the procedure. Permanent deformation of the five survivors was negligible. Four of the survivors showed surprisingly consistent retained strengths: 401, 448, 402, and 400 MPa for applied stresses of 250, 250, 300, and 350 MPa, respectively. The retained strengths are appreciably higher than the reference room-temperature strengths. The increase may be due to a flaw-healing process or to crack blunting.

The intrinsic flaw populations were generally found to be agglomerates and porous zones with a few large grains, inclusions, and process cracks.

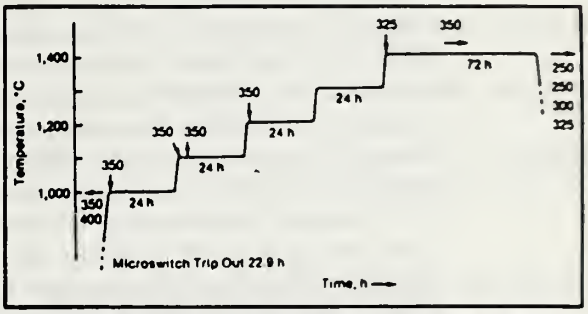

In the **Stepped-Temperature Stress Rupture Procedure**, specimens are subjected to various constant loads while the temperature is periodically increased. In this plot, the arrows indicate the points in time at which a failure occurred. The number associated with an arrow indicates the load on the specimen in megapascals. The asterisk indicates an anomaly: the specimen survived intact at 350 MPa when the furnace was inadvertently shut down after 22.9 hours at 1,400 °C.

Time-dependent failures occurred only from surface-connected porous zones.

Project officer George D. Quinn
(617) 923-5980 or AV 478-5980.

FOR ADDITIONAL INFORMATION:

You can learn more details about this technology by ordering the NTIS report(s):
Mechanical Property Evaluation at Elevated Temperatures of Sintered Beta Silicon Carbide
Order number: AD-A169593/NAA
Price code: A02

Order from:
National Technical Information Service
5285 Port Royal Road
Springfield, VA 22161

This document was prepared under the sponsorship of the U.S. Government. Neither the United States Government nor any person acting on behalf of the United States Government assumes any liability resulting from the use of the information contained in this document, or warrants that such use will be free from privately owned rights.

MANUFACTURING TECHNOLOGY NOTE

U.S. ARMY MATERIEL COMMAND

Deputy Chief of Staff for Manufacturing Technology, Alexandria, VA

Project Number: 1B-3-2B180-18EF

Filing Code: 71H024

Rubber-Processing Studies

Processing of natural rubber and styrene/butadiene was studied.

The U.S. Army Belvoir R&D Center conducted processing studies on styrene/butadiene-rubber (SBR) and natural-rubber (NR) compounds typical of those used in the fabrication of tank-track pads. The effects of purposely implemented variations in formulating and mixing of the compounds were ascertained through visual examination of ingredient dispersion and physical/mechanical testing of vulcanized samples obtained for each variant/rubber combination. Results were analyzed in terms of the ultimate positive or negative impact upon quality and expected performance of the end items.

Rheological data (see figure) for the SBR compounds indicate that overloading of a Banbury mixer has the most significant effect on processability, whereas other formulation or procedural variables evidenced negligible to slight influences. Examination of the rheological data for the NR compounds reveals that processing is less subject to formulation and procedural variations than is the case for the SBR compounds. This difference is a manifestation of the chemical structure and inherently better processing characteristics of NR and of the more reactive copolymer structure of SBR.

Project officer Jacob Patt
(313) 574-5814 or AV 786-5814.

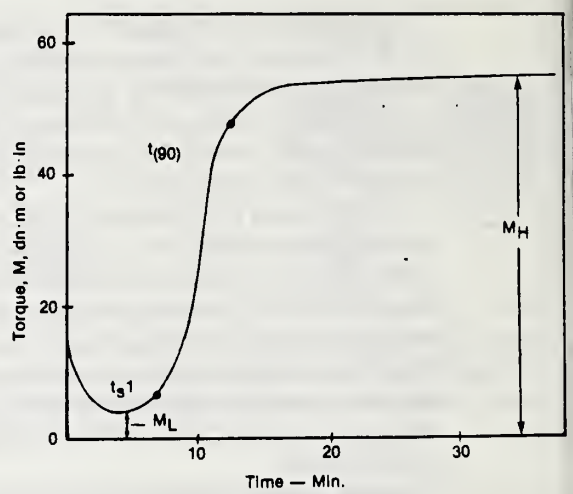

1. M_L — Minimum torque
2. M_H — Maximum or equilibrium torque
3. T_s1 — Time to 1 lb × in., rise above M_L
4. $T_{(90)}$ — Time to 90% of maximum torque
5. $T_{(50)}$ — Time to 50% of maximum torque
6. CRI — Cure Rate Index $\frac{100}{T_{(90)} - T_s1}$

A **Representative Rheometer Curve** illustrates parameters used to evaluate ingredient dispersions prior to curing.

FOR ADDITIONAL INFORMATION:

You can learn more details about this technology by ordering the NTIS report(s):
Effect of Compounding and Mixing Variables on the Physical Properties of Elastomeric Tank Pad Formulation.
Order number: AD-A167728/NAA
Price code: A05

Order from:
National Technical Information Service
5285 Port Royal Road
Springfield, VA 22161

This document was prepared under the sponsorship of the U.S. Government. Neither the United States Government nor any person acting on behalf of the United States Government assumes any liability resulting from the use of the information contained in this document, or warrants that such use will be free from privately owned rights.

Hypersonic Plane Material

Basic tests on aluminum-lithium alloys will be conducted.

As now conceived, the space plane would be a hypersonic aircraft capable of lifting off from conventional runways and reaching orbital speeds. To achieve such a performance the material used to make this vehicle will have to be stronger, more resistant to fracturing, and able to stand up to more extreme temperature changes than the aluminum alloys currently used in aircraft.

"The driving force behind the aluminum-lithium project is the desire on the part of the aerospace industry to create lighter metals for all aircraft," says William Morris, a metallurgist with LBL's Center for Advanced Materials, who heads the project. "Many countries are working on the problem because the payoff will be not only hypersonic aircraft, but also conventional planes that can fly faster or carry greater loads while burning less fuel."

Aluminum-lithium alloys hold great promise in such a capacity because they possess low density and good mechanical properties. They can also be formed into complex shapes.

The research team headed by Morris has designed and arranged the construction of a small melting furnace which they will use to manufacture their own aluminum-lithium compositions. Since aluminum-lithium alloys become lighter in weight as the concentration of lithium becomes greater, the LBL scientists will

attempt to find what the maximum concentration of lithium can b

without affecting the material's strength and stability.

FOR ADDITIONAL INFORMATION:

Public Information Department
Lawrence Berkeley Laboratory
1 Cyclotron Road, Berkeley, CA 94720
(415) 486-5771
Refer to: Hypersonic Plans Material 1/30/87/TN.

New Anisotropic Ceramic-Air Composites Improve the Strength and Operational Capability of Ceramic Electronic Devices

A Naval Research Laboratory (NRL) scientist reports the development of an invention that improves the strength and operational capability of ceramic electronic devices used in underwater sensors, microcircuit substrates, and in other Navy and commercial applications.

The development is anisotropic ceramic-air composites that have higher average strengths, are more resilient, and have a lower dielectric constant than their matrix material in conventional homogeneous form.

The improved composites result from the introduction of controlled voids. These voids give the composites a vital crack-resisting capability and provide stress equilibration when used in load-bearing components in operational systems, in sensors, or in electronic substrates. In addition, the ceramic-air composites formed with the NRL technique can be geometrically designed to meet specific engineering requirements for piezoelectric and other electronic ceramic devices.

One advantage of the ceramic-air composites over more conventional ceramic-metal or ceramic-ceramic composites is the absence of interdiffusion during the heating and sintering stages that are used in forming the composites. This is particularly important when compositional purity of the matrix phase of electronic ceramics is desired.

The photolithographic techniques used in the preparation of these composites make it possible to prepare ceramics containing arrays of voids of predetermined size, shape, spacing, and order. This permits the maximization of useful anisotropies and can also provide structured composites having regions of dense matrix phase.

The ordered voids in composites formed by the new NRL technique have a much higher aspect ratio than normal pores formed in more conventional ceramics. This maximizes the arresting of cracks and minimizes excessive stress concentrations at random flaws in the ceramic. As a result, the voids have nearly doubled the average flexure strength of poled lead zirconate titanate (PZT) and more than quadrupled its work of fracture.

Additionally, the ordered void arrays in the new technique also cause an anisotropic (different properties in different directions) reduction in the Poisson's ratio. This together with the presence of solid ceramic columns in the composite increases the hydrostatic sensitivity factor of PZT by 200 times.

Finally, when the spatially defined void regions are designed into multilayer microcircuit substrates, the stray capacitance of critical conductors is reduced by 50 percent and their propagation delays by 30 percent, whereas the full thermal conductance of the substrate can be maintained elsewhere. These properties and others make the new air composites ideal for a host of new applications in Navy systems.

For Additional Information:

Backup material on this effort is available from:

Navy Domestic Technology Fact Sheet
Reader Reply Service
Code E211
Naval Surface Weapons Center
Dahlgren, VA 22448-5000
(703) 663-8921

Refer to 111201/TN

NAVY
Domestic Technology Transfer Fact Sheet

Fracture Analysis of Welded Type 304 Stainless Steel Pipe

An experimental investigation was recently performed at the David Taylor Naval Ship Research and Development Center to determine the fracture resistance of full scale 4 in. diameter circumferentially welded Type 304 stainless steel pipe at 550°F.

Two types of crack geometries were investigated. The first was a circumferential through-wall notch (simple crack) and the second was a circumferential through-wall notch superimposed on a part-through 360 degree radial notch (complex crack). The specimens were loaded in four-point bending until a significant amount of the remaining ligament was fractured.

Test results were analyzed using J-integral and limit load techniques. Additionally, J-integral resistance curve tests were performed on large plan-size laboratory compact tension specimens for comparison with the pipe specimen results.

Results of the J-integral analysis for the pipes containing simple cracks showed that the J level at crack initiation was approximately 6400 in-lb/in^2. Good agreement in the J level at crack initiation between the simple cracked pipe and compact tension specimens indicates that laboratory scale specimens can be used to model the J-integral fracture behavior of welded Type 304 stainless steel pipe provided that the compact tension specimen thickness is similar to that of the pipe wall.

Results of the J-integral analysis for the pipes containing complex cracks indicated an average J-initiation value of 1200 in-lb/in^2. The lower J-initiation level of the complex crack geometry pipe is due to increased constraint at the crack tip due to the internal notch as well as the reduced plasticity away from the crack tip.

The limit load analysis was performed using three values of flow stress for the material. These included the averages of the measured yield and ultimate strengths from the weld and base metals (54.1 ksi and 45.3 ksi, respectively) and an estimate from the ASME Code of three times the design stress intensity (3Sm = 51.0 ksi). Use of the weld metal flow stress and ASME Code estimated flow stress was shown to lead to overpredictions of the load carrying capacity of the pipe specimens. Use of the base metal properties lead to more accurate predictions of the load carrying capacity of the pipe specimens.

For Additional Information:

Backup material on this effort is available from:

Navy Domestic Technology Fact Sheet
Reader Reply Service
Code E211
Naval Surface Weapons Center
Dahlgren, VA 22448-5000
(703) 663-8921

Refer to 120105/TN

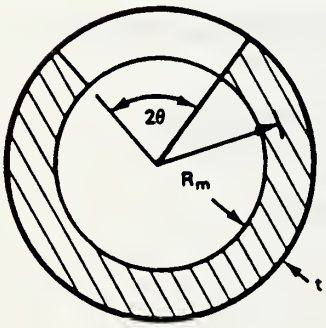

SIMPLE CRACK
2θ = CIRCUMFERENTIAL CRACK LENGTH
R_m = MEAN RADIUS
t = PIPEWALL THICKNESS

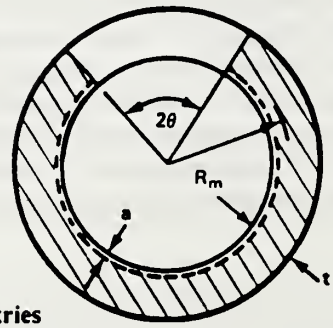

COMPLEX CRACK
2θ = CIRCUMFERENTIAL CRACK LENGTH
R_m = MEAN RADIUS
t = PIPE WALL THICKNESS
a = RADIAL CRACK LENGTH

Simple and complex crack geometries

NASA Tech Brief
National Aeronautics and Space Administration

Microstructure and Aging of Powder-Metallurgy Al Alloys

Peak hardness is achieved at lower aging temperatures than with standard ingot-metallurgy alloys.

A report describes an experimental study of the thermal responses and aging behaviors of three new aluminum alloys. The alloys are produced from rapidly solidified powders and contain 3.20 to 5.15 percent copper, 0.24 to 1.73 percent magnesium, 0.08 to 0.92 percent iron, and smaller amounts of manganese, nickel, titanium, silicon, and zinc. These alloys are of interest for automobile, aircraft, and aerospace applications.

In this study, Rockwell B hardness measurements; optical, scanning-electron, and transmission-electron microscopy; and energy-dispersive x-ray analysis were used to correlate the microstructures with the measured mechanical properties (yield strength, ultimate tensile strength, elongation to failure, and notched tensile strength). These tests were performed on the alloy specimens both as received and after various heat treatments. The fracture surface of each tensile specimen was examined by scanning-electron microscopy.

This study led to the following conclusions:

- Increased temperatures of solution heat treatment were effective in re-dissolving coarse primary constituents in the alloy containing 5.15 percent copper, but had little effect on the microconstituents in the alloys containing less copper.
- Studies of aging at room temperature, 120, 150, and 180 °C for times ranging up to 60 days indicated that classic aging-response curves, as determined by hardness measurements, occurred at aging temperatures lower than those previously studied or generally used for ingot-metallurgy alloys of similar compositions. The principal microstructural feature associated with peak hardness is an extremely fine and homogeneously distributed S′ or θ′ phase.
- High tensile strengths of notched specimens were typically associated with fine, homogeneous distributions of strengthening S′ or θ′ phases and decreases in the sizes and volumes of dispersoids or large soluble precipitates, as compared to those of the specimens of lower strength. The fracture surfaces of notched specimens of low strength exhibited homogeneous distributions of equiaxial dimples resulting from microvoid coalescence initiated at second-phase particles. The fracture surfaces of the stronger notched specimens were more irregular, exhibiting numerous smooth regions attributed to matrix shear.
- Variations in heat-treatment procedures, including changes in the temperatures and times of the solution heat treatments and of aging, produced mechanical properties comparable to those achieved previously by cold working and natural aging.

This work was done by Linda B. Blackburn of **Langley Research Center**. *"Microstructure-Mechanical Property Relationships for Various Thermal Treatments of Al-Cu-Mg-X PM Aluminum Alloys," LAR-13298 /TN*

FOR ADDITIONAL INFORMATION: *Contact: Director, Technology Transfer Division, P.O. Box 8757, BWI Airport, MD. 21240; (301) 621-0100 Ext. 241*
REFER TO THE NUMBER LISTED AT THE END OF THE ARTICLE

NASA Tech Brief
National Aeronautics and Space Administration
NASA's Jet Propulsion Laboratory, Pasadena, California

Fast-Response Heating of Silicon Melts

Heating would be confined to a small mass near the growing crystal.

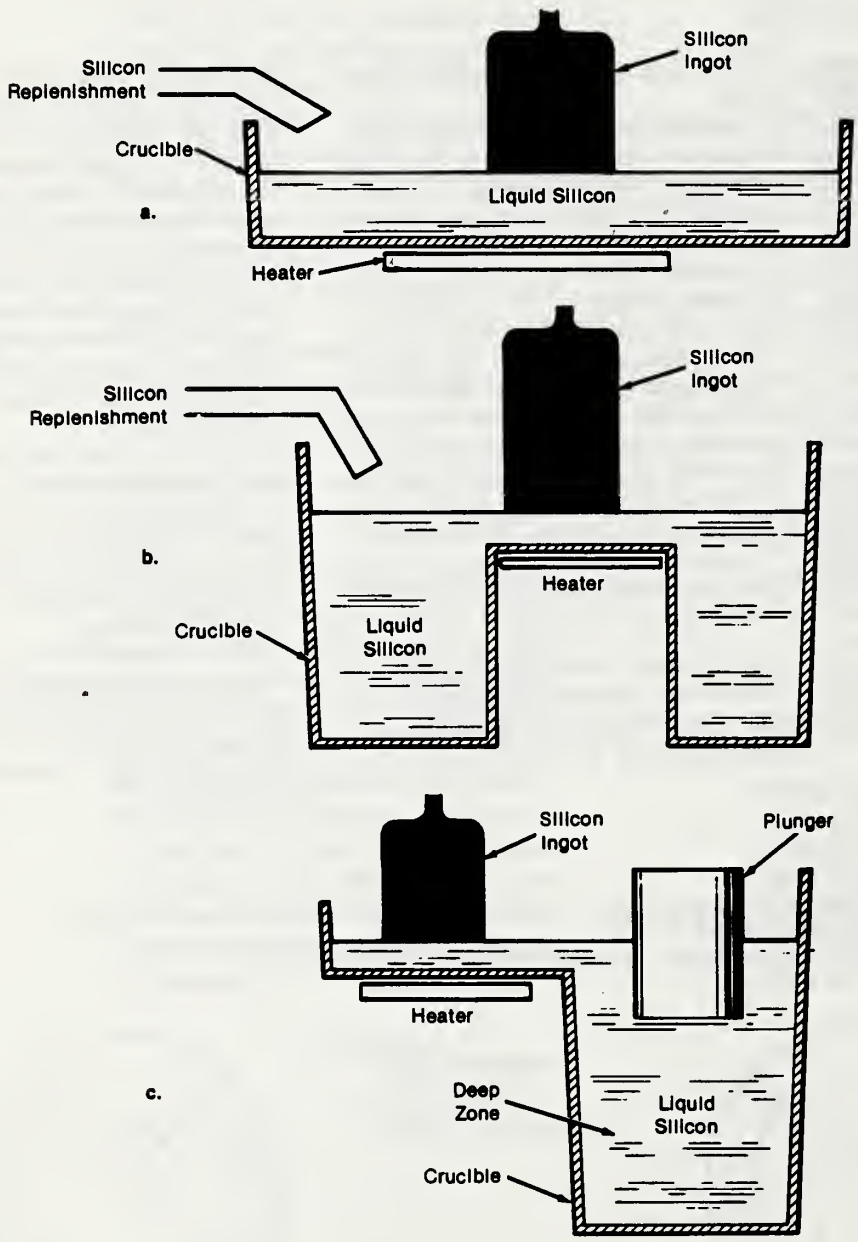

In versions b and c, a **Deep Zone Adjoins a Shallow Zone** of molten silicon. A heater can raise the temperature of the shallow zone quickly. In all three versions, the melt level is maintained by replenishment with silicon (top and middle) or by immersing a plunger in the liquid (bottom).

A proposed improvement for silicon crystal growing would enable rapid heating of the melt in the vicinity of the liquid-solid interface to compensate for decreases in melt temperature, to ensure a uniform diameter and composition in the ingot. The improvement is intended for growing large silicon ingots by the Czochralski process, in which a cylindrical single-crystal ingot is pulled from molten silicon.

At present, it is impossible to respond quickly to sudden drops in melt temperature by boosting the power to the electrical heating elements that surround the melt crucible, because the melt is too massive to heat up quickly enough. Instead, an industrial crystal grower automatically raises the pulling rate to compensate and thereby maintain a constant ingot diameter. However, this practice is not entirely satisfactory: Rapid changes in the pulling rate cause changes in the solidification rate and in the inclusion of impurities and defects. (These effects were previously masked by the effects of convection currents but will become increasingly important as controlled convection furnaces are developed.)

For the purpose of effecting a rapid heating of the melt in the vicinity of the interface, a shallow melt would underlie the growing ingot (see figure). A heater under the shallow zone would provide heat when the melt cooled. With a relatively small mass of molten silicon above it, the heater can rapidly raise the melt temperature to the proper level. At the same time, there is ample liquid silicon in the deep zone adjacent to the shallow center to replace the material consumed by the growing ingot.

This work was done by Andrew D. Morrison of Caltech for **NASA's Jet Propulsion Laboratory**. *NPO-16730 /TN*

FOR ADDITIONAL INFORMATION: *Contact: Director, Technology Transfer Division, P.O. Box 8757, BWI Airport, MD. 21240; (301) 621-0100 Ext. 241*
REFER TO THE NUMBER LISTED AT THE END OF THE ARTICLE

NASA Tech Brief
National Aeronautics and
Space Administration

Evaluation of GaAs Fracture Mechanics

These data can aid the design of solar cells.

A report provides data on the fracture properties of single-crystal GaAs. These data are required for the design of reliable GaAs solar cells and modules.

Measured by ultrasonic-velocity techniques, the elastic moduli of GaAs single crystals were found to be highly anisotropic. The Young's moduli in the <100>, <110>, and <111> crystal orientations are 8.93×10^{11}, 12.50×10^{11}, and 14.40×10^{11} dyn/cm^2, respectively. The effect of temperature on the elastic modulus was not appreciable in the range of −130 to 450 °C, and no effect of dopant (Si vs. Te) was observed.

The measured coefficients of thermal expansion in the range of −130 to 450 °C were 5.6×10^{-6} (°C)$^{-1}$ for Si-doped GaAs and 5.3×10^{-6} (°C)$^{-1}$ for Te-doped GaAs: The small difference between these values was not statistically significant. These values were also not significantly affected by the temperature or the crystal orientation.

The fracture toughness was measured under four-point bending, with a controlled flaw produced by a pyramid-shaped diamond indentation. GaAs was found to be extremely fragile, with fracture toughnesses of 0.43, 0.31, and 0.45 MN/m$^{3/2}$, respectively, in the {100}, {110}, and {111} cleavage planes. In comparison, single-crystal silicon has corresponding fracture toughnesses of 0.95, 0.90, and 0.82 MN/m$^{3/2}$. The fracture toughness of GaAs was not affected by Te vs. Si doping or by temperatures in the range of −8 to 121 °C.

The delayed emergence of cracks after the removal of the indentor suggests that crystalline GaAs is susceptible to subcritical crack growth. This is important because subcritical cracks introduced during manufacture could cause the fracture of GaAs solar cells long after installation.

Similar fracture tests were also performed on GaAs wafers after successive processing stages in the manufacture of solar cells. Wafers were tested as cut and polished, coated by chemical-vapor deposition, metallized, and soldered. The fracture-stress data were then analyzed using Weibull statistics. Chemical-vapor deposition appeared to produce some damage on the wafer surface, possibly as a result of the thermal shock during deposition. However, the wafer edges were not damaged. Antireflection coating and soldering materials increased the apparent strengths of cells. Mechanical polishing of cut wafers did not produce significant increases in their strengths. The strengths of GaAs wafers were not affected by temperatures within the range of −87 to 121 °C. Preliminary results indicate that the strength of GaAs tends to increase with increasing etch-pit density within the range of 5,000 to 20,000 etch pits per cm^2.

A long tail at the low-stress portion of the strength-distribution curve was found for several types of samples. The wafers or cells in the low-strength distribution are likely to be fractured during subsequent cell processing and handling. A proof test would be useful to eliminate these weak samples.

This work was done by Chern P. Chen of Caltech for **NASA's Jet Propulsion Laboratory.** *NPO-16604 /TN*

FOR ADDITIONAL INFORMATION: *Contact: Director, Technology Transfer Division, P.O. Box 8757, BWI Airport, MD. 21240; (301) 621-0100 Ext. 241*
REFER TO THE NUMBER LISTED AT THE END OF THE ARTICLE

NASA Tech Brief
National Aeronautics and
Space Administration

Radiation Effects on Polymer Properties

Tables present lowest doses for which effects are noticeable.

A report compiles data on the effects of radiation on the physical properties of synthetic organic materials. Emphasis is on materials of interest to nuclear-equipment and nuclear-reactor designers. The data cover five categories of polymeric materials: Insulators, elastomeric seals and gaskets, lubricants, adhesives, and coatings. More than 250 materials are represented. The document reflects a continuation of the work reported in the preceding article.

A table gives available data on physical, electrical, and optical properties for each material in terms of the lowest reported threshold dose (LTD), which indicates the radiation level at which radiation effects become apparent and the dose for a 25 percent change in the specified property. The literature source for the data is indicated.

Both the LTD and the 25-percent-change dose vary widely within each of the five categories of polymer. Most of the polymeric materials have thresholds above 10^5 rads. Five materials have thresholds below 10^5 but above 10^4 rads; namely, fluorocarbons, nylons, epoxy resins, polyethylene oxides, and polyalphamethyl chloroacrylates.

The LTD data are useful for setting a lower limit at which changes can be expected. They may also be used as a guide for deciding when the expected radiation is low enough to be disregarded for a given polymer. The 25-percent-change dose is a valuable radiation statistic because changes are real at this dose level and are neither artifacts of the experiments nor results of sample variations.

This work was done by Frank L. Bouquet and John W. Winslow of Caltech for **NASA's Jet Propulsion Laboratory.** *"Radiation Data Definitions and Compilation for Equipment Qualification Data Bank," NPO-16426/TN*

FOR ADDITIONAL INFORMATION: *Contact: Director, Technology Transfer Division, P.O. Box 8757, BWI Airport, MD. 21240; (301) 621-0100 Ext. 241*
REFER TO THE NUMBER LISTED AT THE END OF THE ARTICLE

NASA Tech Brief
National Aeronautics and Space Administration

Licensing Opportunity

Fire-Retardant, Decorative Inks

The effectiveness of fire-retardant additives is evaluated.

The fire retardance of decorative acrylic printing inks for aircraft interiors may be enhanced by certain commercial and experimental fire-retardant additives, according to a study. In the study, standard brominated fire retardants and new polymeric brominated retardants were incorporated into a commercial acrylic ink. The resulting formulations were evaluated for solubility in methyl ethyl ketone (the acrylic-ink solvent), thermal stability, compatibility with acrylic-ink processing, flammability, and smoke emission.

The following retardants were evaluated:

- 2,3-dibromopropyl acrylate, a commercial vinyl-terminated product;
- Bis(β-chloroethyl)vinyl phosphonate, another vinyl-terminated product;
- Brominated polymeric additive (BPA) F2001P, a commercial brominated fire retardant containing 50 percent bromine largely as aromatic bromine, which is highly thermostable;
- F2001P with tribromophenol (TBP) — the TBP increases the bromine content to 58 percent;
- F2001P with rubberized TBP — carboxy-terminated butadiene acrylonitrile rubber gives this additive greater resistance to impact;
- F2001P with pentabromophenol (PBP) — the PBP increases the bromine content to 63 percent, even higher than TBP; and
- F2001P with rubberized PBP.

The limiting oxygen index (LOI) was used as one of the measures of flammability. The inks with the commercial vinyl-terminated additives proved to be slightly more effective than the neat acrylic ink in retarding fire. The derivatives of F2001P produced LOI's higher than those of the commercial additives. The higher the rubber content, the higher the LOI.

Thermogravimetric analysis and differential scanning calorimetry were used to evaluate thermostability. The rank order turned out to be somewhat different from that for flammability. The simple F2001P additive produced the most stable ink and was followed by the rubberized formulations. The inks with commercial additives and the plain acrylic ink were lowest on the scale of stability.

This work was done by D. A. Kourtides of **Ames Research Center,** *Z. Nir of the National Research Council, and J. A. Mikroyannidis of the University of Patras. "Fire-Retardant Decorative Inks for Aircraft Interiors,"*

Inquiries concerning rights for the commercial use of this invention should be addressed to the Patent Counsel, Ames Research Center Refer to ARC-11499 / TN

Ames Research Center
Technology Utilization Officer:
Laurance A. Milov
Mail Code 204-10
Moffett Field, CA 94035
(415) 694-5761
Patent Counsel:
Darrell G. Brekke
Mail Code 200-11
Moffett Field, CA 94035
(415) 694-5104

FOR ADDITIONAL INFORMATION: *Contact: Director, Technology Transfer Division, P.O. Box 8757, BWI Airport, MD. 21240; (301) 621-0100 Ext. 241*
REFER TO THE NUMBER LISTED AT THE END OF THE ARTICLE

NASA Tech Brief
National Aeronautics and Space Administration
Lewis Research Center, Cleveland, Ohio

Polyimide Prepregs With Improved Tack

Drape and tack are improved without loss of strength.

Composites made with PMR-15 (or equivalent) polyimides have gained acceptance as viable engineering materials for high-use-temperature applications. This acceptance is due to both the thermo-oxidative stability of PMR-15 (or equivalent) and the ease with which PMR-15 (or equivalent) prepreg materials can be processed into composite structures. An important factor contributing to the processability of PMR-15 (or equivalent) is the volatility of the alcoholic solvents used in preparing prepregging solutions. These low-boiling-point solvents (methanol or ethanol) are easily removed during fabrication, making it possible to obtain void-free or low-void composites. However, the volatility of these solvents does limit the tack and drape retention of PMR-15 (or equivalent) prepreg exposed to the ambient. Retention of these two important material-handling properties is essential for consistent performance during layup of composite structures, particularly large composite structures that require long layup times.

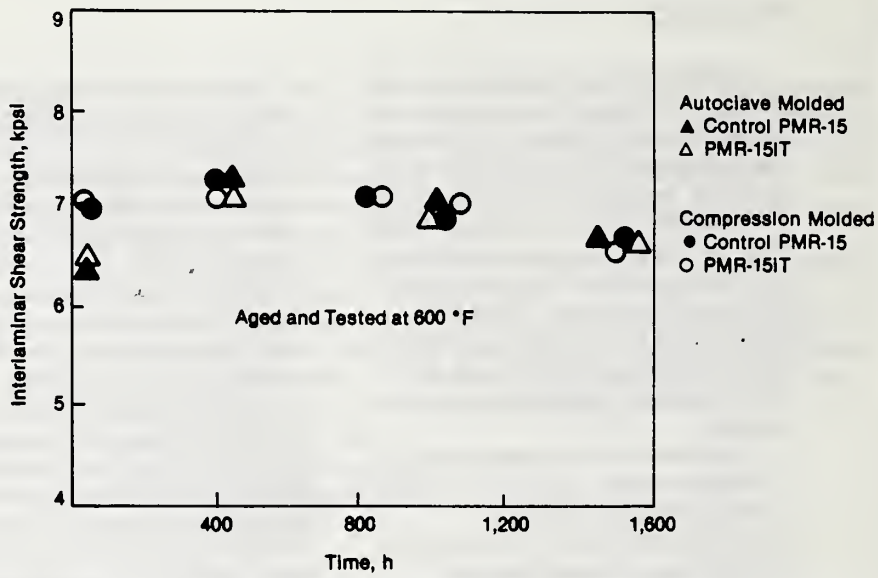

The **Interlaminar Shear Strength** of composites made with the improved polyimide nearly matches that of its predecessor.

In a recent study, PMR-15 (or equivalent) resin compositions, designated "PMR-15IT," were identified that provide improved tack and drape retention for graphite-fiber/PMR-15 (or equivalent) prepreg materials without adversely affecting processability or composite mechanical properties (see figure). The improved tack system identified to provide the best overall processability, along with excellent composite properties, was obtained by utilizing methyl ester monomers and a solvent containing methanol/1-propanol in a 3:1 weight ratio. Graphite-fiber/PMR-15 (or equivalent) prepreg prepared from the above PMR-15IT (or equivalent) resin and exposed to ambient conditions exhibits excellent tack retention for at least 10 days — approximately four times longer than current-technology PMR-15 (or equivalent) prepreg exposed under the same conditions. The figure shows that the 600 °F (320 °C) mechanical properties of composites fabricated from the PMR-15IT (or equivalent), by either compression- or autoclave-molding methods, are equivalent to those exhibited by the composites fabricated from state-of-the-art PMR-15 (or equivalent) prepreg.

This work was done by R. D. Vanucci of **Lewis Research Center.** *Further information may be found in:*

NASA TM-82951 [N83-12175/NSP], [A02] "PMR-15 Polyimide Modification for Improved Prepreg Tack" and NASA TN-D-7257 [N72-29598/NSP], [A02] "Addition Type Polyimides from Solutions of Monomer Reactants."

Copies may be purchased from the National Technical Information Service, Springfield, Virginia 22161. /TN

FOR ADDITIONAL INFORMATION: *Contact: Director, Technology Transfer Division, P.O. Box 8757, BWI Airport, MD. 21240; (301) 621-0100 Ext. 241*
REFER TO THE NUMBER LISTED AT THE END OF THE ARTICLE

MANUFACTURING TECHNOLOGY NOTE

U.S. ARMY MATERIEL COMMAND

Deputy Chief of Staff for Manufacturing Technology, Alexandria, VA

Project Number: 1L162105AH84 Filing Code: 73D098

Mechanical Tests of Coated Carbon/Carbon Composite

The duplex coating performs its function despite nonuniformity, cracks, and debonding.

The strength of a carbon/carbon composite having a proprietary silicon carbide coating with silicate glass interlayers was evaluated at ambient and elevated temperatures in air. In the evaluation by the U.S. Army Materials Technology Laboratory, a duplex-coating system with a silicon carbide outer layer was applied by the controlled nucleation thermochemical deposition (CNTD) process. Earlier studies had shown that such duplex-coated systems are most durable.

Bars were strength-tested at room temperature, 1,200, 1,800, 2,200, and 2,400 °F (650, 980, 1,200, and 1,300 °C, respectively) in air (see figure). Uncoated bars were also tested at room temperature. Strength measurements, either in terms of maximum load or approximate coating stress, were appreciably higher at all elevated temperatures than at room temperature. However, stress-rupture experiments showed that these high strengths could not be maintained for significant times at elevated temperatures. Alternatively, several specimens with more conservative loads endured very well for thousands of hours at 1,832 and 2,372 °F (1,000 and 1,300 °C). The composite beam had favorable thermal shock resistance, as demonstrated by cyclic-fatigue torch airblast testing and by limited water-quench testing.

Although the coating was not uniform, was cracked, and tended to debond from the substrates, it performed its function of protecting the substrates. There was some indication that the silicate interlayer in the coating had crack-healing ability. Further refinements in the two-layer coating process may enhance the coating-to-substrate bond and thus give better mechanical properties. Project officer George D. Quinn (617) 923-5980 or AV 478-5980.

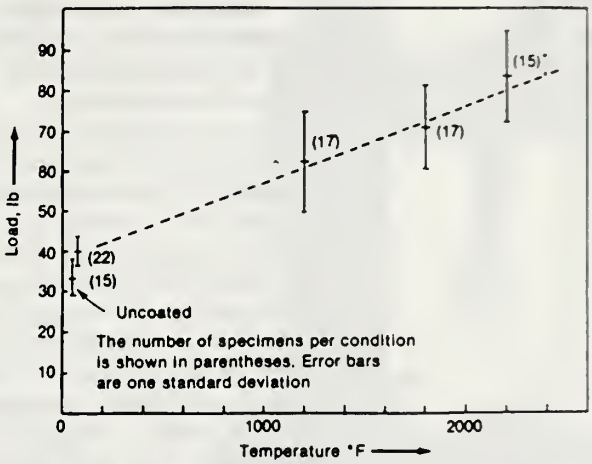

Flexure Strength (load) is plotted against temperature for uncoated and coated bars tested in air. The number of specimens per condition is shown in parentheses. Error bars are one standard deviation.

FOR ADDITIONAL INFORMATION

You can learn more details about this technology by ordering the NTIS report(s):

Mechanical Testing of a Coated Carbon/Carbon Composite at Elevated Temperature in Air.
Order number: AD-A169355
Price code: A02

Order from:
National Technical Information Service
5285 Port Royal Road
Springfield, VA 22161

This document was prepared under the sponsorship of the U.S. Government. Neither the United States Government nor any person acting on behalf of the United States Government assumes any liability resulting from the use of the information contained in this document, or warrants that such use will be free from privately owned rights.

energygram

Damping Capacity Measurements for Characterization of Degradation in Advanced Materials

DOE/TIC/EG-86/113
OFFICE OF SCIENTIFIC AND TECHNICAL INFORMATION

This technical note was based on research conducted by Idaho National Engineering Laboratory for the U.S. Department of Energy.

INEL
Idaho National Engineering Laboratory

A recently developed impulse-frequency response technique has been used to obtain damping capacity measurements of advanced materials for characterization of degradation.

The recently published paper describes the analysis of the response of structural components to imposed vibration as a way to characterize the integrity of the components of a structure to material damping. The paper correlates the response of such components to changes in damping.

The analysis of the response of components can be enhanced, in many cases, by looking at its frequency spectrum rather than its time history. Real-time frequency domain analysis has been made possible by Fast Fourier Transform analyzers, which are now common. The recently developed technique reported in this paper uses the frequency-domain transfer function under impulsive excitation. Damping is found by curve-fitting to the transfer function.

This technique holds considerable potential for nondestructive in situ testing on full-scale engineering structures. The work described in this paper, which is essentially experimental and exploratory in nature, involves the use of this technique as a nondestructive evaluation method for obtaining damping capacity measurements for predicting degradation and also for possible correlation with mechanical property data. The research reported on examines the application of the techniques as described on several types of materials, including composite materials in general and E-glass/epoxy composite specimens in particular and A710 stainless steel.

Overall, the study has shown that damping data at high strains does correlate with the mechanical property data.

This information is of immediate interest to materials testing laboratories, industrial research organizations, and universities.

FOR ADDITIONAL INFORMATION

DOE report(s):
Damping Capacity Measurements for Characterization of Degradation in Advanced Materials.
Report number: EGG-M-30485/NAB
Order number: DE86007656/NAB
Price: $9.95

Order from:
National Technical Information Service
5285 Port Royal Road
Springfield, VA 22161

For additional information, contact:
J. M. Welch
EG&G Idaho, Inc.
P.O. Box 1625
Idaho Falls, ID 83415
Telephone No.: (208) 526-8318

or

R. F. Gibson
Associate Professor
Engineering Science
University of Idaho
Moscow, ID 83843
Telephone No.: (208) 885-6111

NASA Tech Brief
National Aeronautics and Space Administration
Ames Research Center, Moffett Field, California

Licensing Opportunity

Furnace for Tensile Testing of Flexible Ceramics

Ceramic cloth and thread are tested quickly at temperatures up to 1,250 °C.

Tensile strengths of ceramic cloths and threads can be measured conveniently in a new furnace at specified temperatures up to 1,250 °C, using an ordinary mechanical tester. The samples are heated along part of their lengths in the furnace slots. The interchangeable furnace chambers and the matching heating elements are sized to match the size of the tested ceramic material.

The furnace is made of foamed silica with temperature-controlled embedded resistant-wire heating elements powered by a 110-V, 25-A supply. Designed to heat strips about 1 in. (2.5 cm) wide or threads that are less than 0.06 in. (0.15 cm) thick, the furnace is 4 in. (10.2 cm) wide, 5 in. (12.7 cm) deep, and 3 in. (7.6 cm) high. The furnace test chambers are one-half in. long, one-half in. wide, and 1 in. high (1.27 by 1.27 by 2.54 cm) for thread, and 1-1/2 in. long, one-half in. wide, and 1 in. high (3.81 by 1.27 by 2.54 cm) for cloth.

There are two type "K" thermocouples — one for the temperature control, the other for temperature monitoring — mounted one-eighth in. (3 mm) from the tested material. The small furnace opening — a 1/16-in. (1.6-mm) slot — allows the furnace to be slid into place around, or removed from, the specimen, with insignificant loss of heat at the test temperature.

The tensile-test specimen is mounted in the mechanical tester with a 4-in. (10.2-cm) opening between the tensile grips (see figure). Mounted on a horizontal sliding bar, the preheated furnace is moved forward to enclose the tensile specimen, the strength of which is then measured in the standard way. After the specimen breaks, the furnace is moved away from the test specimen, a new specimen is mounted in the tensile grips, and the furnace is slid into place for the next test. Because the furnace remains hot and does not enclose the mechanical tester, no time is lost waiting for the furnace to reheat.

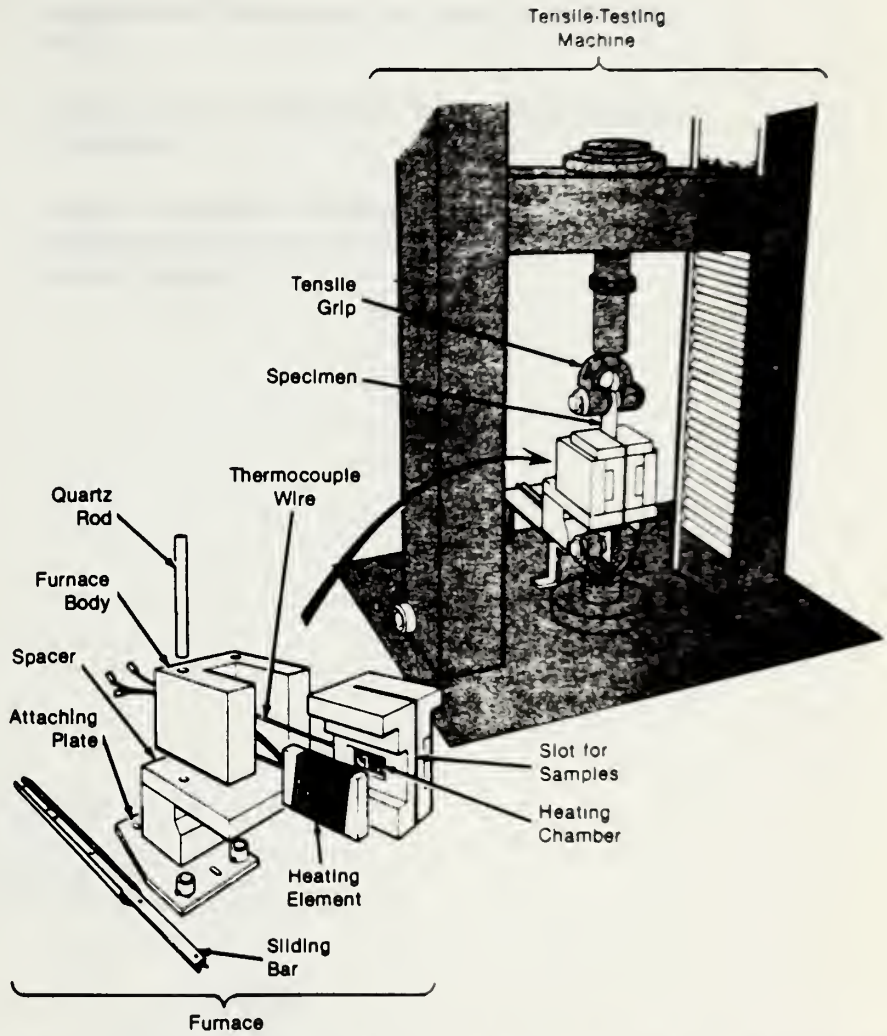

The Modular Design of the Furnace allows the tensile-strength testing of both ceramic thread and cloth.

This work was done by Marnell Smith, Carlos A. Estrella, and Victor W. Katvala of **Ames Research Center**. *No further documentation is available.*

Inquiries concerning rights for the commercial use of this invention should be addressed to the Patent Counsel, Ames Research Center. Refer to ARC-11589 /TN

Ames Research Center
Technology Utilization Officer
Laurance A. Milov
Mail Code 204-10
Moffett Field, CA 94035
(415) 694-5761
Patent Counsel:
Darrell G. Brekke
Mail Code 200-11
Moffett Field, CA 94035
(415) 694-5104

FOR ADDITIONAL INFORMATION: *Contact: Director, Technology Transfer Division, P.O. Box 8757, BWI Airport, MD. 21240; (301) 621-0100 Ext. 241*
REFER TO THE NUMBER LISTED AT THE END OF THE ARTICLE

Medicine & Biology

690 Neural Tissues Available

691 Advance Computer System Probes Molecular Structure of Proteins

Testing & Instrumentation

692 Portable Beta Spectrometer for Tissue Dose Measurement

693 Magnetic Study of Bioelectric Phenomena (Licensing Opportunity)

694 Surgical Borescopes Remove Contaminants—Borescope instruments are put to use in extracting hard-to-reach particles.

IIH
Research & Technology

Federal
Technology
Resource

S. Department of Health and Human Services Public Health Service National Institutes of Health

Neural Tissues Available

Samples from human brains, peripheral nerves, spinal fluids, and sera are available from the National Neurological Research Bank at the Veterans Administration Wadsworth Medical Center in Los Angeles, California. Tissues are intended for scientists researching neurological and psychiatric diseases.

The main goal of the resource, which is supported by the National Institute of Neurological and Communicative Disorders and Stroke, the National Institute of Mental Health, the National Multiple Sclerosis Society, the Hereditary Disease Foundation, and the Veterans Administration, is to make available to scientists high-quality tissues from clinically well-studied patients with pathologically confirmed disorders. Most of the specimens are from patients with disorders with no known cure. The tissues are obtained during autopsy, as well as at surgery, and are needed to study neurological disorders for which animal models do not exist. Scientists use the samples in biochemical, immunological, virological, and other analytical studies.

Currently more than 600 cryopreserved specimens of various conditions are in the bank. Among the samples are tissues taken from people who had multiple sclerosis, Alzheimer disease, Huntington disease, Parkinson disease, amyotrophic lateral sclerosis, epilepsy, depressive disorders, schizophrenia, and neurofibromatosis, as well as from people who abused drugs or alcohol or who committed suicide. Samples from normal people are also available for comparison. The diseased specimens are matched with normal control specimens by several characteristics, including age and gender, and time elapsed from death to cryopreservation (autolysis time).

The brains are examined in the fresh state. Full transverse sections are quick-frozen to minimize the formation of ice artifact, permitting application of histochemical techniques. In contrast to chemical preservation—for example, the use of formalin which promotes and enhances cell changes—cryopreservation as soon after death as possible preserves the in vivo chemical anatomy.

Researchers choose the samples according to specific criteria, including anatomical site, disease, age, gender, medical treatment, and degree of postmortem autolysis. A computerized inventory allows the staff to quickly identify the sections that are appropriate for each request. Photomacrographs are taken of each transverse brain section in order to locate those with the anatomical and/or neuropathological features requested by the investigators.

The tissue samples are accompanied by a comprehensive patient history file, which describes all significant diseases, their course and treatment, as well as age, gender, and race.

Photo courtesy of NIH News and Features

Tissues from the brains of patients who had Huntington disease or other neurological diseases may be obtained from the National Neurological Research Bank.

Also included is a complete neuropathology report summarizing the findings and diagnostic impressions. In some cases, for example in patients with Huntington disease, a family pedigree is prepared and included with the samples.

The staff at the repository plan to increase the extensiveness of the collection by including brain tumor samples. More samples, particularly from patients with herpes encephalitis, Down syndrome, Friedreich ataxia, Tourette syndrome, and subacute sclerosing panencephalitis, are being sought because the repository's supply is limited.

—Barbara Proujan

For more information on either obtaining research specimens or on the "Gift of Hope" anatomical donor program, contact:
Wallace W. Tourtellotte, M.D., Ph.D
Director, National Neurological Research Bank
Neurology Research (W127A)
Veterans Administration
Wadsworth Medical Center
Los Angeles, California 90073
Telephone: (213) 824-4307.

Photo courtesy of the National Neurological Research Bank

A technician at the resource examines photomicrographs of brain sections to locate tissues requested by investigators.

NIH Research & Technology

U.S. Department of Health and Human Services Public Health Service National Institutes of Health

Advance Computer System Probes Molecular Structure of Proteins

A computer system, imitating the reasoning of human experts, is building models of proteins. The system, called PROTEAN, uses nuclear magnetic resonance (NMR) spectroscopy measurements and other data to analyze protein structure. High-resolution NMR provides detailed information about protein molecules as they exist naturally—suspended in solution. In solution proteins can change shape and carry out the enzymatic, transport, and regulatory functions that sustain life. By providing a clearer picture of protein structure, the PROTEAN system helps explain how proteins perform their many functions.

Eventually, PROTEAN might be used to develop drugs by showing how compounds bind to target proteins and produce physiological effects. At this point, however, it "is still very much a research project," says Dr. Oleg Jardetzky, director of the Stanford magnetic resonance laboratory. "Computers are needed in the analysis of proteins simply because of the enormous wealth of information that you get from an NMR spectrum." Computers are widely used to study protein structure, but PROTEAN is the only research project using artificial intelligence (AI) to analyze NMR data. "In that respect we are unique—at the moment," he says.

In theory a team of human experts could eventually obtain the same result, but that would require a much longer period of time. The computer has the crucial advantage of speed. "I don't think there is a qualitative difference between the way a human mind solves the problem and the way the computer solves the problem," says Dr. Jardetzky, professor of pharmacology in the Stanford University Medical School.

By using artificial intelligence, the Stanford researchers have greatly increased the efficiency of data analysis. Still, PROTEAN requires about 24 hours of computer time to analyze the structure of a single protein.

The project began in 1983, when Dr. Jardetzky started working with Dr. Bruce Buchanan, professor of computer science and director of Stanford's Knowledge Systems Laboratory. Using the nationally shared computing facilities of SUMEX-AIM (Stanford University Medical Experimental Computer for Artificial Intelligence in Medicine), they set out to develop a computer program that could accurately determine protein structures using NMR data. Although x-ray crystallography was—and still is—the most precise method for analyzing protein structure, many proteins are difficult to crystallize. And when proteins are crystallized their normal structures are often altered in the process.

In 1984 the Stanford research team used an early version of PROTEAN to calculate the structure of the 51-amino-acid "lac-repressor headpiece," part of a bacterial protein. By 1985 a more powerful version of PROTEAN was available. It could determine a protein's general form but could not pinpoint small-scale, atomic structures.

Finally, a complete working version of PROTEAN was finished in 1986. "This is the first version that can put together a molecule from NMR data and display it at atomic resolution," Dr. Jardetzky says. Because of limits in the available data the program does not define all atomic positions, "but we can at least display the options."

The Stanford team has successfully tested PROTEAN on several well-known proteins, including sperm-whale myoglobin, a protein of 153 amino acids that has been fully characterized by x-ray crystallography. PROTEAN reconstructed the complete structure of the myoglobin molecule from data on the distances between adjacent atoms in the protein.

Most computer programs plow straight ahead, using the available data to compute a single "best fit" model. A problem often arises when additional data are incorporated into the model. "A major advantage of our approach is that it doesn't focus on a single structure, but it tries to define the family of all structures that are compatible with the data," Dr. Jardetzky explains.

By keeping track of all possible structures, PROTEAN can identify structural changes the protein may undergo while performing its functions. A single subunit may actually occupy more than one position at different times. Identifying such conformational changes may be crucial for understanding how the protein works. Says Dr. Jardetzky: "We try to converge on the correct structure or structures by adding more and more experimental data, rather than by invoking theoretical constraints."

PROTEAN begins with a protein's basic sequence of amino acids. The program then constructs a three-dimensional model of the protein by positioning secondary structures such as alpha helices and random coils. Starting with the largest and most stable structures, PROTEAN builds the model by attaching other structures and requesting further data as needed.

PROTEAN displays the evolving structure on a high resolution color monitor. The computer sketches out the approximate outlines of the protein, then eliminates configurations that do not fit the data. "You can watch the process of building up the protein structure, observing at each step the difference that adding each bit of information makes," Dr. Jardetzky explains.

The details of protein structure are functionally important and need to be included in the final model. For example, the posi-

tions of amino acid side chains help determine the molecules to which the protein will bind. Because the side chains can change their orientation in solution, "defining the allowed positions of the side chains is really all one can hope to do," he says.

To characterize a protein completely, PROTEAN depends on a set of interacting program components. The "knowledge base" contains the necessary data; "knowledge sources" devise a problem-solving strategy and carry out specific instructions; the "geometry system" performs the actual computations; the "blackboard" keeps track of the ongoing process; and a graphics display program provides the resulting three-dimensional images.

"These programs are based, of course, on human reasoning; they could not be written without it," Dr. Jardetzky says. Although some parts of the PROTEAN system are strictly computational, the symbolic or inferential elements reflect the Stanford investigators' own scientific experience and their methods for drawing conclusions.

In this way the PROTEAN project goes beyond the study of proteins to the study of problem solving itself. The researchers are even exploring ways to make their system introspective, allowing PROTEAN to monitor its own performance and use that experience to improve its strategies.

Despite its sophistication, PROTEAN does not require a supercomputer. In fact, the program's capabilities are limited less by computer power than by the software itself. PROTEAN can operate on an IRIS work station that costs about $40,000, which means the program may eventually be useful in many laboratories, Dr. Jardetzky says.

Given enough data and sufficient computer memory, the program should be able to determine the structure of even the largest proteins. But extending the system to large proteins will require improvements in NMR data collection. "I would not venture to do very large structures in the next couple of years. We have to go slowly in increasing molecular size," Dr. Jardetzky says.

The larger the protein, the more complex the resulting NMR spectrum. One way to handle the massive amounts of data obtained from large proteins is to replace specific hydrogen atoms in the molecule with deuterium isotopes. This produces simpler spectra that are easier to analyze in detail.

The Stanford research team is now using the selective deuteration method to study proteins too large to be fully characterized by conventional NMR. After obtaining multiple spectra using selective deuteration, "we will get from the combined data set all of the structural information that one can get by NMR," Dr. Jardetzky explains. This approach should allow PROTEAN to derive the complete protein structure.

But Dr. Jardetzky notes that the goal of the PROTEAN project is not just to analyze the structure of proteins but also to explain how proteins function. The researchers want to know how drugs or other molecules recognize and bind to a specific protein, cause structural changes, and thereby alter the protein's behavior.

Dr. Jardetzky and his associates are now studying the structure of the tryptophan repressor protein, a DNA binding protein that helps regulate production of the amino acid tryptophan. In the presence of tryptophan, the protein forms a stable complex with a specific DNA site. Without the tryptophan, the protein assumes a different shape and the DNA-protein complex falls apart.

To explore this conformational change in the tryptophan repressor, the researchers will first use PROTEAN to work out the protein's detailed structure. They will then study how the structure changes when the protein binds to tryptophan and to DNA.

Dr. Jardetzky says other re-
fevre, J. F., Lichtarge, O., Hayes-Roth, B., Altman, R., and Buchanan, B., A new method for the determination of protein structures in solution from NMR. In *Proceedings XXIII Congress Ampere*, Rome, Italy, September 15–19, 1986, pp 64–69.
searchers have expressed interest in collaborating on studies of this kind. "We intend to make PROTEAN generally available," he says, "but we are not quite ready to do that yet." In about a year other laboratories may be able to use an improved version of the system.

Additional reading:

1. Jardetzky, O., and Lane, A., Determination of the solution structure of proteins from NMR. *Proceedings of the International School of Physics Enrico Fermi*, Varenna, Italy, July 8–18, 1986 (in press).
2. Jardetzky, O., Lane, A., Le-
3. Altman, R., and Jardetzky, O., New strategies for the determination of macromolecular structure in solution. *Journal of Biochemistry* (in press).
4. Hayes-Roth, B., Buchanan, B., Lichtarge, O., Hewitt, M., Altman, R., Brinkley, J., Cornelius, C., Duncan, B., and Jardetzky, O., Elucidating protein structure from constraints in PROTEAN. In *Insight Series in Applied AI* (Engelmore, R., and Morgan, T., eds.). New York, Addison-Wesley (in press).
5. Duncan, B., Buchanan, B. G., Hayes-Roth, B., Lichtarge, O., Altman, R., Brinkley, J., Hewett, M., Cornelius, C., and Jardetzky, O., PROTEAN: a new method for deriving solution structures of proteins. *Bulletin of Magnetic Resonance* (in press).
6. Jardetzky, O., and Roberts, G. C. K., *NMR in Molecular Biology*. New York, Academic Press, 1981.

The research described in this article was supported by the Biomedical Research Technology Program of the NIH Division of Research Resources and by the National Science Foundation.

For Additional Information:

To locate information or professional contacts on this effort, contact:

Research Resources Information Center, 1601 Research Blvd., Rockville, MD 20850 (301) 984-2870

Refer to item XI, No. 1/TN

energygram

Portable Beta Spectrometer for Tissue Dose Measurement

DOE/TIC/EG-86/109
OFFICE OF SCIENTIFIC AND TECHNICAL INFORMATION

This technical note was based on research conducted by Idaho National Engineering Laboratory for the U.S. Department of Energy.

INEL
Idaho National Engineering Laboratory

A technique for measuring the radiation dose rates at depths of 0.07 [Ḋ(.07)] and 10 millimeters [Ḋ(10)] in tissue in mixed beta/gamma radiation fields through the use of a tissue equivalent detector and portable multichannel analyzer has been developed and field tested.

The key element of the portable beta spectrometer is the 2.5-cm diameter by a 0.9-cm-thick tissue equivalent plastic scintillator used as the detector. The energy spectrum from the tissue equivalent detector for both betas and photons is almost exactly proportional to the energy that would have been deposited in an equal volume of tissue.

In field applications, two spectra are collected at each location, the first with an open window (2.5 mg/cm of aluminized mylar) and a second with a 1-cm-thick lucite cap covering the window to shield the betas and allow the photon component to pass through with minimal attenuation. Because the plastic scintillator detector is nearly tissue equivalent, the unfiltered spectrum represents the energy deposited by betas plus energy deposited by the Compton electrons resulting from photon interactions. The low effective atomic number of tissue essentially precludes photoelectric interactions of photons with energies above 50 keV.

Two energy spectra are collected for each measurement, an open window spectrum representing the tissue response to betas plus photons, and a second filtered spectrum representing the photon response. The D(.07) dose rate is calculated from the net beta spectrum, which is obtained by subtracting the photon spectrum from the total (photon and beta) spectrum. The total energy deposited is obtained by summing the product of the number of counts in each channel and the energy associated with that channel over the entire spectrum. Similarly, the dose rate at a tissue depth of 10 millimeters [D(10)] is calculated by multiplying each channel count of the total spectrum by the calibrated energy value associated with the channel number and summing these results to obtain the total energy deposited.

FOR ADDITIONAL INFORMATION

DOE report(s):
A Portable Beta Spectrometer for Tissue Dose Measurement.
Report number: EGG-M-04985/NA8
Order number: DE86004106/NAB
Price: $9.95
Field Tests of a Tissue Equivalent Beta Survey Meter.
Report number: EGG-M-06585/NAB
Order number: DE86004139/NAB
Price: $9.95

Order from:
National Technical Information Service
5285 Port Royal Road
Springfield, VA 22161

For additional information, contact:
Jane M. Welch
EG&G Idaho, Inc.
P.O. Box 1625
Idaho Falls, ID 83415
Telephone No. (208) 526-8318

or

D. E. Martz
EG&G Idaho, Inc.
P.O. Box 1625, WCB-E2
Idaho Falls, ID 83415
Telephone No. (208) 526-0146

energygram

Licensing Opportunities

DOE/TIC/EG-86/131
OFFICE OF SCIENTIFIC AND TECHNICAL INFORMATION

Magnetic Study of Bioelectric Phenomena

This technical note was based on research conducted by Idaho National Engineering Laboratory for the U.S. Department of Energy.

INEL

Idaho National Engineering Laboratory

A device and method have been designed for magnetic detection of bioelectric activity associated with muscle action or with other living tissue. This method is intended to supplement known diagnostic techniques of electrocardiography and electromiography by providing an analogous magnetic technique to study the electric currents flowing in living tissue.

The device is comprised of a magnetic shielding facility to establish an enclosed region, within which the ambient level of magnetic noise is below the level of the magnetic fields to be measured. A highly sensitive magnetic field detector is positioned within the enclosed space. An adjustable chair to comfortably support the subject to be studied and suitable electronic circuitry connected to the magnetic field detector for processing a visual display of the magnetic fields to be measured are also included within the space.

The magnetic field detector is arranged to produce an electrical indication of a component of the magnetic field in a relatively localized region; so a direct mapping of the magnetic fields associated with the bioelectric activity being studied can be made by measurement of a single magnetic field component at a number of locations.

Current technology for measurement of the bioelectric effect measures the effect as an electrical potential in the tissue. This signal is a scalar value, whereas the current flow is a vector quantity. The method described here allows the study of the electrical currents flowing in living tissue by a direct mapping of the magnetic fields associated with such currents. Such vectors can then be used in the diagnosis of heart and other muscle diseases. This technique might be termed magnetomiography and magnetocardiology with regard to study of muscles and heart, respectively.

Owing to its inherently low noise and its magnetically quiet environment, the system as described here is capable of achieving considerable spatial resolution, whereby magnetic detection of the electrical activity in a localized area of muscle tissue may be possible without the need for insertion of detector probes into the muscle itself. Other diagnostic uses of the device, such as magnetic study of electric activity of the brain, might also be achieved.

FOR ADDITIONAL INFORMATION

U.S. Patent 3,557,777

Order from:
Commissioner of Patents
Washington, DC 20231

For licensing information, contact:
Office of Assistant General Counsel for Patents
U.S. Department of Energy
Washington, DC 20585

For additional information, contact:
Jane M. Welch
EG&G Idaho, Inc.
P.O. Box 1625
Idaho Falls, ID 83415
Telephone No.: (208) 526-8318

NASA Tech Brief
National Aeronautics and Space Administration
Marshall Space Flight Center, Alabama

Surgical Borescopes Remove Contaminants

Borescope instruments are put to use in extracting hard-to-reach particles.

Surgical instruments in flexible borescopes are being used for a new purpose: removing contaminant particles from normally inaccessible places within equipment. The instruments readily enter small openings, turn corners, and reach far.

Previously, the equipment to be cleaned often had to be shaken, otherwise manipulated, or flushed with gas; sometimes makeshift tools had to be used. The surgical borescope instruments offer an easier, quicker, and more effective answer to the contamination problem.

The instruments are about 0.070 in. (1.8 mm) thick and up to 6 ft (1.8 m) long. They can be used by themselves or through the borescope channel. One type of instrument has a claw at its end, another has a retractable loop, and a third has forceps — a variety of end effectors that can grasp many different forms of contaminants.

This work was done by Karen Vallow of Rockwell International Corp. for **Marshall Space Flight Center**. *No further documentation is available. MFS-29156 /TN*

FOR ADDITIONAL INFORMATION: *Contact: Director, Technology Transfer Division, P.O. Box 8757, BWI Airport, MD. 21240; (301) 621-0100 Ext. 241*
REFER TO THE NUMBER LISTED AT THE END OF THE ARTICLE

Natural Resources Technology & Engineering

695 Underground Channels Mapped by Radar

Software

696 Tidal Data Available through Microcomputer Software

697 HARPA (Hamiltonian Acoustic Ray-tracing Program for the Atmosphere)—Traces the three-dimensional paths of acoustic rays through continuous model atmospheres

698 Program for Thermospheric Calculations—Atmospheric properties at high altitudes are predicted.

United States
Department of
Agriculture

Research Technology
Agricultural Research Service

Underground Channels Mapped by Radar

Ground-penetrating radar that can detect hidden water channels is helping U.S. Department of Agriculture researchers predict what happens to pesticides after they are applied to crops.

"Our research is like doing bookkeeping for an ecosystem. We establish a budget for water, pesticides, and fertilizer use on a watershed, then try to account for how much was spent and where," says Ralph A. Leonard, soil scientist with the USDA Agricultural Research Service.

"Radar's role is vital in accounting for agrichemical movement that can't be seen," says Leonard, who is a member of a research team at the agency's Southeast Watershed Research Laboratory in Tifton, GA.

One of Leonard's uses for radar is as a surveying tool for charting topographic maps, not of land surfaces but of underground features. As the trailer-mounted unit is towed across a field, a series of echoes from radar signals bounce from the soil at various depths to give researchers clues to where and how chemicals are likely to move underground.

"Radar gives scientists underground data that they can use in computer models to help devise better ways of keeping agrichemicals out of groundwater," says David A. Farrell, the agency's national program leader for groundwater research.

"Our studies at Tifton and other locations are expected to yield new answers for protecting groundwater supplies," Farrell says.

At Tifton, the radar work is pinpointing the depths at which changes, such as different densities, occur in soil.

"Recording changes in soil density on a map lets us make a profile of the contour of an impervious soil layer. Its ups and downs are much like slopes, ridges, and valleys," Leonard says.

Watertight soil layers can form channels that intercept water and associated chemicals from beneath a crop's root zone and direct to either an aquifer or a body of water. Aquifers are reservoirs for the groundwater that supplies one-half the nation's drinking water.

When such a channel lies above the main aquifer it is called a perched aquifer. On Georgia's coastal plain, a perched aquifer may be only a few feet below the surface, while the main aquifer may be 60 to several hundred feet down.

A perched aquifer is just one thing to consider when tracking the movement of water in complex and out-of-sight groundwater systems, Leonard says.

Among others are the direction and rate of waterflow and location and thickness of the main aquifer, its geologic formation, and its ability to store and transport water. Radar helps in obtaining this information.

Leonard's research team is unraveling the intricacies of pesticide movement across and beneath field-sized watersheds. The land, which supports woods as well as field crops, is dotted by springs and ponds and crossed by sluggish streams.

Leonard says that besides pinpointing the location and depth of perched and main aquifers, radar can help:

- Determine where water flowing laterally in a perched aquifer eventually goes, whether to a main aquifer, a spring, a pond, or a stream.
- Select the best locations to place observation wells for monitoring fluctuations in the level of the water table or for collecting water samples for chemical analysis.
- Measure how much water is in a pond by sending signals from a boat-carried unit to the pond bottom.

"Radar can help in solving special problems of tracking groundwater movement in regions underlain by limestone," Leonard says. "For example, its signals may pick up fractures or large openings in limestone through which water pours as through a pipe."

Geologist Loris Asmussen reviews a soil density profile chart produced by the radar as it moves over a test area (background).

It can also probe sinkholes formed when limestone dissolves and collapses. These sinkholes often fill with drainage water, becoming surface lakes. Radar can help tell whether the water stays in the lake or enters an aquifer.

Leonard's research team is developing data for GLEAMS, a computer model that predicts potential effects of pesticides on groundwater. The model, whose full name is Groundwater Loading Effects of Agricultural Management Systems, is under test by the research agency and the USDA Soil Conservation Service.

GLEAMS will also be tested in a groundwater research project in cooperation with the U.S. Geological Survey.

Ralph A. Leonard is at the USDA-ARS Southeast Watershed Research Laboratory, P.O. Box 946, Tifton, GA 31793. (404) 546-3433

NOAA Technology Brief

National Oceanic and Atmospheric Administration
National Ocean Service
Office of Oceanography and Marine Assessment

Computer Software

Tidal Data Available through Microcomputer Software

A new NOAA software program is available that allows users to acquire near real-time water level data from selected tide stations equipped with telephone telemetry. The program is called Tides ABC and is designed for use with IBM-compatible personal computers and Hayes-compatible modems.

By using Tides ABC, 17 stations can now be accessed to obtain water level measurements. Water level is measured every 6 minutes at NOAA tide stations. Tides ABC can retrieve and display water levels for periods up to 5 days prior to the present date and compute any predictions from 1985-1997.

Tides ABC can generate graphic and tabular information in both video and printed displays that compare actual water level at a station against water levels predicted in NOAA tide tables. It can also compare predicted water levels with anomalies.

Near real-time water level data from Tides ABC can be used for navigation, vessel traffic control, channel dredging and maintenance, and coastal management by businesses and governments involved in transportation, fishing, boating, coastal recreation, and planning.

The current Tides ABC software provides access to some water level data that has not been processed or analyzed by NOAA; therefore, NOAA makes no warranties, either expressed or implied, concerning the accuracy, completeness, reliability, or suitability of that data.

The program diskette and user manual can be purchased from NOAA for $1,400. For additional information, write Joseph Mullin, Physical Oceanography Division (N/OMA1231), Office of Oceanography and Marine Assessment, National Ocean Service, NOAA, 6001 Executive Boulevard, Rockville, Maryland 20852, or telephone (301) 443-8469.

National Oceanic and Atmospheric Administration

HARPA (Hamiltonian Acoustic Ray-tracing Program for the Atmosphere)

Traces the three-dimensional paths of acoustic rays through continuous model atmospheres

HARPA stands for Hamiltonian Acoustic Ray-Tracing Program for the Atmosphere developed by the National Oceanic and Atmospheric Administration's Wave Propagation Laboratory in Boulder, Colorado. The modular FORTRAN 77 computer program traces the three-dimensional paths of acoustic rays through continuous model atmospheres by numerically integrating Hamilton's equations -- a differential expression of Fermat's principle. The user specifies an atmospheric model by writing closed-form formulas for its three-dimensional wind and temperature (or sound speed) distribution, and by defining the height of the reflecting terrain vs. geographic latitude and longitude. In addition to computing the geometry of each raypath, HARPA can calculate pulse travel time, phase time, Doppler shift, absorption, and geometrical path length.

The program is written in the FORTRAN programming language for implementation on a CDC Cyber-840 using a NOS 2.X operating system. Special features and/or requirements in hardware: Any FORTRAN 77 compiler. DISSPLA is useful but not essential. Source tape is in the ASCII character set. This restricts preparation to 9 track, one-half inch tape only. Identify recording mode by specifying density only. Price includes documentation, PB87-132031/NAC.

For Additional Information:

For information about ordering this software, contact the
NTIS Computer Products Center, NTIS, 5285 Port Royal Road, Springfield, VA 22161; (703) 487-4763.
Refer to PB87-132023//NAC

Program for Thermospheric Calculations

Atmospheric properties at high altitudes are predicted.

MSIS83 is a computer program for an empirical model of the thermosphere based on mass-spectrometer and incoherent-scattering data. It provides a description of the atmospheric temperature, density, and composition at altitudes higher than 85 kilometers. There are coefficients in MSIS83 to account for yearly and daily variations, geodetic latitude and longitude, and solar activity. Variations due to magnetic storms are represented by 3-hour magnetic a_p indices. The MSIS83 model enables a more timely prediction of aeronomic densities for such specific events as rocket flights.

The data base for this model is a comprehensive summary of rocket flight, satellite, incoherent-scattering radar, grenade, and falling-sphere measurements. Subsets of data were formed by random selection after sorting on altitude, latitude, time of day, etc. Curve fitting was done with 4- to 5-thousand data points at a time. The resulting coefficients are presented in subroutines that calculate the thermospheric composition and temperature for a position and time supplied by the user.

MSIS83 is written in FORTRAN 77 for use with batch or interactive programs and has been implemented on a DEC VAX-series computer operating under VMS with a central-memory requirement of approximately 18K of 8-bit bytes. MSIS83 is based on a 1977 implementation of a thermospheric model and was last updated in 1983.

This program was written by A. E. Hedin of **Goddard Space Flight Center.**

GSC-12989 /TN

FOR ADDITIONAL INFORMATION

CONTACT:

COSMIC®
112 Barrow Hall
University of Georgia
Athens, GA 30620
(404) 542-3265

Physical Sciences

699 Cleaning With Ultraviolet Radiation and Ozone—The combustion of radiation and active oxidation removes contaminants quickly and clearly.

700 Chemist's Workbench for Molecular Mechanics—A suite of programs allows modeling, analysis, and display

701 Temperature and Concentration Profiles in Hydrogen/Nitrous Oxide Flames—Raman spectroscopy and laser-induced fluorescence yield data on constituents and temperatures over a range of flame mixtures.

702 New Fischer-Tropsch Catalysts Derived from Zeolitic Aluminoferrisilicates

703 High Pressure Studies Show Rare Behavior of Bonding in Actinide Metals

704 Determining Optical Axes of Uniaxial Crystals

705 Monolithic Isolated Single-Mode Ring Laser—The MISER uses a four-sided ring to lase nonreciprocally. (Licensing Opportunity)

706 Rapid Synthesis of Nonstoichiometric Lanthanum Sulfide—A new process is relatively fast and simple.

707 Thermoelectric Properties of Lanthanum Sulfide—At 300 to 1,400 K, Gamma-phase La(3-x)S4 is an extrinsic semiconductor.

708 A Model-Parameter Extraction Procedure—The procedure accommodates multiple input excitations.

709 Preventing Cracks in Silicon-Reactor Liners—Correct placement may help to prevent contamination while eliminating crack-causing deposits.

Testing & Instrumentation

710 Monitoring Ion-Implantation Progress—A conventional implanter can be modified to perform ion acoustic microscopy.

711 Automatic Measurement of Rain Rate—Standard rain gauges are assembled into an electronic collection, storage, and processing sytem.

712 One-Dimensional Simulation of Isotropic Radiation—Solar cells are tested for effects of radiation in a unidirectional beam.

713 Versatile X-Ray Telescope—Spatial and spectral resolutions are increased. (Licensing Opportunity)

714 Wide-Angle, Flat-Field Telescope—An all-reflective system is unvignetted. (Licensing Opportunity)

Other items of interest

639 New Polymer Electrolyte for Batteries

660 Air Monitoring Device Developed—New meter measures light scattered by particulates.

675 Self-Propagating High-Temperature Synthesis—A new method of preparing ceramics offers many advantages.

684 Radiation Effects on Polymer Properties—Tables present lowest doses for which effects are noticeable.

697 HARPA (Hamiltonian Acoustic Ray-tracing Program for the Atmosphere)—Traces the three-dimensional paths of acoustic rays through continuous model atmospheres

MANUFACTURING TECHNOLOGY NOTE

U.S. ARMY MATERIEL COMMAND

Deputy Chief of Staff for Manufacturing Technology, Alexandria, VA

Project Number: AH94 Filing Code: 68A006

Cleaning With Ultraviolet Radiation and Ozone

The combustion of radiation and active oxidation removes contaminants quickly and clearly.

In a study by the U.S. Army Laboratory Command, cleaning with ultraviolet radiation and ozone has been shown to be a highly effective method of removing a variety of contaminants. It is a simple-to-use dry process, which is inexpensive to set up and operate (see figure). It can produce clean surfaces at room temperature, either in a room atmosphere or a controlled atmosphere.

The cleaning mechanism seems to be a photosensitized oxidation process in which the contaminant molecules are excited and dissociated by the absorption of short-wavelength ultraviolet light. Simultaneously, atomic oxygen is generated when molecular oxygen and ozone are dissociated by the absorption of short- and long-wavelength radiation. The products of the excitation of contaminant molecules react with atomic oxygen to form simpler molecules, such as CO_2 and H_2O, which desorb from the surface.

The variables of the cleaning procedure are the contaminants, the precleaning method, the wavelengths emitted by the ultraviolet source, the atmosphere between source and sample, the distance between source and sample, and the time of exposure. For surfaces that are properly precleaned and placed within a few millimeters of an ozone-producing ultraviolet source, the process can produce a clean surface in less than 1 minute.

Project officer John R. Vig
(201) 544-4275 or AV 995-4275.

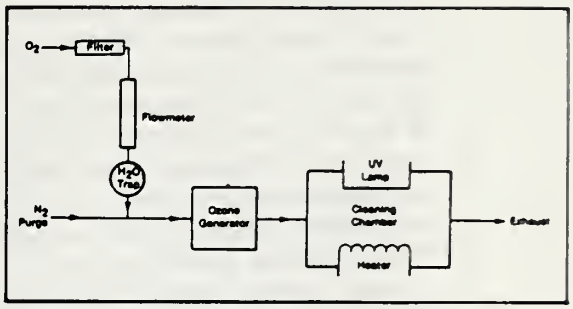

Representative **Application** of ultraviolet and ozone cleaning removes photoresist from semiconductor devices. With the setup shown here, removal rates as high as 1,600 angstroms/minute have been achieved. The apparatus uses auxiliary ozone generation.

FOR ADDITIONAL INFORMATION:

You can learn more details about this technology by ordering the NTIS report(s):
Basic and Applied Research in the Field of Electronics and Communications.
Order number: AD-A169024/NAA
Price code: A03
Order from:
National Technical Information Service
5285 Port Royal Road
Springfield, VA 22161

This document was prepared under the sponsorship of the U.S. Government. Neither the United States Government nor any person acting on behalf of the United States Government assumes any liability resulting from the use of the information contained in this document, or warrants that such use will be free from privately owned rights.

MANUFACTURING TECHNOLOGY NOTE

U.S. ARMY MATERIEL COMMAND

Deputy Chief of Staff for Manufacturing Technology, Alexandria, VA

Project Number: 1L162706 Filing Code: 62B112

Chemist's Workbench for Molecular Mechanics

A suite of programs allows modeling, analysis, and display

The Molecular Modeling, Analysis, and Display System (MMADS) is a "chemist's workbench," a user-friendly, integrated suite of programs organized around a common data structure. Developed by the U.S. Army Chemical Research, Development, and Engineering Center, MMADS incorporates application programs for quantum, physical, and physical organic chemistry, as well as state-of-the-art molecular graphic routines.

Every molecule entered into MMADS is described via a structure file. These files specify the type, location, and bonding environment for each atom, along with the number of atoms in the molecule and a descriptor line for the file.

All actions performed by MMADS are initiated by commands entered by the user. Structure entry commands allow the user to enter a great variety of structures, whether from a traditional chemical structure, fragments from structures already determined, or data from x-ray crystallography.

Structure modification commands allow the user to make changes in a structure already entered, while preserving the information necessary for compatibility with the other parts of the system. Structure maintenance commands allow the user to obtain information on the run time and revision status of MMADS, tailor the execution parameters, perform interrogation and preparation operations on structure files, and maintain the set of equilibrium values and force constants needed for molecular-mechanics calculations.

Structure optimization commands allow the user to optimize the geometry of a structure by minimizing the molecular potential function. Property determination commands allow the user to determine the steric and electronic properties of a structure without altering the molecular geometry. Four physical properties can be calculated: (1) the molecular surface area, (2) the molecular volume, (3) the volume shared between two molecules, and (4) the solvent-accessible surface area.

Graphical display commands allow the user to employ the various graphic display devices available to view the geometry created by MMADS. With these commands, the user can obtain a rough geometry on a nongraphics terminal, obtain a projection about any bond, obtain a colored stick-figure representation, view structures with crystallographic data base, and obtain real-time, three dimensional representations. Theoretical calculation commands allow the user to do both semiempirical and analytical computations.

FOR ADDITIONAL INFORMATION:

You can learn more details about this technology by ordering the NTIS report(s):
A User's Guide to the Molecular Modeling, Analysis, and Display System (MMADS).
Order number: AD-A171019/NAA
Price code: A03

This document was prepared under the sponsorship of the U.S. Government. Neither the United States Government nor any person acting on behalf of the United States Government assumes any liability resulting from the use of the information contained in this document, or warrants that such use will be free from privately owned rights.

MANUFACTURING TECHNOLOGY NOTE

U.S. ARMY MATERIEL COMMAND

Deputy Chief of Staff for Manufacturing Technology, Alexandria, VA

Project Number: 1L161102AH43 Filing Code: 81A006

Temperature and Concentration Profiles in Hydrogen/Nitrous Oxide Flames

Raman spectroscopy and laser-induced fluorescence yield data on constituents and temperatures over a range of flame mixtures.

An experimental study of atmospheric-pressure hydrogen/nitrous oxide flames has measured temperature and nitric oxide, oxygen, and nitrogen concentration profiles. The proportions of H_2 and NO_2 ranged from lean to stoichiometric. Spontaneous Raman spectroscopy was the primary measurement technique in the study, which was done by the U.S. Army Ballistic Missile Research Laboratory. Laser-induced fluorescence was used to measure hydroxyl concentration profiles.

It is possible to observe the Raman spectra simultaneously for four molecules with the experimental detection system (see figure). The Raman signals for NO, N_2, and O_2 were individually analyzed by an interactive, multivariate least-squares fitting procedure, which incorporates the necessary molecular and experimentally specific information; an analysis of the N_2O Raman signals has not been done.

Measured NO concentrations were found to be much higher than the equilibrium values for all the H_2/N_2 ratios studied. This result provides further evidence that detailed chemistry is required to describe the flame system. Both line-of-sight and spatially resolved optical techniques give similar results for flame temperature and NO concentration.

Large differences are observed when the OH concentration of a lean atmospheric-pressure flame is compared with the same flame at low pressure. Possible pressure effects or the inherent differences between the optical technique and mass spectrometric sampling may be responsible. Project officer Anthony J. Kotlar (301)278-2170 or AV 283-2170.

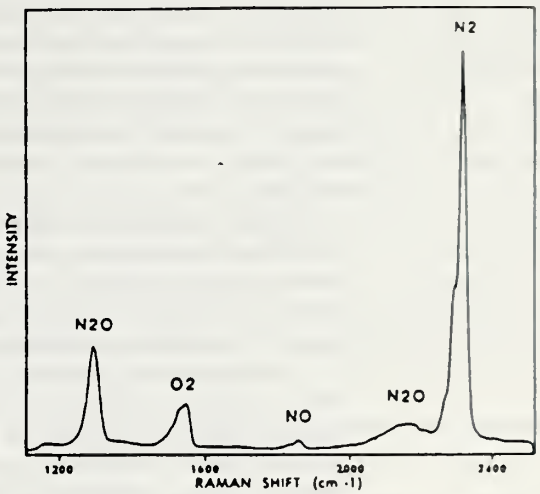

Five Peaks Representing Four Different Molecules appear in Stokes Q-branch Raman spectra of a hydrogen-nitrous oxide premixed flame. The laser excitation wavelength here is 350.742 nanometers.

FOR ADDITIONAL INFORMATION

You can learn more details about this technology by ordering the NTIS reports:
Temperature and Concentration Profiles in Hydrogen/Nitrous Oxide Flames.
Order number: AD-A171085/NAA
Price code: A02
Order from:
National Technical Information Service
5285 Port Royal Road
Springfield, VA 22161

This document was prepared under the sponsorship of the U.S. Government. Neither the United States Government nor any person acting on behalf of the United States Government assumes any liability resulting from the use of the information contained in this document, or warrants that such use will be free from privately owned rights.

energygram

New Fischer-Tropsch Catalysts Derived from Zeolitic Aluminoferrisilicates

DOE/TIC/EG-86/137
OFFICE OF SCIENTIFIC AND TECHNICAL INFORMATION

This technical note summarizes a project achievement selected from the U.S. Department of Energy 1985 Basic Energy Sciences Program.

Argonne National Laboratory

Fischer-Tropsch catalysts have been in use for decades. Developed in the early twentieth century, these iron-based catalysts have been the workhorse for the petroleum and petrochemical industries for conversion of crude oil to more-desirable, lower-molecular-weight hydrocarbons. Research has been focused on understanding their mechanisms with the goal of improving the selectivity of conversions promoted by this class of solid catalysts.

Zeolites are naturally occurring materials with an open structure of molecular dimensions that have been found to be selective in admitting certain sizes or shapes of molecules into their open structures. This property of selectivity can be controlled through altering the zeolite's composition and dimensions. This current research has successfully wedded the selectivity of a zeolite with the properties of a Fischer-Tropsch catalyst.

At Argonne National Laboratory, a new approach has been successfully applied to the formation of extremely small metallic iron particles (diameter <20 Å) within an aluminoferrisilicate (AFS) zeolitic structure. The iron particles are highly dispersed and have been produced in two different structures, both of which have now been shown to be active Fischer-Tropsch catalysts. A further modification procedure permits the activity and selectivity of this new Fischer-Tropsch zeolite catalyst to be modified by introduction of other elements, such as nickel or cobalt. Good selectivity for producing high yields of light hydrocarbons (less than five carbons in the molecule) has been found in preliminary tests of these new catalysts.

Employing shape-selective materials, e.g., zeolites, is a potentially powerful method for improving selectivity in heterogeneous catalytic conversions. One of the most important long-range technological targets in catalysis is the efficient production of feedstock chemicals from coal or biomass sources via hydrogenation of carbon monoxide. Iron-based catalysts are preferred due to iron's availability and cost relative to other metals with similar catalytic properties. Improved performance with increasing metal dispersion has been reported for iron Fischer-Tropsch catalysts, but achieving very high dispersions has been very difficult. This new method for producing highly dispersed iron particles on zeolites is a promising new direction and is potentially applicable to incorporation of other elements, either for Fischer-Tropsch conversion or other important energy-related catalytic processes. Currently, direct Fischer-Tropsch conversion at modest operating pressure with good selectivity to light hydrocarbons appears to be a reasonable prospect using zeolite catalysts. (Argonne National Laboratory, L. Iton)

FOR ADDITIONAL INFORMATION

For additional information, contact:
L. Iton
Argonne National Laboratory
9700 South Cass Avenue
Argonne, IL 60439
Telephone No.: (312) 972-5536

energygram

High Pressure Studies Show Rare Behavior of Bonding in Actinide Metals

DOE/TIC/EG-86/161
OFFICE OF SCIENTIFIC AND TECHNICAL INFORMATION

This technical note summarizes a project achievement selected from the U.S. Department of Energy 1985 Basic Energy Sciences Program.

ornl
Oak Ridge National Laboratory

In a collaborative effort between Oak Ridge National Laboratory and the University of Tennessee, a discovery has been made of a scientific phenomenon rare in the metallic elements. It has been seen in the actinide series of elements, and it provides insights into the understanding of electronic structure and chemical bonding of all elements.

The first clear evidence has been obtained that the f-electron type of metallic chemical bonding can be induced by enormous pressures in elements above atomic number 94, plutonium. The experimental evidence comes from both X-ray studies of actinide metal crystal structures and volume changes for four transplutonium elements: americium, curium, berkelium, californium, and berkelium-californium alloys. Only two other examples of f-electron metallic bonding under extreme pressure are known.

It was found that when extreme pressures squeeze the atoms together, at a certain threshold pressure for each higher actinide studied, the 5f electrons enter metallic bonding, volume collapse occurs, and the crystal geometry suddenly changes. The volume collapse in some cases is striking: for curium at 440,000 atmospheres, it is 2.1%.

FOR ADDITIONAL INFORMATION

For additional information, contact:
Oak Ridge National Laboratory
P.O. Box X
Oak Ridge, TN 37831

NASA Tech Brief
National Aeronautics and
Space Administration
Lewis Research Center, Cleveland, Ohio

Determining Optical Axes of Uniaxial Crystals

The polarizing-microscope concept is adapted for thick samples.

Uniaxial crystals such as sapphire, quartz, calcite, and ice exhibit the property known as birefringence. A single laser beam entering such a material is generally split into two beams, each having a different polarization. Single-beam transmission is possible if the optical axis of the crystal is perpendicular to the direction of the beam propagation or if the polarization of the incoming beam is identical to that of either of the outgoing beams. These polarization directions can be calculated if the directions of the incident beam and the optical axis are known.

The optical axis of a crystal is usually found by examining a sample thinner than 1 mm between crossed polarizing plates. Because it is frequently impractical to cut off a small sample of a crystal for testing, the technique was modified to accommodate large crystals.

A vertically polarized, expanded laser beam is first passed through the crystal under study and then through a horizontally polarizing plate. The crystal is rotated until light ceases to be transmitted through the final polarizing plate. This places the optical axis in the plane containing the initial beam and the axis of rotation of the crystal. The crystal is then rotated 90°, and the initial polarization is rotated until transmission again ceases. This polarization is now parallel or perpendicular to the optical axis. The correct orientation is chosen by observing the interference pattern created by light passing through the final polarizing plate.

The ability to circumvent the effect of birefringence has applications where laser beams must be transmitted through uniaxial crystals, as in laser diagnostics of contained flows in systems requiring windows for optical access.

This work was done by Harold J. Schock and Carolyn A. Regan of **Lewis Research Center** *and James A. Lock of Cleveland State University. Further information may be found in NASA TM-86892 [N86-22915/NSP], "The Determination of the Direction of the Optic Axis of Uniaxial Crystalline Materials."*

Copies may be purchased from the National Technical Information Service, Springfield, Virginia 22161, [A02]
LEW-14452 /TN

FOR ADDITIONAL INFORMATION: *Contact: Director, Technology Transfer Division, P.O. Box 8757, BWI Airport, MD. 21240; (301) 621-0100 Ext. 241*
REFER TO THE NUMBER LISTED AT THE END OF THE ARTICLE

NASA Tech Brief
National Aeronautics and Space Administration
Langley Research Center, Hampton, Virginia

Licensing Opportunity

Monolithic Isolated Single-Mode Ring Laser

The MISER uses a four-sided ring to lase nonreciprocally.

Lasers of a single, very-stable frequency are desirable for a number of purposes. Frequency stability makes possible coherent detection of laser radiation with a low-bandwidth detector, which is useful for communications. It also allows very-high-resolution spectroscopy. Any application where it is desired to use a laser in the way microwaves have been used traditionally can be enhanced if the frequency is very stable. This laser concept should provide a very-compact, efficient, and stable source of coherent radiation.

Laser materials that are homogeneously broadened, such as Nd:YAG, should lase easily in a single mode, at least when pumped continuously. In a conventional linear resonator, Nd:YAG lases in five or more modes due to a phenomenon known as spatial hole burning. Spatial hole burning occurs when there is a standing wave in the resonator with a sinusoidal intensity pattern. At points of low intensity, there is poor saturation of the gain, and the other modes will be above threshold.

One successful technique for achieving single-longitudinal-mode operation in materials such as Nd:YAG is to build the laser resonator as a nonreciprocal ring. When there is a traveling wave instead of a standing wave, there is uniform saturation of the gain, and only one mode should lase. What is needed is a ring resonator that has a slightly greater loss in one direction than in the other.

The Monolithic (no external mirrors) Isolated (from external reflections) Single-Mode End-Pumped Ring Laser (MISER) consists of a single piece of solid-state laser material with a ring path for the laser beam. The simplest ring would be three sided. However, the two possible directions for lasing in a single-crystal triangle ring will be equivalent. Nonreciprocity is impossible, and the laser will lase in both directions. For nonreciprocity to exist, it is necessary for the ray path to be in two different planes.

The MISER design is a four-sided ring. Three of the corners utilize total internal reflection, while the fourth is the output coupler. The output coupler is at nonnormal incidence, so it acts as a polarizer. The corners at which total internal reflection takes place act as birefringent elements. There is a magnetic field that causes magneto-optic rotation of the direction of polarization.

Because the planes of incidence for the four faces are not all the same, there is some nonmagnetic rotation of the polarization. The strength of the magnetic field and the orientation of the total-internal-reflection faces are such that light traveling in one direction "sees" each face in the proper orientation for no birefringence to take place, while light traveling in the other direction is fairly strongly polarized. Since the output coupling will be substantially greater for the P-polarization than for the S-polarization, the laser will operate in the S-polarization. Only for one direction of travel will a ray leaving the coupler in the S-polarization return in that polarization. This is the direction in which the laser will operate.

Because the laser will be a nonreciprocal ring, it will lase in a single-axial mode. The ring also isolates it from outside reflection, because light entering the output coupler parallel to the output beam will travel the wrong way through the ring and thus will not be amplified. Matching the pump radiation (from a mostly-coherent diode laser array) into the mode volume will result in easy single-transverse-mode operation. Frequency stability is possible, because the natural acoustic modes of the crystal are at very high frequencies, which cannot propagate through the mounting hardware into the crystal. Thermal stability is also possible, since the diode pumping results in little waste heat, and cooling may be done by conduction or thermoelectrically.

This work was done by Thomas J. Kane and Robert L. Byer of Stanford University for **Langley Research Center**. *No further documentation is available.*

In accordance with Public Law 96-517, the contractor has elected to retain title to this invention. Inquiries concerning rights for its commercial use should be addressed to:

Office of Technology Licensing
Stanford University
Stanford, CA 94305
(ref. invention S83-081).

Refer to LAR-13191, /TN

Langley Research Center
Technology Utilization Officer
John Samos
Mail Stop 139A
Hampton, VA 23665
(804) 865-3281
Patent Counsel:
Howard J. Osborn
Mail Code 279
Hampton, VA 23665
(804) 865-3725

FOR ADDITIONAL INFORMATION: *Contact: Director, Technology Transfer Division, P.O. Box 8757, BWI Airport, MD. 21240; (301) 621-0100 Ext. 241*
REFER TO THE NUMBER LISTED AT THE END OF THE ARTICLE

NASA Tech Brief
National Aeronautics and
Space Administration
NASA's Jet Propulsion Laboratory, Pasadena, California

Rapid Synthesis of Nonstoichiometric Lanthanum Sulfide

A new process is relatively fast and simple.

An improved method of synthesizing nonstoichiometric lanthanum sulfide is faster and simpler than the former method. The product may be purer because some of the prior sources of contamination are eliminated.

In the former method, a lanthanum ingot was cut or ground into small chips. Along with the required amount of sulfur, the chips were sealed under vacuum in a quartz ampoule. The ampoule was placed in a resistance-heated furnace at a temperature of 500 to 800 °C, which was below the melting point of lanthanum. The reaction took several days because the sulfur had to diffuse through and into the lanthanum chips.

In the new method, the lanthanum ingot is placed directly in a flat-bottomed graphite boat and enclosed in a heat- and chemical-resistant glass ampoule. The sulfur is placed in a sulfur reservoir that communicates with the ampoule, and the ampoule/reservoir system is sealed under vacuum.

The lanthanum ingot is melted by radio-frequency heating of the graphite boat. The liquid lanthanum spreads over a large area in the boat. The sulfur is heated to 300 to 450 °C, causing it to vaporize. This vapor reacts quickly with the lanthanum; the reaction is complete in about 2 hours.

The reaction is faster in the new process because the lanthanum is molten. The elimination of grinding or cutting not only simplifies the process but also eliminates contamination from the grinding or cutting machinery. In the new method, the oxidation of the lanthanum by oxygen in the glass is suppressed in two ways: (1) The lanthanum does not touch the glass, and (2) the glass remains below 400 °C during the radio-frequency heating, thereby reducing the rates at which oxygen diffuses from within and permeates through the glass.

This work was done by Seigo Matsuda, Edik Shapiro, Lee Danielson, and Harold Hardister of Thermo Electron Corp. for **NASA's Jet Propulsion Laboratory**. *NPO-16631 /TN*

FOR ADDITIONAL INFORMATION: *Contact: Director, Technology Transfer Division, P.O. Box 8757, BWI Airport, MD. 21240; (301) 621-0100 Ext. 241*
REFER TO THE NUMBER LISTED AT THE END OF THE ARTICLE

NASA Tech Brief
National Aeronautics and Space Administration

Thermoelectric Properties of Lanthanum Sulfide

At 300 to 1,400 K, γ-phase $La_{3-x}S_4$ is an extrinsic semiconductor.

A report describes the measurement of the Seebeck coefficient, electrical resistivity, thermal conductivity, and Hall effect in γ-phase lanthanum sulfide with composition of $La_{3-x}S_4$ ($0.04 \leq x \leq 0.3$). Results of this study, part of the search for high-temperature thermoelectric energy-conversion materials, indicate that this sulfide behaves like an extrinsic semiconductor over the temperature range of 300 to 1,400 K, with a degenerate carrier concentration controlled by the stoichiometric ratio of La to S.

Lanthanum sulfide was prepared by the reaction of lanthanum ribbon with sulfur in quartz ampoules, the melting of the product in tungsten crucibles, and then the grinding of the powder. The specimens for thermoelectric study were then prepared by hot pressing in vacuum at a temperature of approximately 1,800 K and at a mechanical pressure of 10^4 psi (69 MN/m^2) for about 1 h. X-ray diffraction showed the hot-pressed pellets to be γ-phase. The composition of the pellets was determined by the amount of hydrogen evolved when they were dissolved in acid.

A four-probe method was used to measure the electrical conductivities. The Seebeck coefficients were determined by use of small temperature gradients. These measurements were confirmed by measurements at large temperature gradients; that is, by the Seebeck voltages measured as functions of temperature and then differentiated to obtain the Seebeck coefficients. The dc van der Pauw technique was applied to obtain the Hall-effect measurements. These were made as a function of temperature on 1-mm-thick slices cut perpendicularly to the axes of cylindrical samples.

Thermal conductivities were calculated from the thermal diffusivities, the densities (determined by Archimedes' principle), and the specific heat (measured between 300 and 900 K by a differential scanning calorimeter). The mass loss rate of the sulfide was determined in situ as a function of temperature by a mass-spectrometer thermal gravimetric apparatus in a vacuum of 10^{-8} torr (1.3×10^{-6} N/m^2).

Results showed that all Seebeck coefficients are n-type, and both the resistivities and Seebeck coefficients increase approximately linearly with increasing temperature. In these respects, the materials resemble metals. There is no indication from the data that the materials in this composition and temperature range become intrinsic semiconductors. The Hall constants and thus the carrier concentrations are almost invariant with temperature. The Hall mobilities are low and are approximately proportional to the reciprocal of temperature, as expected for metallike behavior.

The data are consistent with lanthanum sulfide in the specified composition range being an extrinsic semiconductor; i.e., the conduction process is by the itinerant motion of large (nearly degenerate) concentrations of quasi-free electrons undergoing acoustic-mode scattering. A theoretical analysis of the data yielded fairly high values for the electron effective mass (in the range of 2 to 3) and low values for electron mobilities (in the range of 1 to 6 $cm^2V^{-1}s^{-1}$), which suggest that the energy bands are fairly narrow.

Experimental results and theoretical analysis showed that the optimum figure of merit (Z) should occur for compositions in the range $x = 0.30$ to 0.32. The highest experimental value for Z was approximately 5×10^{-4} at 1,000 °C. Although it may be possible to exceed this value slightly by a slight adjustment in composition, large improvements are not anticipated because of the low electron mobilities. These results suggest that to realize higher Z, a search should be made for rare-earth chalcogenides of comparable electron effective masses but having higher charge-carrier mobilities.

This work was done by Charles Wood, R. Addis Lockwood, James B. Parker, Andrew Zoltan, Leslie D. Zoltan, Lee Danielson, and Valvo Raag of Caltech for **NASA's Jet Propulsion Laboratory**. *"Thermoelectric Properties of Lanthanum Sulfide," NPO-16662 /TN*

FOR ADDITIONAL INFORMATION: *Contact: Director, Technology Transfer Division, P.O. Box 8757, BWI Airport, MD. 21240; (301) 621-0100 Ext. 241*
REFER TO THE NUMBER LISTED AT THE END OF THE ARTICLE

NASA Tech Brief
National Aeronautics and
Space Administration

A Modal-Parameter Extraction Procedure

The procedure accommodates multiple input excitations.

An improved modal-parameter extraction procedure applicable to linear, time-invariant systems is derived in a 92-page report. The algorithm allows multiple noncoherent input excitations to be applied to a structure and generates a consistent set of modal parameters.

The procedure is an extension of simultaneous frequency-domain (SFD) techniques that was achieved through an investigation of two automatic methods for reducing the effective problem size while minimizing the amount of user interaction. (Problem-size reduction is an important consideration because practical modal analyses often require numerous measurement locations.) In several sample runs, the independent-coordinate reduction method is shown to be the more accurate method for small sample size. The principle-component method can be used to estimate the number of modes active in a given frequency range.

No restrictive assumptions are made concerning the damping matrix. In contrast to the prior SFD techniques, the derivation provides for skew-symmetric and nonproportional damping matrices. Accurate damped frequencies, decay rates, and complex modes are calculated for such a system despite relatively high noise levels.

The procedure uses solution methods more stable than those of the prior SFD techniques. Of two solution methods noted for accuracy and stability, Householder's method is preferable to the singular-value decomposition techniques because of its faster execution and easier use.

The procedure accurately resolves closely spaced modes. An experimental comparison showed that the parameters obtained by the new method are comparable to those obtained with the Polyreference and the complex-exponential algorithms.

The report also notes topics worthy of further investigation; for example, it recommends numerical study of the methods suggested in the report for calculating standard and residual attachment modes from experimental data. As another potential application of the procedure, it recommends the investigation of the use of the experimental reduced systems matrices directly in a substructure-coupling procedure. Possible avenues for modifying and improving the procedure are also given.

This work was done by Andrew H. Kurdila and Roy R. Craig, Jr., of the University of Texas at Austin for **Marshall Space Flight Center**. *Further information may be found in NASA CR-178509 [N85-33747/NSP], "A Modal Extraction Procedure Applicable to Linear Time Invariant Dynamic Systems."*

Copies may be purchased from the National Technical Information Service, Springfield, Virginia 22161, [A05]
MFS-27139 /TN

FOR ADDITIONAL INFORMATION: *Contact: Director, Technology Transfer Division, P.O. Box 8757, BWI Airport, MD. 21240; (301) 621-0100 Ext. 241*
REFER TO THE NUMBER LISTED AT THE END OF THE ARTICLE

NASA Tech Brief
National Aeronautics and Space Administration
NASA's Jet Propulsion Laboratory, Pasadena, California

Preventing Cracks in Silicon-Reactor Liners

Correct placement may help to prevent contamination while eliminating crack-causing deposits.

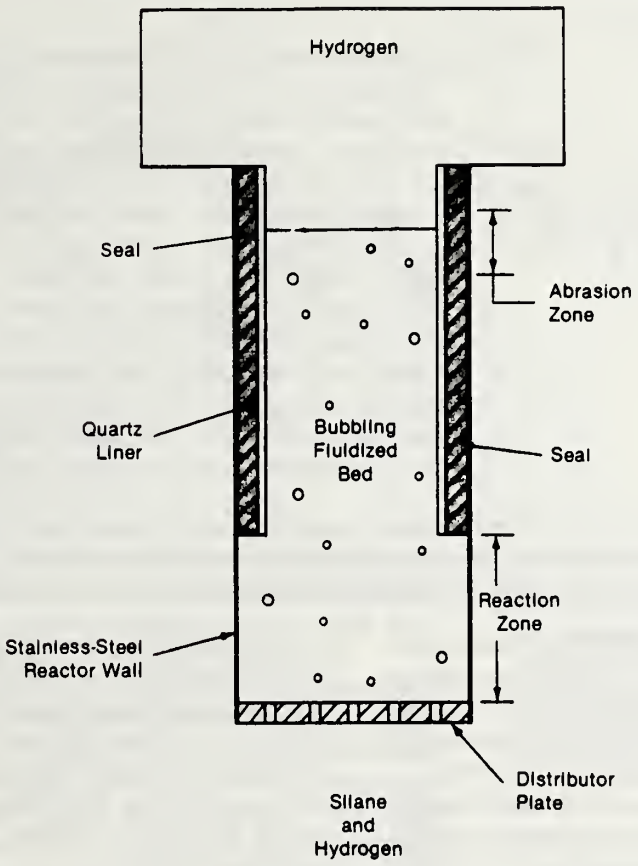

The **Bottom of the Quartz Liner** is raised above the reaction zone. The liner still covers the abrasion zone at the top of the fluidized bed.

Repositioning the quartz liner in a silicon fluidized-bed reactor prevents cracking of the liner when it cools. The liner protects the stainless-steel walls of the reactor from abrasion by the particles in the fluidized bed. It thus prevents contamination of the newly formed silicon by material abraded from the wall and ensures a high-quality product.

However, silicon tends to deposit on the liner as it decomposes from the silane flowing with hydrogen through the bed. When the quartz cools, the difference in contraction between it and the accumulated silicon layer tends to crack the liner. A costly replacement is then necessary before the reactor can be used again.

If the liner is positioned so that it covers the abrasion zone at the top of the bed but not the reaction zone at the bottom, the problem is avoided (see figure). The liner still protects the reactor wall but is not exposed to deposition of significant amounts of silicon.

This work was done by Ralph Lutwack of Caltech for **NASA's Jet Propulsion Laboratory**. *NPO-16708 /TN*

FOR ADDITIONAL INFORMATION: *Contact: Director, Technology Transfer Division, P.O. Box 8757, BWI Airport, MD. 21240; (301) 621-0100 Ext. 241*
REFER TO THE NUMBER LISTED AT THE END OF THE ARTICLE

MANUFACTURING TECHNOLOGY NOTE

U.S. ARMY MATERIEL COMMAND

Deputy Chief of Staff for Manufacturing Technology, Alexandria, VA

Project Number: NONE

Filing Code: 73D096

Monitoring Ion-Implantation Progress

A conventional implanter can be modified to perform ion acoustic microscopy.

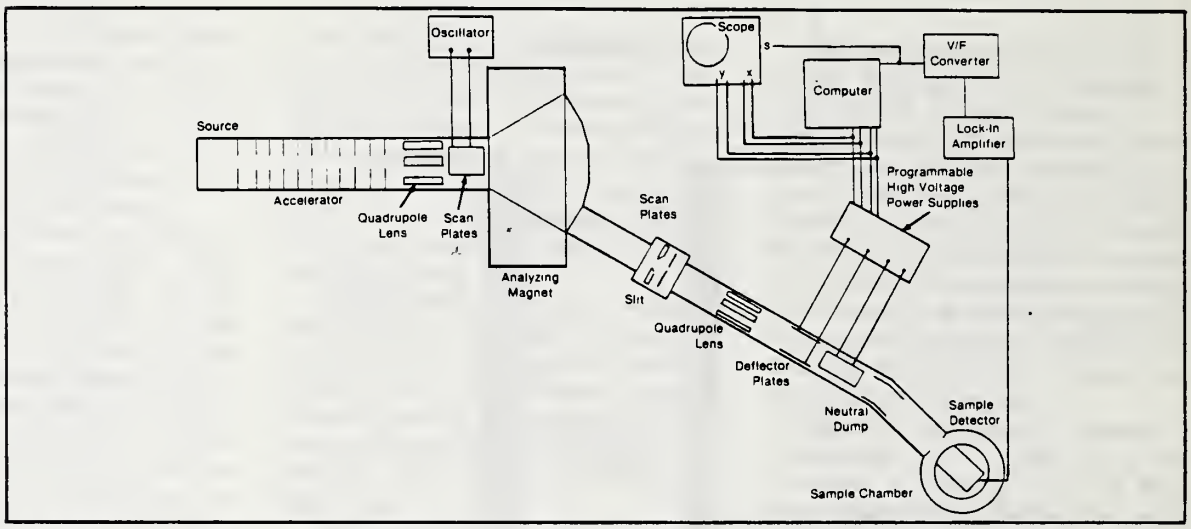

A **Standard Ion Implanter** was modified to function as a monitor of implantation progress. The components of the standard implanter are labeled below the diagram, and the added components are labeled above.

An ion-implantation apparatus has been modified so that it can be used for ion acoustic microscopy. The apparatus, developed for the U.S. Army Tank-Automotive Command, can monitor the progress of implantation in metals and ceramics.

Vertical scanning plates were added to the apparatus, positioned before the analyzing magnet (see figure). A movable plate with a 0.5- or 2-mm aperture was placed directly behind the normal slit aperture. A sinusoidal voltage of up to 50 V peak to peak on the plates scanned the ion beam across the aperture to produce a 10-to 20-percent variation in beam current through the aperture.

By scanning the beam and sending a portion of the scanning voltages to the x and y inputs of an oscilloscope, with a signal proportional to the Faraday cup current going to the z (intensity) axis, it was possible to obtain an image of the beam spot. The shape and position of the beam could then be adjusted with the quadrupole lenses to provide a well-focused, properly positioned beam.

The scan drive was modified to permit scanning plates to be driven by a computer interfaced to a set of programmable high-voltage power supplies. Programming was designed to scan the beam alternately up and down across a sample in a series of 48 vertical lines. Each line was divided into 48 points, so that the acoustic signal it generated could be recorded.

With a fairly intense ion beam 1 cm in diameter, modulated at megahertz frequencies, ion acoustic microscopy appears to be a viable method for monitoring the progress of implantation.

Project officer Douglas N. Rose
(313) 574-7752 or AV 786-7752.

FOR ADDITIONAL INFORMATION:

You can learn more details about this technology by ordering the NTIS report(s):
Ion Acoustic Microscopy
Order number: AD-A169492/NAA
Price code: A02
Order from:
National Technical Information Service
5285 Port Royal Road
Springfield, VA 22161

This document was prepared under the sponsorship of the U.S. Government. Neither the United States Government nor any person acting on behalf of the United States Government assumes any liability resulting from the use of the information contained in this document, or warrants that such use will be free from privately owned rights.

MANUFACTURING TECHNOLOGY NOTE

U.S. ARMY MATERIEL COMMAND

Deputy Chief of Staff for Manufacturing Technology, Alexandria, VA

Project Number: NONE

Filing Code: 68D043

Automatic Measurement of Rain Rate

Standard rain gauges are assembled into an electronic collection, storage, and processing system.

A report describes a means of electronically instrumenting off-the-shelf tipping-bucket rain gauges so that each gauge is an autonomous real-time recording unit. The gauge system, which was developed for the U.S. Army Missile Command, accurately measures rainfall with respect to time.

The heart of the system is a real-time-clock integrated circuit (see figure). The circuit, a low-threshold, metal-gate complementary metal-oxide semiconductor (CMOS) device, is designed to function as both clock and calendar is bus-oriented microprocessor systems. This device, coupled with supporting logic and a 4 K random-access memory (RAM), provides data recording and retention facilities.

Each gauge contains a small pivoted bucket having a volume equivalent to 0.1 in. (2.5 mm) of rainfall. When a bucket becomes full of rainwater, it tips, discharges its contents, and returns to its upright position to receive more rainwater.

Each time a rain gauge bucket tips, the time of the event is recorded and retained in RAM. The sequence continues until testing is terminated. Data retrieval ensues; a microprocessor is connected to the memory board and sequentially reads each RAM location. As the data are extracted from memory, the microprocessor software formats it and sends it to a port, which transmits the data to a terminal or printer.

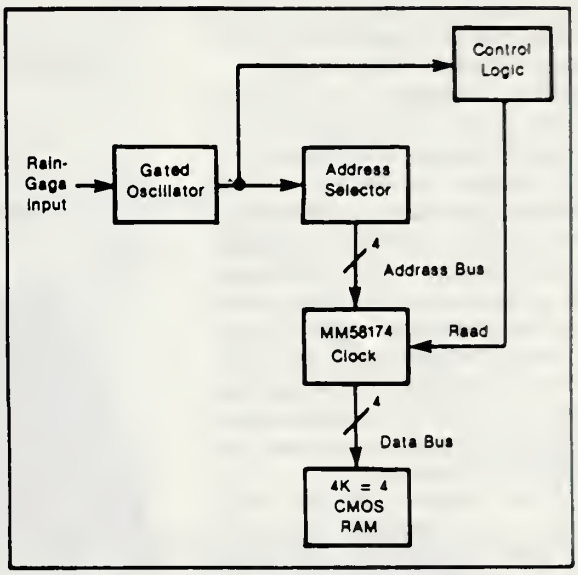

The **MM58174 Clock Integrated Circuit** synchronizes collection and storage of rain gauge data on tipping times of the rainwater buckets. The integrated circuit was chosen for its compatibility with the microprocessor used to format the data after collection.

FOR ADDITIONAL INFORMATION:

You can learn more details about this technology by ordering the NTIS report(s):

An Autonomous Real-Time Data Logging Rain Gauge System.
Order number: AD-A169911/NAA
Price code: A03

Order from:
National Technical Information Service
5285 Port Royal Road
Springfield, VA 22161

This document was prepared under the sponsorship of the U.S. Government. Neither the United States Government nor any person acting on behalf of the United States Government assumes any liability resulting from the use of the information contained in this document, or warrants that such use will be free from privately owned rights.

NASA Tech Brief
National Aeronautics and Space Administration
NASA's Jet Propulsion Laboratory, Pasadena, California

One-Dimensional Simulation of Isotropic Radiation

Solar cells are tested for effects of radiation in a unidirectional beam.

A test setup (see figure) exposes solar cells to the time-average equivalent of isotropic electron and proton radiation, even though the particles come from a single direction. A motor-driven cam rotates a target plate back and forth at a speed proportional to the cosecant of the angle of the incident radiation beam.

In isotropic irradiation, the frequency distribution of the incident particles is proportional to the sine of the angle of incidence. Therefore, to simulate isotropic irradiation of a sample by a unidirectional source of constant intensity, the sample is irradiated at each angle of incidence, with an exposure time inversely proportional to the sine of the angle; in other words, directly proportional to the cosecant. This will ensure that in the average over time, the radiation produces a dose-versus-depth profile that duplicates that from isotropic irradiation.

The motor rotates the cam continuously in one direction. The cam follower slides a carriage back and forth on rails. A rack at the rear of the carriage turns a pinion gear at the lower end of the shaft that holds the solar cells. The rack rotates the shaft back and forth to expose the sample at all angles of incidence between +90° and −90°. The cam groove is shaped to drive the cam follower in a pattern that makes the shaft rotational speed proportional to the cosecant of the angle. The beam is fairly large, encompassing the reciprocating cell specimens as well as stationary cells mounted above for comparison.

This work was done by Bruce E. Anspaugh and R. Gil Downing of Caltech for **NASA's Jet Propulsion Laboratory**.

NPO-16412 /TN

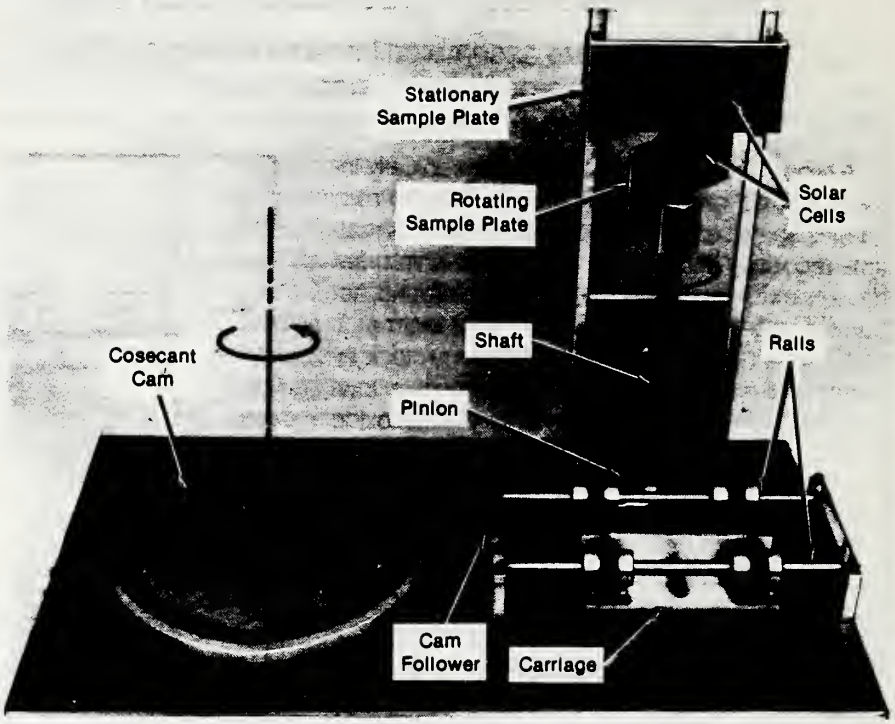

The Cam Groove Imparts a Cosecant-Function velocity to solar cells on a rotating target plate. The cells on the stationary plate above the rotating one absorb steady perpendicular radiation from a test source.

FOR ADDITIONAL INFORMATION: *Contact: Director, Technology Transfer Division, P.O. Box 8757, BWI Airport, MD. 21240; (301) 621-0100 Ext. 241*
REFER TO THE NUMBER LISTED AT THE END OF THE ARTICLE

NASA Tech Brief
National Aeronautics and Space Administration

Licensing Opportunity

Versatile X-Ray Telescope

Spatial and spectral resolutions are increased.

A proposed telescope for x-rays and extreme ultraviolet rays would feature high spectral and spatial resolution. Like previous telescopes of its class, it would include a glancing-incidence primary reflector. However, unlike its predecessors it would include a concave, non-glancing secondary reflector more like those used in telescopes for visible light.

The primary reflector (see Figure 1) consists of adjacent annular segments of a paraboloid and a confocal, coaxial hyperboloid. Paraxial rays that strike these surfaces produce an image at the primary focus, F_1. The secondary reflector is a concave, off-axis ellipsoid with one of its focuses at F_1 and the other at F_2. A high-resolution x-ray detector or photographic film is placed at F_2.

The secondary reflector functions well with x-rays at or near normal incidence because it is coated with alternating thin layers of two different materials (usually, metals) that support Bragg reflection at the wavelengths of interest. Such coatings, called synthetic layered microstructures, are described more fully in "Computation of Bragg Reflection for Layered Microstructures" (NPO-15880), page 41, *NASA Tech Briefs,* Vol. 8, No. 1 (Fall 1983).

Figure 2 illustrates some variations of the new telescope concept. At the top, several off-axis secondary reflectors of identical curvature are mounted on a cylinder. Any of these reflectors can be selected by simply rotating the cylinder to bring it into the focal position. Because a synthetic layered microstructure reflects primarily in a narrow wavelength band at a given angle of incidence, each reflector can be given a different coating so that it will produce an image at a different part of the x-ray spectrum.

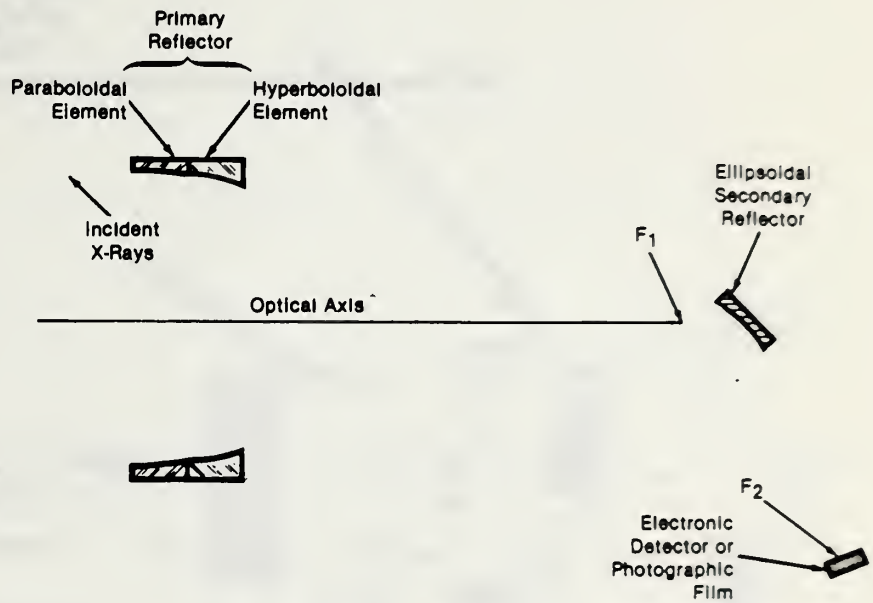

Figure 1. The Basic **X-Ray Telescope** includes a glancing-incidence, two-element primary reflector and a concave, off-axis ellipsoidal secondary reflector.

The middle of Figure 2 shows two secondary mirrors and two detectors in use with the same primary mirror. The image produced by mirror A is larger than that produced by mirror B. The lower magnification of B is selected by moving mirror A out of the focused x-ray beam. If the synthetic layered microstructure of B is the same as that of A, then mirror B can be used to image a band of wavelengths slightly shorter than those of A, because B has a slightly lower glancing angle.

A normal-incidence concave ellipsoidal reflector with a synthetic layered microstructure can be used to reflect the x-rays back along the optical axis (see Figure 2, bottom). In this case, a pair of nested primary reflectors is used.

This work was done by Richard B. Hoover of **Marshall Space Flight Center.**

Inquiries concerning rights for the commercial use of this invention should be addressed to the Patent Counsel, Marshall Space Flight Center. Refer to MFS-28013 /TN

George C. Marshall Space Flight Center
Technology Utilization Officer
Ismail Akbay
Code AT01
Marshall Space Flight Center, AL 35812
(205) 544-2223
Patent Counsel:
Leon D. Wofford, Jr.
Mail Code CC01
Marshall Space Flight Center, AL 35812
(205) 544-0014

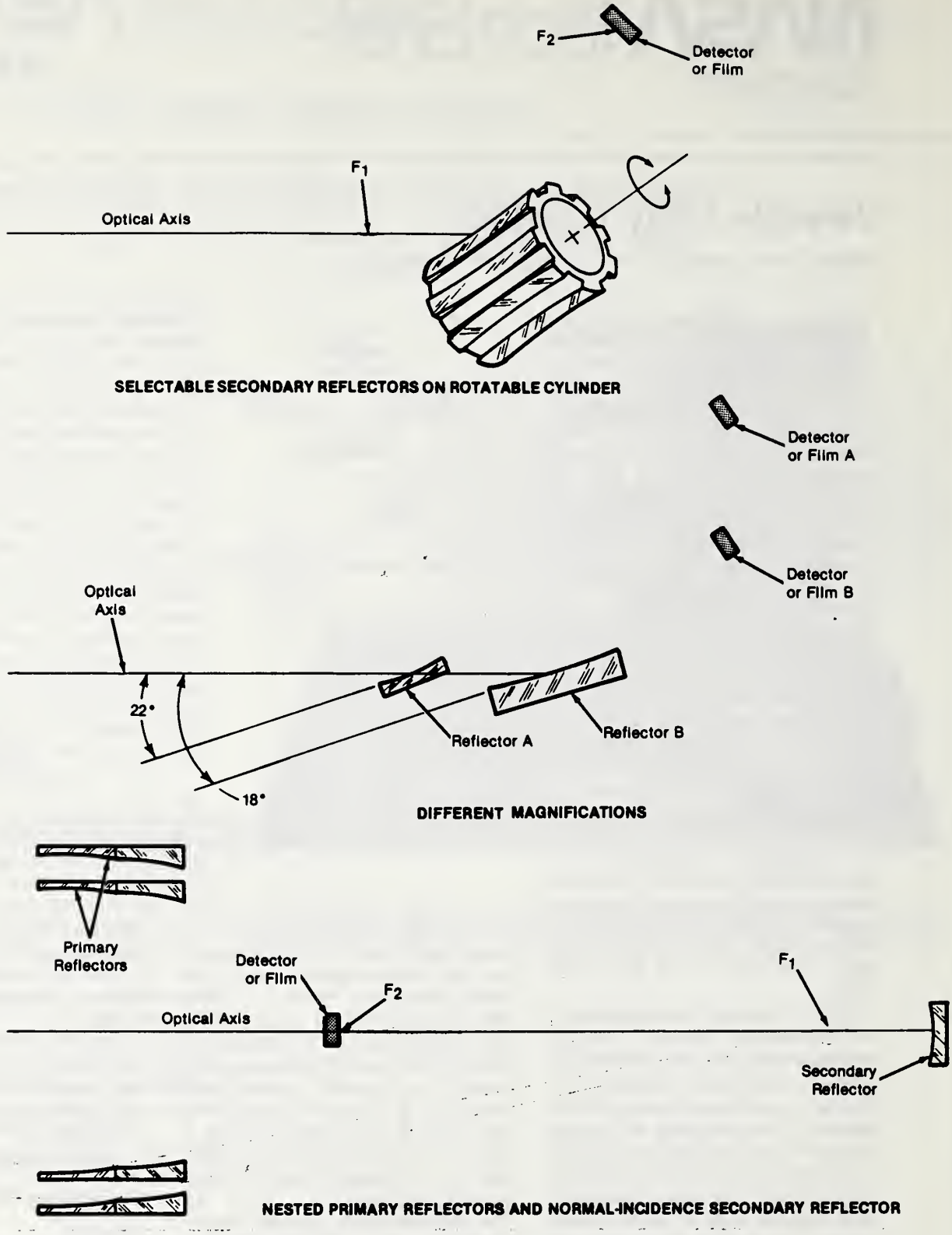

Figure 2. **Different Versions of the Telescope** are obtained by the use of different reflector and detector configurations.

FOR ADDITIONAL INFORMATION: *Contact: Director, Technology Transfer Division, P.O. Box 8757, BWI Airport, MD. 21240; (301) 621-0100 Ext. 241*

REFER TO THE NUMBER LISTED AT THE END OF THE ARTICLE

NASA Tech Brief
National Aeronautics and Space Administration
Goddard Space Flight Center, Greenbelt, Maryland

Licensing Opportunity

Wide-Angle, Flat-Field Telescope

An all-reflective system is unvignetted.

A wide-angle telescope uses unobstructed reflecting elements to produce a flat image. Because there are no refracting elements, there is no chromatic aberration, and the telescope operates over the spectral range from infrared to far ultraviolet. The telescope can be used with such image detectors as photographic film, vidicons, and solid-state image arrays.

The telescope (see figure) includes three reflectors: A spherical primary mirror, M_1; an ellipsoidal secondary mirror, M_2; and a spherical tertiary mirror, M_3. The centers of curvature of the spheres and the foci of the ellipsoid lie on the common optical (Z) axis. Practical values of the effective focal length of the three-mirror system could range from 20 to 100 mm.

To eliminate vignetting, the mirrors are offset portions of the parent reflector surfaces. An input baffle helps define the field of view, which is 20° about the X axis and 30° about the Y axis. Additional masks and baffles define further the field of view and suppress stray light.

The incoming light beam first strikes M_1 and is reflected to M_2. After M_2, the beam narrows to a waist where it crosses the common optical axis. An iris diaphragm placed there serves as an aperture stop, with its center on the common optical axis. None of the rays that pass through the iris is obscured by any of the mirror segments. The iris is adjusted to produce any desired focal ratio between f/4 and f/22.

The curvatures of M_1, M_2, and M_3 are balanced so that their combined spherical aberration is nearly zero. Coma is corrected by balancing the contribution of M_1 and M_3 against that of M_2. Astigmatism is corrected by balancing the contribution of M_1 against that of M_3, leaving a small residue from M_2. The curvatures of M_1, M_2, and M_3 are selected so that a distant object produces a flat image.

After passing through the iris, the light is reflected and focused by M_3 onto the detector. Because the image is flat, the detector can be flat. The image on the detector plane has about 10 percent barrel

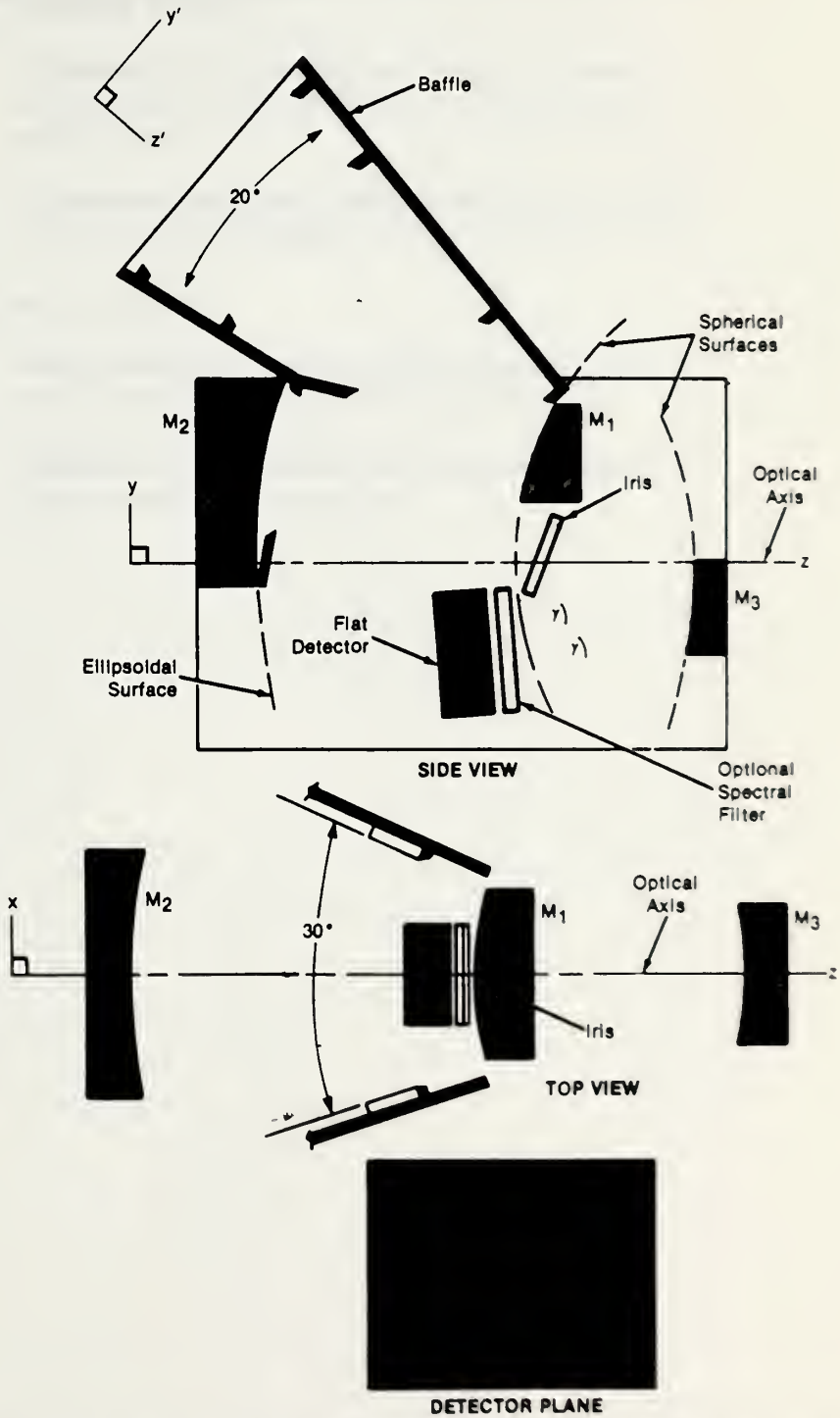

The Wide-Angle Telescope includes offset mirrors to achieve an unobstructed field of view. The mirror curvatures are chosen to produce a flat image on the detector.

distortion, which in most cases would be acceptable as the price of maintaining high resolution throughout the entire image field, and can be corrected with automatic processing of the image data.

This work was done by Kenneth L. Hallam, Barton J. Howell, and Mark E. Wilson of **Goddard Space Flight Center.**

quiries concerning nonexclusive or exclusive license for its commercial development should be addressed to the Patent Counsel, Goddard Space Flight Center Refer to GSC-12825 /TN

Goddard Space Flight Center
Technology Utilization Officer:
Donald S. Friedman
Mail Code 702-1
Greenbelt, MD 20771
(301) 286-6242
Patent Counsel:
John O. Tresansky
Mail Code 204
Greenbelt, MD 20771
(301) 286-7351

FOR ADDITIONAL INFORMATION: *Contact: Director, Technology Transfer Division, P.O. Box 8757, BWI Airport, MD. 21240; (301) 621-0100 Ext. 241*

REFER TO THE NUMBER LISTED AT THE END OF THE ARTICLE

Transportation

715 Small-Scale and Full-Scale Models of Helicopter Rotors—Data on noise and on hovering and forward flight are compared.

716 Testing Helicopter Crashworthiness—A simulated crash shows that an energy-absorbing design is effective in protecting the crew.

717 Circulation-Control Variable-Pitch Propeller—Blown aerodynamics concept would improve reliability and reduce costs.

718 Acceptance, Verification, and Performance Test Results for the Bedford CF Electric Van

Other items of interest

647 Energy-Absorbing Passenger Seat for Aircraft—Tests show probability of passenger survival to be high.

678 Hypersonic Plane Material—Basic tests on aluminum-lithium alloys will be conducted.

MANUFACTURING TECHNOLOGY NOTE

U.S. ARMY MATERIEL COMMAND

Deputy Chief of Staff for Manufacturing Technology, Alexandria, VA

Project Number: NONE

Filing Code: 51A058

Small-Scale and Full-Scale Models of Helicopter Rotors

Data on noise and on hovering and forward flight are compared.

A 1/6-scale model helicopter main rotor, 2.1 m in diameter, was tested in hover in a 40- by 80-ft (12.1-by 24.4-m) wind tunnel. Subsequently, it was tested in forward flight in a 7- by 10-ft (2.1- by 3.0-m) tunnel.

The primary objective of the tests by the U.S. Army Aviation Research and Development Activity — AVSCOM was to obtain performance and noise data on a small-scale rotor at various thrust coefficients, tip mach numbers, and advance ratios. The data were compared with data measured on full-scale helicopter rotors. A secondary objective was to contribute to a data base that will help researchers to estimate the effects of the testing facility on acoustic measurements.

The hover performance (see figure) and acoustic results for the model-scale and full-scale rotors compared quite well. The expected influence of Reynolds number on profile power was evident. Acoustic low-frequency harmonic levels were found to scale geometrically. At full-scale midfrequencies; the spectral levels rolled off much more rapidly than with model-scale data at equivalent frequencies.

In forward flight, both the performance and acoustics of the small-scale rotor compared poorly with the full-scale data. Significant Reynolds-number effects were found in the lift-to-drag comparison. The acoustic spectra of both the model- and full-scale rotors showed similar trends; however, there was an overall difference in levels of 5 to 10 dB.

Project officer Cahit Kitaplioglu
(415) 694-6679 or FTS 443-6679.

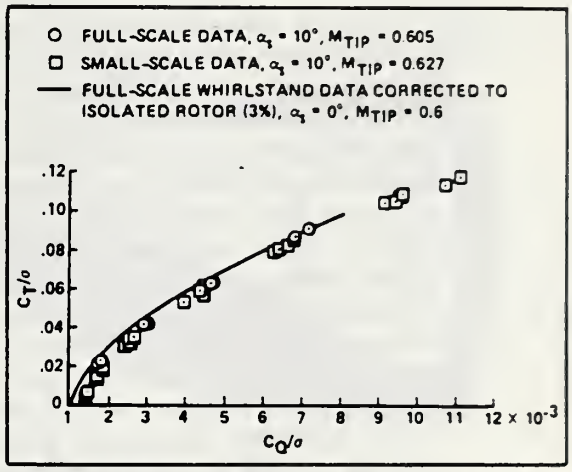

Model-Scale and Full-Scale Data for hovering flight agree closely. The vertical and horizontal axes represent thrust and torque, respectively.

FOR ADDITIONAL INFORMATION:

You can learn more details about this technology by ordering the NTIS report(s):
Hover and Forward Flight Acoustics and Performance of a Small-Scale Helicopter Rotor System.
Order number: AD-A165948/NAA
Price code: A03

Order from:
National Technical Information Service
5285 Port Royal Road
Springfield, VA 22161

This document was prepared under the sponsorship of the U.S. Government. Neither the United States Government nor any person acting on behalf of the United States Government assumes any liability resulting from the use of the information contained in this document, or warrants that such use will be free from privately owned rights.

MANUFACTURING TECHNOLOGY NOTE

U.S. ARMY MATERIEL COMMAND

Deputy Chief of Staff for Manufacturing Technology, Alexandria, VA

Project Number: NONE

Filing Code: 51A059

Testing Helicopter Crashworthiness

A simulated crash shows that an energy-absorbing design is effective in protecting the crew.

A test has assessed the effectiveness of the structural crashworthiness features and systems designed into the YAH-63 helicopter to improve the survivability of the crew during crashes. The test, which was conducted for the U.S. Army Aviation Research and Technology Activity (AVSCOM), offers unique data for predicting the crash impact behavior of future helicopters.

In the test, the helicopter was dropped onto a concrete apron so that its tail gear struck first and its main landing gear slightly thereafter. The impact velocity was 60.1 ft/s (18.3 m/s). The helicopter traveled 27 ft (8.2 m) along the apron after impact.

The crashworthy landing gear, energy-absorbing fuselage structure, and forward crewseats performed at or above their design levels of energy absorption. For example, although both of the pilot's seat energy attenuators buckled in compression after stroking only 2.5 in. (6.4 cm), the seat continued to absorb energy (see figure). The peak seat acceleration was 17 g. The pilot's seat began stroking 139 milliseconds after tail impact and 13 milliseconds before the copilot's seat began stroking.

Since the vertical loads do not exceed the 23-g Eiband criterion, a pilot would have survived the impact without spinal injury. In addition, the lateral and longitudinal loads were well within tolerance for a properly restrained human.

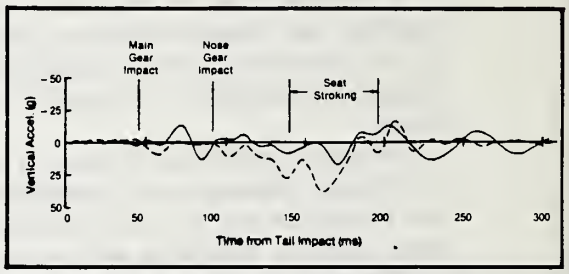

The **Pilot-Seat Pan Acceleration** during impact (solid line) is compared with the crewseat-mounting bulkhead. Throughout, the energy-absorbing seat prevents acceleration from exceeding safe levels, even though the bulkhead does.

Project officer Kent F. Smith
(804) 878-5875 or -2103 or FTS 988-5875 or -2103.

FOR ADDITIONAL INFORMATION:

You can learn more details about this technology by ordering the NTIS report(s):
Full-Scale Crash Test (T-41) of the YAH-63 Attack Helicopter.
Order number: AD-A167813/NAA
Price code: A05

Order from:
National Technical Information Service
5285 Port Royal Road
Springfield, VA 22161

This document was prepared under the sponsorship of the U.S. Government. Neither the United States Government nor any person acting on behalf of the United States Government assumes any liability resulting from the use of the information contained in this document, or warrants that such use will be free from privately owned rights.

NASA Tech Brief
National Aeronautics and
Space Administration
Langley Research Center, Hampton, Virginia

Circulation-Control Variable-Pitch Propeller

Blown aerodynamics concept would improve reliability and reduce costs.

A variable-pitch propeller based on the circulation-control airfoil concept has no moving parts other than those needed for propeller rotation. When substituted for a conventional variable-pitch propeller airfoil, it would lower manufacturing costs, reduce maintenance, and improve reliability.

In previous designs to vary pitch for different flight regimes (such as takeoff and cruise), the individual propeller blades are rotated about their span axes by hydraulic or electric motors. These approaches require precise, moving machine elements, increasing costs, maintenance requirements, and opportunities for failure.

The circulation-control airfoil concept (see figure), under development for a number of years, involves blowing a tangential stream of air from a thin upper-surface slot over the airfoil rounded trailing edge. The jet sheet remains attached to and turns around the trailing edge, thus controlling the circulation around the airfoil. In the current design, this principle controls the effective pitch of the propeller.

Air for the blowing slot is supplied by an engine-driven air pump through a labyrinth seal at the propeller hub. By controlling the flow of air to the propeller, the effective pitch of the propeller may be changed in flight.

Since large changes in angle-of-attack have little effect on coefficient-of-lift, a propeller using this airfoil would tend to be self-compensating for changes in aircraft forward speed, even without an adjustment of the air supply. However, an automatic system for sensing engine speed and controlling the airflow to maintain constant speed over a range of power settings could be easily incorporated into the design. This would be done preferably by fluidic control, for maximum reliability.

With the circulation-control variable-pitch propeller, the effective pitch of the

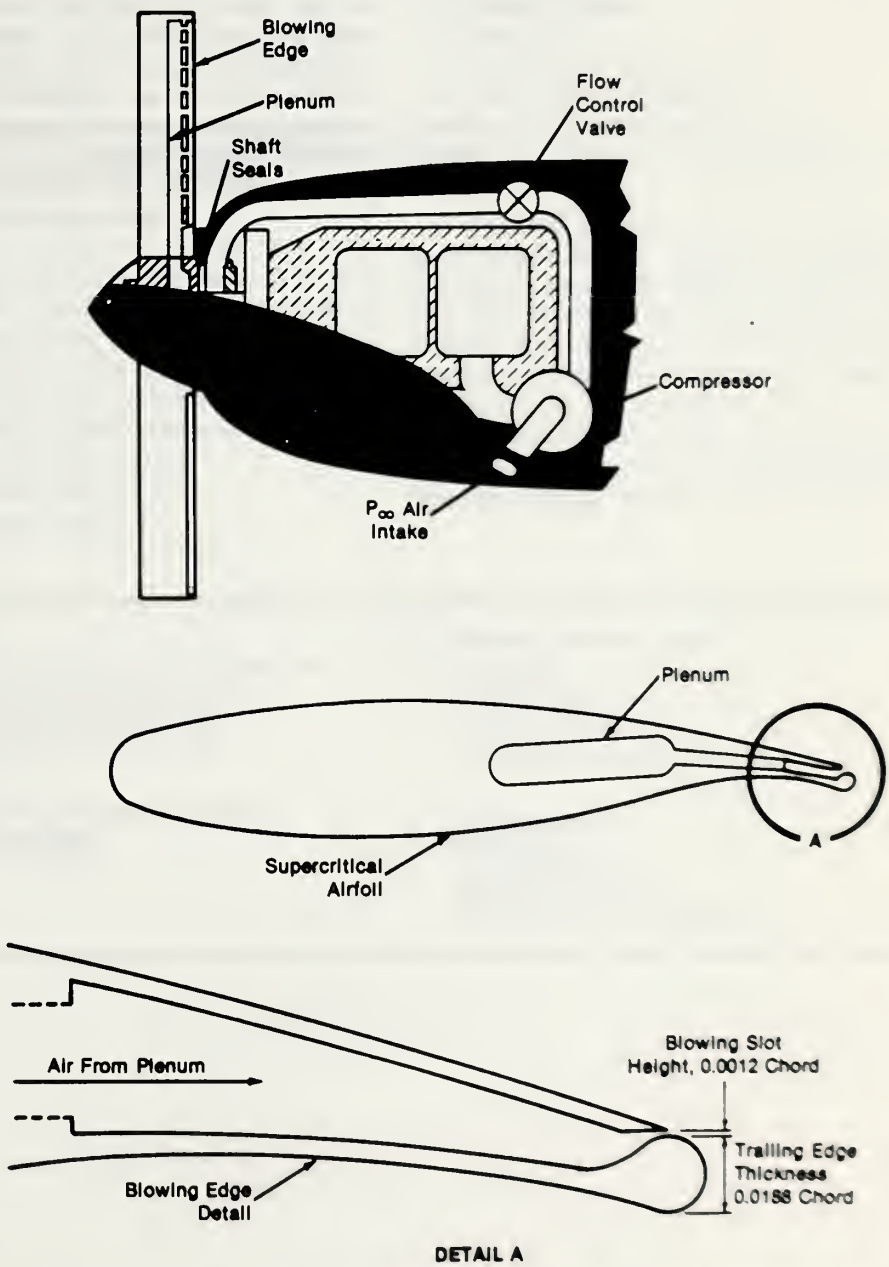

Circulation-Control Variable-Pitch Propeller has a large lift value at very moderate blowing coefficients.

propeller could be varied over a wide range, simply by controlling the flow of air to the blowing slot. In small aircraft, it would improve takeoff performance and increase fuel economy at little or no additional cost.

This work was done by H. Douglas Garner of **Langley Research Center.** *Further information may be found in NASA CR-165968 [N85-29959/NSP], "Circulation Control Propellers for General Aviation, Including a Basic Computer Program."*

Copies may be purchased from the National Technical Information Service, Springfield, Virginia 22161, [A05]

LAR-12740 /TN

FOR ADDITIONAL INFORMATION: *Contact: Director, Technology Transfer Division, P.O. Box 8757, BWI Airport, MD. 21240; (301) 621-0100 Ext. 241*

REFER TO THE NUMBER LISTED AT THE END OF THE ARTICLE

energygram

Acceptance, Verification, and Performance Test Results for the Bedford CF Electric Van

DOE/TIC/EG-86/114
OFFICE OF SCIENTIFIC AND TECHNICAL INFORMATION

This technical note was based on research conducted by Idaho National Engineering Laboratory for the U.S. Department of Energy.

INEL
Idaho National Engineering Laboratory

Acceptance, verification, and performance testing of a production Bedford CF electric van has been performed. Battery characterization as well as vehicle track and dynamometer tests was performed. The report cited herein presents results of such testing as well as summary recommendations.

The primary objective of the tests was to evaluate the vehicle characteristics and performance relative to the *U.S. Code of Federal Regulations,* Title 10, Part 475 (10 CFR 475). During the testing, the following parameters were addressed:

- Acceptance inspection and testing
- Battery characterization
- Coastdown testing
- Acceleration testing
- Range
- Forward speed
- Braking
- Gradeability limits
- Environmental factors
- Dynamometer/vehicle testing
- Federal Urban Driving Schedule testing

A detailed discussion of the results of each phase of the testing is included in the report as well as a summary of results. The document cited here contains supporting data for acceptability and performance of a commercial electric vehicle. Test matrices are identified.

This information is of value to potential users and designers of short-range commercial transportation.

FOR ADDITIONAL INFORMATION

DOE report(s):
Acceptance, Verification, and Performance Test Results for the Bedford CF Electric Van.
Report number: EGG-SE-7033/NAB
Order number: DE86007650/NAB
Price: $16.95

Order from:
National Technical Information Service
5285 Port Royal Road
Springfield, VA 22161

For additional information, contact
J. M. Welch
EG&G Idaho, Inc.
P.O. Box 1625
Idaho Falls, ID 83415
Telephone No.: (208) 526-8318

or

H. W. Heiselmann
EG&G Idaho, Inc.
P.O. Box 1625
Idaho Falls, ID 83415
Telephone No.: (208) 526-0897

NTIS Order Form

NTIS Telephone Numbers

To Order Reports
(703) 487-4650

For Subscription Questions
(703) 487-4630

Other Information
(703) 487-4600

Editorial Questions
(703) 487-4838

Postage:
NTIS uses First Class Delivery, or equivalent service, on all shipping. For information about one day RUSH ordering, call (703) 487-4600.

NTIS PRICE CODE SCHEDULE *

This schedule gives the current values to the price codes cited in those Tech Notes having a backup report available from NTIS.

Microfiche	
A01	$6.50
Paper copy	
A02	9.95
A03	11.95
A04 through A05	13.95
A06 through A09	18.95
A10 through A13	24.95
A14 through A17	30.95
A18 through A21	36.95
A22 through A25	42.95
A99	Call for price

Customers in Canada, United States, and Mexico use this schedule. Other addresses should write for the price listing, number PR-360-4.

Prices effective January 1, 1987

Use this form ONLY to order reports designated as available from NTIS

MAIL ORDER TO: National Technical Information Service
U.S. DEPARTMENT OF COMMERCE
5265 Port Royal Road
Springfield, VA 22161
(703) 487-4650

Send me the reports I have selected on this form. I have placed order numbers in appropriate blanks and have indicated the quantity. IF ADDRESS LABEL IS NOT CORRECT, CALL OUR SUBSCRIPTIONS DEPARTMENT.

Last Name: .....

Title: .....

Company/Organization: .....

Address: .....

.....

City/State/Zip: .....

Telephone Number: .....

METHOD OF PAYMENT

☐ Check enclosed payable to NTIS for $ .....

☐ Charge to my NTIS Deposit Account, No: ....-.....

☐ Purchase order number: .....

Charge to: ☐ American Express ☐ VISA ☐ MasterCard

Card Number: .....

Expation date: .....

Signature: .....
(Required to validate order)

NTIS ORDER NUMBER (Use only for backup reports stated as available from NTIS)

NTIS Order Number	*Price**	*Quantity*	*Total Price*
.....	.....	.....	.....
.....	.....	.....	.....
.....	.....	.....	.....
.....	.....	.....	.....
.....	.....	.....	.....
		Shipping and handling fee	$3.00
		Total	.....

- Agriculture & Food
- Computers
- Electrotechnology
- Energy
- Engineering
- Environmental Science & Technology
- Manufacturing, Machinery, & Tools
- Materials
- Medicine & Biology
- Natural Resources Technology & Engineering
- Physical Sciences
- Transportation

PENN STATE UNIVERSITY LIBRARIES
A000072009857

PARTMENT OF COMMERCE
al Technical Information Service
ld, Va. 22161

L BUSINESS
for Private Use, $300

AN EQUAL OPPORTUNITY EMPLOYER

Route To:

BULK RATE
POSTAGE & FEES PAID
NTIS
Permit No. G-292